SYNTHESIS OF MULTIFILAMENT SILICON CARBIDE FIBERS BY CHEMICAL VAPOR DEPOSITION

Vithal Revankar and Vladimir Hlavacek

Laboratory for Ceramic and Reaction Engineering
Department of Chemical Engineering
State University of New York at Buffalo
Buffalo,New York 14260

Final Technical Report for the Project Grant No. NAG3-863 submitted to:

NASA Lewis Research Center, Cleveland, OH 44135-3191
for the Period 1988-1991

May 1991

Contents

Department of Chemical Engineering
School of Engineering and Applied Sciences
Clifford C. Furnas Hall
Buffalo, New York 14260
Telephone: (716) 636-2911
Fax: (716) 636-3822

UNIVERSITY AT BUFFALO
STATE UNIVERSITY OF NEW YORK

August 20, 1991

Technical Officer
NASA Lewis Research Center
M.Stop 500-315
21000, Brookpark Road
Cleveland,Ohio 44135

Dear Sir:

Re: Final Technical Report for the Program No. NAG3-863 for six

List of Figures

List of Tables

1 ABSTRACT

A need exists for a cheap silicon carbide fiber with a small diameter (10-20 μm), which would exhibit consistently high values of fiber strength. A promising candidate for the manufacture of such inorganic fibers with good mechanical properties is Chemical Vapor Deposition (CVD) of silicon carbide on a carbon core. Our report highlights a process for the development of clean fiber with a small diameter and high reliability (a low degree of scatter of values of mechanical properties along the fiber). Our CVD process takes advantage of a carbon tow core (with individual 5-7 μm filaments) which is pulled through a tubular reactor. Experiments in a batch system indicated that the silicon carbide fibers consisting of many individual filaments can be prepared by a CVD process. The fiber exhibits a geometrical form of nicalon and mechanical properties of TEXTRON material. This report focuses on (a) an experimental evaluation of operating conditions for SiC fibers of good mechanical properties;(b) devising an efficient technique which will prevent welding together of individual filaments.Our efforts on synthesis of these small diameter individual mono filaments are also detailed.The problems and remedies are discussed.The kinetic studies on the tungsten and carbon substrate were carried out.The reported mechanical properties gave an indication for further improvement.

The thermodynamic analysis of different precursor system was analyzed vigorously. Thermodynamically optimum condition for stoichiometric SiC deposit were obtained.Our analysis on different precursor system gave the order of reactivity for CH_3SiCl_3,$(CH_3)_4Si$, $(CH_3)_2SiCl_2$, $SiH_4 + CH_4$,$SiCl_4 + CH_4/CCl_4$ system with hydrogen.The 3-D picture explained the effect of the α ratio(concentration),the pressure, and the temperature on the stoichiometry of SiC.Various other thermodynamic analysis which covers the whole spectrum of conditions are discussed in the report.The different morphological changes of the deposit with all the parameter of operation is discussed. Overall, the project is fairly successful.

2 Introduction

A new class of processes, with enormous technological flexibility and capability, so called Chemical Vapor Deposition (CVD) was developed and successfully applied in the last two decades. CVD is a unique way to deposit solid materials by making use of

the surface-vapor chemical reactions. Even though the application of CVD technology in the electronic industry was extremely successful and certain deposition techniques seem to mature, there is a lack of knowledge in fundamental chemistry and chemical engineering principles to apply this process in the synthesis of inorganic fibers.

Motivated by aerospace applications, under NASA support, the Laboratory for Ceramic and Reaction Engineering launched research and development activities leading to a CVD method for the synthesis of high performance continuous non-oxide ceramic fibers. These materials offer many outstanding properties at high temperature. The achievement of consistent high fiber strength over long length is important for successful implementation in many composite systems [Edie, 1987; Edie and Dunham, 1987; Richerson, 1984]. Keeping this goal in mind, we decided to develop the silicon carbide fiber by chemical vapor deposition using carbon tow as a core material. The application of this material in bulk form has often been limited by a poor understanding of reaction mechanism which resulted in poor physical properties, high residual stress and high cost (Revankar et al., 1988a, 1989b).

Over the past few years, numerous patents and publications have revealed the use of polymer precursors and CVD methods to manufacture silicon carbide fibers. There are only two sources available commercially (NICALON and TEXTRON). The existing Textron and Nicalon fibers are susceptible to oxidation at relatively low temperature and are very costly. Hence, our research is to make available the silicon carbide fiber at lower cost and may share some of the key reinforcing characteristics of boron but with higher thermal stability (T>1400°C) and toughness. The metal matrices of silicon carbide can be manufactured and machined more easily than boron. In addition Al, Ti and Mg parts can be cast into shape with SiC reinforcement [Reisch, 1987].

2.1 Critical Analysis of Silicon Carbide Fibers and Future Developments Required

Commercially available silicon carbide fibers, Nicalon (prepared by polymer pyrolysis) and TEXTRON material (prepared by chemical vapor deposition) have completely different chemistry and mechanical properties. Nicalon's small fiber diameter ($\approx$17μm) provides a high surface-to-volume ratio, thus allowing large numbers of potential crack stoppers in a ceramic composite. Moreover, intricate composite shapes can be fabricated because the small diameter can tolerate radical bending. TEXTRON's fiber produces

composites of good fracture toughness, however, it cannot be used for reinforcing areas with sharp bending (<1/2 inch loop diameter) due to its high diameter ($\approx$125-150μm). Both of these fibers degrade or lose strength at relatively low temperature when exposed to air (Nicalon's >1000°C, AVCO's >1400°C) [Mah et al., 1984; DiCarlo, 1985, 1986].

The TEXTRON fiber, manufactured by chemical vapor deposition (similar to the process which we are following), is essentially comprised of silicon carbide and carbon with discrete regions of each [Wawner et al, 1983]. Thick carbon monofilament is used as a core material; the bulk of the fiber is β-SiC and the outer coating ($\approx$1-6μm) is a graded combination of silicon carbide and free amorphous carbon. The microstructure of Nicalon is not discrete, but consists of an intimate amorphous combination of silicon, carbon and oxygen [$\approx$14%] that separates into β-SiC, graphite and amorphous silicon dioxide when heat treated above 1200°C [Mah et al., 1984]. Although the data characterizing strength as function of temperature is limited, TEXTRON's fiber appears to be slightly stronger. Theoretically, stoichiometric SiC-fiber should retain strength up to 1700°C. One of the reasons for reduction in strength is due to surface pitting which is associated with metallic impurities (Johnson et al., 1987) and the conversion of excess carbon to carbon monoxide. Due to the low solubility of Si and C in silicon carbide, a laminae structure is formed with alternating thin Si/SiC layers or C/SiC layers [Weiss and Diefendorf, 1974; Knippenberg et al., 1974; Gulden, 1968; Merz, 1960]. The free Si and C and morphology of the fiber entirely depends on deposition parameters. The thermal instability of these ceramic composites, which is often a result of fiber-matrix interfacial degradation, has prevented prolonged application of these composites at high temperature. Hence, our development will be concentrated on stoichiometric deposition of ultraclean silicon carbide.

High fracture toughness is one of the main characteristics required for the fiber. The understanding of a complex nature of the dependence of toughness on deposition parameters, morphology, composition and impurities is not clear. Several factors are considered important. The ratio of fiber modulus to matrix modulus should be at least 2:1 to allow greater load transfer from the matrix to the fiber. Secondly, thermal expansion mismatches are also important because higher thermal expansion in the fiber produces radial tensile forces around the fiber. When a crack approaches the fiber, it tends to bend around it, thus increasing the toughness by dissipating fracture energy. However, excessive thermal expansion mismatch causes prestressing of the fiber and decreases the strength and toughness. Good mechanical bond between the fiber and matrix is desirable and strong chemical bond tends to cause fiber degradation and

adversely affects the fracture toughness. Hence, future development will be to increase the strength and toughness by suitable secondary coating materials on the fiber. For example, the TEXTRON Company coats carbon on SiC fiber, thereby improving tensile strength almost by a factor two.

One of the ways to stabilize the strength of the fibers is through a plasticizing effect [Shorshorov et al., 1978]. Applying a nickel coating $\approx 1\mu$m thick with subsequent annealing at 1000°C forms a surface solid solution of free carbon of the fiber in nickel. Plasticizing can also be achieved by pulling the fiber through Al or an Al-alloy melt. The reported data show that the physicochemical interaction of the fibers with the coating indicates a selective dissolution of the atoms of the fiber material in the coating at stress concentrators, with the result that the stress concentrators are smoothed out. In addition, the plasticizing effect is promoted by relaxation of stresses in the coating at the stage of micro-plastic strain of the fiber [Shorshorov et al., 1978]. Wettability of the fiber is very important for metal matrix. This can be achieved by secondary coatings. Molybdenum is found to be the best bet in this situation.

Finally, for most reinforcements, the critical aspect ratio is about 20. Long fibers (continuous), therefore reinforce a composite more efficiently than short fibers. Another dominant advantage is that their orientation in the composite can be controlled precisely. The internal structure of the composite can thereby be designed to anticipate the stress it will face in use.

Design engineers have been hesitant to work with materials having low component reliability such as a large degree of scatter in strength, brittle nature and catastrophic failure. These problems can be solved if proper control of deposition is achieved.

3 CVD Synthesis

Broadly defined, chemical vapor deposition, or CVD, is the formation of solid products via chemical reactions of gaseous precursors. A typical CVD process would involve a dynamic flow system in which gaseous reactants pass over a heated substrate. The gases react chemically to produce a condensed coating on the substrate plus product gases, which, together with any remaining reactant gases, dynamically exit from the hot reaction zone.

The application of CVD processes centers around the production of thin films

for semi-conductors and other solid state electronic devices (Hess et al., 1985), coating of cutting tools and surfaces needing erosion and/or corrosion protection (Yee, 1978), coating of fibers used in forming composite materials (DiCarlo, 1985 and Guinn and Middleman, 1989), and containment coatings for nuclear fuel and nuclear waste particles (Spear, 1982). CVD processes are also used in the manufacturing of objects with complex shapes (e.g., refractory crucible) out of materials such as tungsten, molybdenum and rhenium which resist conventional machining and fabrication techniques (Iwasa et al., 1987; Shinko and Lennartz, 1987).

A vast number of chemical compounds are considered for these applications (Blocher et al., 1984). Important materials being prepared by CVD for electronic and optic devices include Si, Ge,Si_3N_4, SiO_2, GaAs, CdS, ZnSe and related compounds. Superconducting materials such as Nb_3Sn, Nb_3Ge, and NbC_xN_y can be deposited as well (Wahl and Schmanderer, 1989). Erosion and corrosion resistant coatings commonly applied by CVD to tooling materials are TiC, TiN and Al_2O_3. In addition, an appreciable amount of CVD research is being performed on coatings of TaC, TaN, W_2C, TiB_2, SiC, Si_3N_4, B_4C, BN and B for use on cutting tools, tubes, fibers and applications in which the materials are subjected to high temperatures, and corrosive and erosive environments.

3.1 Synthesis of High Performance Ceramic Fibers by CVD

The CVD process involves the formation of solid by decomposition or reduction of one or more gaseous components upon a heated substrate. Typically, a small-diameter substrate wire is run through the glass reaction tube, and suitable gases are introduced. The substrate is resistance heated causing the gas to react and deposit on the heating wire. Uniformity of the coating mainly depends on the uniform surface structure of the base fiber, temperature and rate of supply of fresh reacting gas to the fiber surface [Pierson and Randich, 1978]. The non-uniform temperature distribution results in heavier deposits on the hotter region and thereby introduce some flaws in the material. Deposition non-uniformities due to the fluctuations in the concentration of a coating gaseous reaction mixture along the fiber might be overcome by lowering pressure in the system [Sherman, 1987].

The coating adhesion is excellent when some kind of physical/chemical bond is formed by diffusion, or reaction between the coating material and the base. However, this diffusion (or interaction) should be at the "optimum" level to maintain the strength

and modulus of the fiber. Cleanliness of the surface of the base material is very important where the surface and base material interaction is necessary to obtain good adhesion. Cleanliness of the matrix is not so important when only physical adhesion of the material is required.

The supersaturation and temperature of the reaction process are important factors affecting the type of deposit. Low temperature or higher supersaturation of gases leads to a gas phase nucleation, thereby decreasing the efficiency of coating and adhesion. Higher temperature or low supersaturation gives epitaxial growth or dendrites kind of growth which is determental for the coating process. Hence, optimum temperature and supersaturation is necessary to obtain the required deposit such as amorphous deposit or fine grain polycrystal [Naslain et al., 1979; Schlichting, $1980_{a,b}$].

Deposition rates vary with the material deposited and the process used. Coating efficiency is the measure of material deposited to material supplied as volatilized compound, might vary greatly with the coating process and strongly depends on operating conditions and geometry of a reactor.

Generally, the material necessary for the CVD process can be supplied by a source gas. For the CVD process, two general reaction routes can be followed:

- Reduction of volatile halides
- Pyrolytic methods

The hydrogen reduction of halides process is an effective technique for the synthesis of ceramic fibers by CVD. The principle of this technique is as follows: Hydrogen saturated with metal halides (e.g., $TiCl_4$, $ZrCl_4$, etc.) or nonmetal halides (e.g., CCl_4, BCl_3, etc.) or mixture of these halides is passed into a reactor in which the base filament is heated (resistively or by any other method). Typically, for example, for a TiB_2 filament synthesis, the following reaction occurs:

$$TiCl_4 + 2BCl_3 + 5H_2 \rightarrow TiB_2 + l0HCl \tag{1}$$

The pyrolytic method represents a thermal decomposition of an appropriate component with low boiling point. For example, silicon carbide fiber can be synthesized from CH_3SiCl_3

$$CH_3SiCl_3 \rightarrow SiC + 3HCl \tag{2}$$

The surface deposition reaction rate varies with the material deposited, the reactant composition and temperature. Usually a material is deposited with the rate of 5 to 100 μm/hr. The important parameters which should be considered in this process are:

- Purity of the deposit and uniformity of coating.
- Coating adhesion.
- The effect of supersaturation and temperature on the structure.
- Efficiency of CVD reactions.
- The reactor geometry and operational arrangement.

4 Objective of the Work

The efficiency and performance of aerospace and power systems, such as gas turbine heat engines, can be significantly improved by using materials that are lighter, stronger, can withstand high stress, high heat flux, and aggressive environments. Metal and metal-matrix composites (MMC), carbon and carbon composites (CCC), polymer-polymer composites (PPC) and ceramic- ceramic composites including continuous fiber ceramic composites (CFCCs) are capable of meeting these demands of end user. Monolithic ceramics offer the greatest potential where a combination of reduced weight, high-temperature strength, and environmental stability are needed. But these materials are not fully utilized for engine application because of their poor reliability and catastrophic fracture properties. On the other hand, fiber reinforced ceramic matrix composites offer the promise of maintaining the desirable properties of monolithic ceramic while providing the microstructural mechanisms for improved material reliability and non-catastrophic fracture properties. Considerable effort has been expended in the world to increase the fracture toughness of ceramics. Improvements have been made through better processing to control flaws and by the incorporation of ceramic particulate and or whiskers to form a tougher ceramic composite. However, typical fracture toughness values for monolithic ceramics and whisker particulate-toughened composite remain low, 3 to 6 MPa and 8 to 12 MPa, respectively. In either case, ultimate failure is still catastrophic. This leaves with only fiber reinforced ceramic matrix composite as a means to increase fracture toughness (Vinson, 1989). With the development of silicon carbide, aluminum borosilicate, alumina, silicon nitride, carbon, titanium diboride, and mullite

fibers, continuous fiber reinforcement of ceramic matrices is now possible. With this fracture toughness, values from 15 to greater than 25 MPa have been measured (Prewo, 1989; Bhatt, 1988;). This increase is by mechanisms of fiber sliding, crack deflection and secondary microcracks. As the matrix cracks, the fiber continues to carry the load, thus imparting non-catastrophic failure or metal like behavior of the composites. An additional attractive feature of these composites is the ability to design or tailor properties by selecting not only the fiber and matrix, but also the pattern of the incorporated fibers. Fiber architecture, such as multi-direction fiber weaving, allows the composite manufacturer to tailor or enhance properties in specific directions to meet the needs of an application. Processing of these composites is more complicated. Techniques are needed that allow the matrix to be uniformly introduced throughout the volume of the fiber preform. Densification must take place without chemically or physically degrading the fibers. In addition, the processing techniques must accommodate not only the matrix and the fiber, but also produce the desired fiber-matrix interface bonding which is critical to the toughness and the performance of the composite. Here, considerable understanding of the interrelationship of processing variables, microstructure, and properties is required as well as basic process development and scale-up. This has led to new approaches, both in fabrication of existing materials and in the development of new micro- structural arrangements intended to improve some specific and chemical properties.

Fiber reinforced composites occupy a central role in the development of new materials and has overcome many of the limitations of traditional materials. Some of the potential advantages of fiber reinforced composite materials include: high strength at elevated temperatures, high strength to weight ratio, improved toughness, improved creep and fatigue strength and controlled expansion and conductivity. They also offer the unique advantage to tailor the properties and shape of the high performance material for the application desired.

Therefore, there is a critical need of fibers capable of reinforcing the composites at elevated temperature, even at sharp bending is involved. Even though the application of CVD technology in the electronic industry has been extremely successful, and certain deposition techniques seem to have matured, there still is a lack of knowledge in fundamental chemistry and chemical engineering principles in applying this process to the synthesis of inorganic fibers. This report describes a CVD method for the synthesis of high performance small diameter SiC fibers. The CVD method has several advantages over other conventional methods; hence, it has been adopted for this research.

It is extremely important to produce these fibers with good reproducible and controlled growth rates. Other properties are to be controlled include thickness, composition, purity, crystallinity and surface morphology. These properties are highly dependent on the deposition condition. Hence, it is necessary to correlate the fiber properties with temperature of the substrate, system pressure, gas flow rate and concentration of the reactants. However, the complex interplay of mass and energy transfer, blended with the fluid dynamics makes this a formidable task. Hence, the goals were to design and develop the CVD reactor systems which can synthesize SiC fibers, continuously. These fibers should be in small diameter (10-20μm), hence,carbon tow was used as a substrate material. The thermodynamic and kinetic analysis of SiC system for various precursors with the emphasis on effect of temperature, concentration of reactants, morphology was carried out. Investigation on the mechanical properties and stress distribution was carried out. We decide to analyze the different reactor system theoretically to locate the optimum conditions.

5 CVD of Silicon Carbide

Properties: SiC properties depend on purity, polytype and method of formation. Essentially it is a very hard material occupying a relative position on Moh's scale between alumina at 9 and diamond at 10. Because of its high thermal conductivity and low thermal expansion, SiC is very resistant to thermal shock as compared to other refractory materials. It is also a semiconductor. SiC is comparatively stable with only violent reaction occurring when it is heated with a mixture of potassium dichromate and lead chromate. It forms metal silicides on reaction with oxides of Ca, Mg, Cu above 1000°C.

At high temperature SiC exhibits either active or passive oxidation behavior depending upon ambient oxygen potential(Smoak et.al.,1964). When the partial pressure of oxygen is high, passive oxidation occurs and protective layer of SiO is formed on the surface.

$$2SiC(s) + 3O_2 = 2SiO_2(s) + 2CO(g) \tag{3}$$

Active oxidation occurs where the oxygen partial pressure is low (0.23 mm Hg at 1400°C) and gaseous oxidation products are formed

$$SiC(s) + O_2(g) = SiO(g) + CO(g) \tag{4}$$

$$SiC(s) + 2SiO(g) = 3SiO(g) + CO(g) \tag{5}$$

Silicon Carbide is known to exhibit good physical and mechanical properties and excellent high temperature [800-1600°C] oxidation resistance. CVD is one of the best known processes to obtain the protective coatings on different shaped base materials. The SiC coating has already been tested extensively in nuclear applications and as an abrasive. A large amount of research has been carried out on the CVD via organo-silane compounds or from the mixture of silicon halide and a hydrocarbon onto a hot substrate. However, very few researchers tried to obtain the good quality SiC fiber on suitable substrate and establish the relationship between the composition of the deposit and the deposition parameters as temperature, concentration and gas flow rate. The development of multifilament small diameter (10-20μm) CVD fibers was never tried seriously. These are the major goals of our research.

Pring and Fielding [1909] were first to report the CVD of SiC on graphite substrate using $C_6H_6 + SiCl_4$ with hydrogen at 1700-2000°C. Organic compounds with silicon and carbon in the same molecule is also well reported [Schlichting, 1980]. There exist principally two different methods of preparation:

- the cold wall arrangement and
- the hot wall arrangement of depositions.

In the cold wall arrangement, where the base material is heated in a gaseous atmosphere: and walls are cold, so that deposition takes place on the substrate only. In the hot wall arrangement the substrate is heated inside the furnace. In this system, the inside surface of the furnace is at a higher temperature than that of the substrate leading is poor deposition efficiency and large concentration gradients due to uneven temperature distribution.

A large number of papers, including reviews, appear in literature on CVD process for SiC since the time of Pring and Fielding(1909). Many systems have been used to deposit SiC but methyl trichloro silane has been a common choice in literature (Kaae and Gulden,1971;Ivanova and Pletyushkin,1968;Price,1969), primarily based on its stoichiometric ratio of one carbon to one silicon atom per molecule. However, the temperature necessary to produce pure SiC, the molecule fragments into several reactive species(Susman et.al.,1960) leading to the formation of sub-halides and unsaturated

hydrocarbon. The silicon carbide actually deposits from these. Equilibrium partial pressure calculations have shown the stability of these sub-halides species(Doherty,1976). At 1500 to 1800°C, Pampuch et al.,(1977) observed that for H_2/Cl_2 mole ratio in the gas phase should be about 10, and Si/C mole ratio between 1.0 and 1.3 for $SiCl_4 + CCl_4 + H_2$ system to generate SiC. However, by thermodynamic analysis of MTS system for SiC, Christin et al.,(1979) have shown that the nature of deposit which is formed at equilibrium from CH_3SiCl_3(MTS) -H_2 gas mixture depends on the initial α ratio, $\alpha = [(H_2)_{inlet}/(MTS)_{inlet}]$, at a given temperature and total pressure. The deposit is made of pure SiC for $\alpha_i < \alpha < \alpha_s$ (with $\alpha_i \approx 14$, $\alpha_s \approx 8000$ at 1600 K and 1 atm) and a mixture of SiC and elemental carbon for $\alpha < \alpha_i$. Gas mixtures very rich in hydrogen ($\alpha > \alpha_s$) lead to SiC + Si and even to pure silicon deposit. The change in temperature does not significantly change the α_i value, but strongly modifies the thermodynamic yield. When hydrogen is partly replaced by argon, SiC + C deposits are obtained in a large composition range and finally when gas mixture no longer contains hydrogen (i.e. in the case of MTS-argon mixtures), the deposit is always a mixture of SiC and elemental carbon. In the same manner replacing CH_3SiCl_3 by $(CH_3)_2SiCl_2$(DDS) (i.e., increasing the C/Si ratio) in the gas mixture increases the carbon yield and adding $SiCl_4$ to CH_3SiCl_3(i.e., decreasing C/Si) has a reverse effect. This range of ratio for stoichiometric SiC deposition at 1400°C has been experimentally observed(Cartwright and Popper,1970; or Airey et al.,1974). The range in which the SiC is observed to deposit with interlaminar carbon or silicon layers has been reported by Popper and Mohyuddin(1965). This has been attributed to the excess deposition of either Si or C and their low solubility in silicon carbide(Weiss and Diefendorf,1973; Gulden,1968). The free SiC or C often results in degradation or fiber matrix interface which has prevented prolonged application of composites formed at high temperature.

5.1 Kinetics:

As reported by Schlichting [1980], the deposition of SiC is a linear function of time. The deviation takes place at higher temperature as reported earlier [Revankar et al, 1989]. In case of higher deposition rate, single crystals are formed with lower density material. Many researchers expressed the coating rate in terms of CH_3SiCl_3 partial pressure [Brenner, 1960; Federer, 1977; and Gulden, 1968; Brennfleck,1986]. This shows that the higher the concentration of the reactants, the greater the rate. Knippenberg, (1973) reported the velocity of feed gas relationship with growth rate where growth is square

root of the velocity of gas flow rate. The activation energy is calculated at different systems. Fitzer et al.,(1979) got 209 kJ/mol for cold wall arrangement with CH_3SiCl_3 system which is different than that of other authors which was varied from 68kJ/mol to 410 kJ/mol [Ivanova and Pletyushkin, 1967, Van Kemenade and Stemfoort, 1972], though most agree on linear deposition rate of SiC from different precursors (Motojima et al.,1986;Brennfleck et al.,1984). The value was from 200kJ/mol for $SiCl_4 + CH_4$ system below 1300°C [Nickl and Von Braunmuhl, 1971, 1974]. Deposition rate increased with increase in pressure for different system, which is proved by us in our analysis [Spruiell, 1968; Lavrov et al, 1969].

The kinetic analysis of silane system has been reported by Federer (1977); Gulden(1968); Kaae and Gulden(1971). The morphological studies of deposition in hot wall arrangement of SiC deposits as a function of deposition temperature and degree of supersaturation (H_2/MTS) has been done by Blocher(1974) and Chin et al.,(1977).

5.2 Pyrolytic Carbon Coating/Deposition

Carbon is one of the first vapor deposited materials ever prepared. It has been produced in larger quantities than any other deposited material but the location and nature of the critical steps of deposition reactions are still poorly defined. Secondary dispersive coatings of pyrolytic carbon or graphite is of extreme importance especially in CVD coatings like TiB_2, SiC,Al_2O_3 where deposited material has a very different thermal expansion coefficient than that of the substrate carbon or tungsten. This results in residual stresses at the interface and these stresses considerably weaken the fiber. The stresses can be released by pyrolytic carbon deposition. Diefendorf and Stover(1962) suggested that the deposition of pyrolytic graphite can be done by using methane decomposition.The gas phase reactions create a 'snowstorm' of large flat molecules containing the hexagonal ring structure of graphite. These planes of carbon atoms deposit, overlap and grow on a surface, and also tending to lie flat. One can make random hexagonal orientation so that the structure is not precisely crystalline. This helps in relieving the residual stress in axial direction of the fiber and increasing the tensile strength. Fractured surfaces revealed slight tilts between flakes joined on the same layer, because each layer retraces contours of the surfaces beneath. Various mechanisms have been proposed but it is usually assumed that the decomposition of CH_4 proceeds through the stable intermediates C_2H_6, C_2H_4, C_2H_2 and finally to carbon(Poretr,1955). According to Holliday and Gooderham(1931) the controlling step in the pyrolysis of methane is a bi-molecular

reaction between two methane molecules to yield initially C_2H_2 and H_2 whereas Kassel(1932) and others contended that it is the uni-molecular formation. The CH_2 and H_2 were initial products in a chain of decomposition steps. In any case, it is understood that H_2 strongly retards the reaction and the reaction approximately first order with respect to CH_4 pressure. Kinetic studies show that the activation energy for methane decomposition is 79 kcal/mole(Storch,1932). According to Oxley et al.(1961), at least at low temperature (< 1000°C), the initial reaction step is principally homogeneous, but at some point in the decomposition of chain, the presence of a surface to accept nucleating material becomes a principal factor.

6 Thermodynamic Study

The CVD of SiC on a heated substrate is performed from gas mixture of one of the following compound with hydrogen: methyl trichlorosilane, methyl trichlorosilane + Hydrocarbon, Silane + Hydrocarbon, tetramethyl silane, dimethyl dichlorosilane or silicon halide with hydrocarbon. However, it is difficult to judge which of these precursors are more suitable for our deposition reaction. More than that, only a few of the reported literature tried to establish relationships between the composition of the deposit and the deposition parameters (temperature, pressure, vapor phase initial composition and gas flow rate). The reported thermodynamic calculations for Si-Cl-H-C system can be obtained from the following references: Schlichting, 1980; Doherty, 1976; Naslain et. al., 1983; Buzhdam, et.al, 1979; Harris et. al, 1971; Spruiell, 1970; Gulden, 1968; Chin et. al, 1977; Federer, 1977; Zhao, 1990. However we found a lot of errors and misrepresentations in their results may be due to the small number of species considered in their analysis.

In the present work, the method that is based on the minimization of the total Gibbs free energy of the system. The method gives, for a system of known initial composition studied at a given temperature, pressure, the concentrations of each gaseous or condensed chemical species when equilibrium is established. Thus, the use of this analysis assumes that state close to equilibrium are reached in the CVD apparatus, at least in the vicinity of the substrate. It also implies that all the chemical species able to be present at equilibrium are known.

Program NASAF obtained from NASA was used in determining the equilibrium composition of the gas mixture [Gordon and McBride, 1971]. For calculating the Gibbs

free energy, it requires data for C_p^o, H_T^o, and S_T^o where these are the standard state specific heat enthalpy and entropy respectively to calculate the constants the thermodynamic data from JANAF table [Janaf, 1990] was used. Temperature, pressure of the system, and the concentration of the reactants were the input to the calculations. The criteria of conservation of each element were imposed in calculating the equilibrium composition that had the minimum Gibbs free energy. As I mentioned earlier, this method does not give by its principle, any information on the CVD- mechanism or on the deposition rate. One must remember that in actual use of the results, such a condition rarely exists.

The thermodynamic yield for different condensed and gaseous was obtained as a function of temperature (700< T <1800 K), total pressure (0.001 <P < 2 atm) and initial vapor phase concentration which was defined in terms of hydrogen to silicon containing compound ratio (α) [$10^{-1} < \alpha < 10^5$]. The following species were considered in our calculations for $(CH_3)_4Si + H_2$+ Ar (tetramethyl silane system) reaction.As many as 42 different species were introduced in the calculation. Among them SiC(α), SiC(β), C, Si as condensed species, four liquid species and rest of them in gaseous species. Important among them are Ar, C, $CH_3, CH_4, C_2H, C_2H_2, C_2H_4, C_2H_6, H, H_2$ and SiC.

For $SiH_4 + H_2 + CH_4$ (Silane system) reaction also 42 different species were introduced in the calculations, among which the most important are: Ar, H_2, CH_4, CH_3, H, Si, SiC, SiH, SiH_2, SiH_4, C.

For Si-halide + H_2 + hydrocarbon + Ar (Silicon halide system), 59 different species were introduced, with prominent ones being Ar, C,$CH_3, CH_3Cl, CH_4, C_2H_2, CH_4, C_2H_4$, $C_2H_6, Cl, Cl_2, H, HCl, H_2, SiC, SiCl, SiCl_2, SiCl_3, SiCl_4, SiHCl_3, SiH_2Cl_2, CH_3SiCl_3$.

For methyl trichloro silane System ($CH_3SiCl_3 + H_2$ + Ar) and dimethyldichloro silane system ($(CH_3)_2SiCl_2 + H_2$ + Ar), once again 59 different species were the input data to the calculations. Important species being Ar, C, $CH_3, CH_3Cl, C_2H, C_2H_2, C_2H_4$, $C_2H_6, CH_4, Cl, Cl_2, H, HCl, H_2, SiC, SiCl, SiCl_2, SiCl_3, SiCl_4, SiHCl_3, SiH_2Cl_2, CH_3SiCl_3$. In all the above cases, C, Si, SiC(α) and SiC(β) are the condensed species.

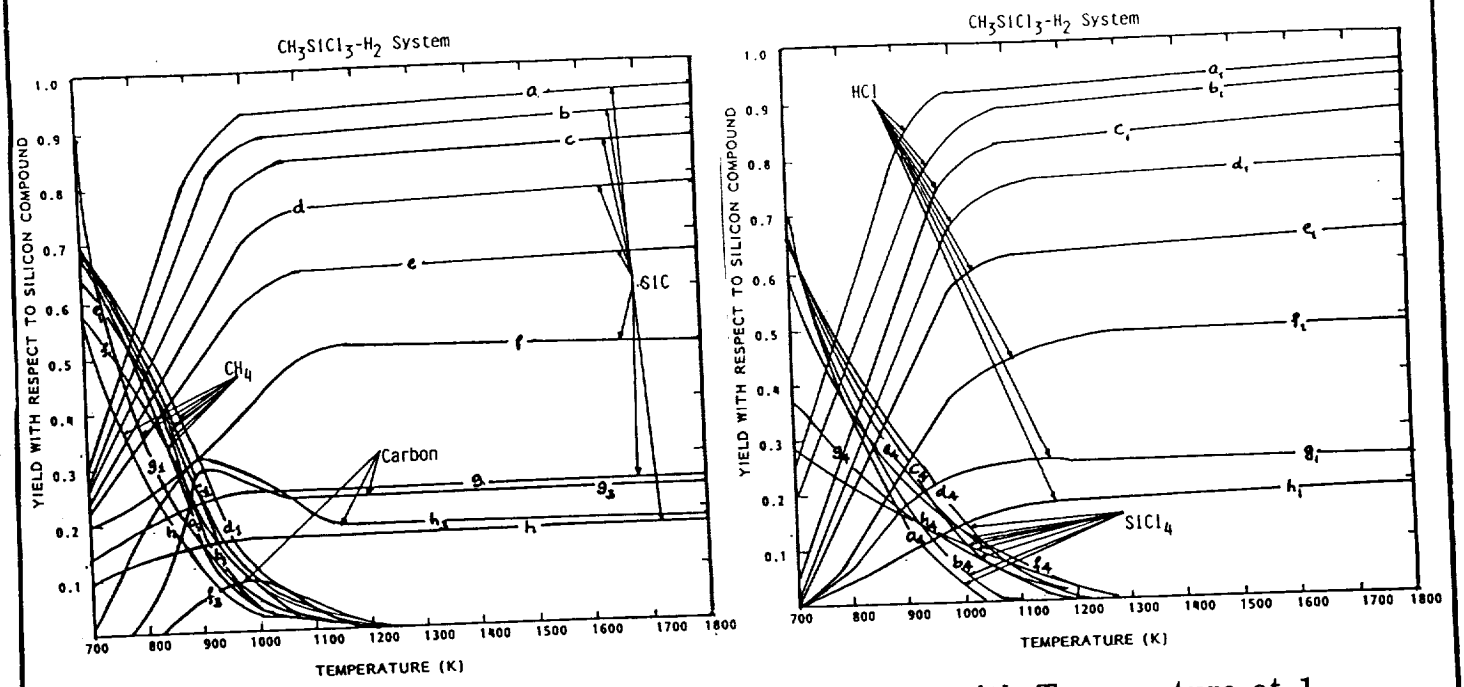

Figure 1: **Product distribution at different α values with Temperature at 1 atm pressure [α is: a=80, b=40, c=20, d=10, e=5, f=2, g=1, h=0.5]**

6.1 Chemical species present, at equilibrium for different systems:

The composition of chemical species at equilibrium depends on both temperature and the initial composition of the reactants at vapor phase at given pressure. The results of the calculations are presented as the yield with respect to original input mole of silicon compound reacted to form at equilibrium chemical species X containing carbon or silicon and belonging to the vapor and solid phases. For example; yield of SiC and CH_4 are defined by

$$\eta_{SiC} = \frac{SiC(moles\ at\ equilibrium)}{[input\ mole\ of\ Si-compound]} \quad and \tag{6}$$

$$\eta_{CH_4} = \frac{|CH_4\ moles\ at\ equilibrium|}{[input\ mole\ of\ C-compound]} \tag{7}$$

In figure 1_a, contains the product distribution of SiC, C, and CH_4. The SiC yield increases linearly with temperature at low temperature region and at high temperature, it remains constant. This yield stabilizes somewhere between 1000-1200 K, above which temperature has negligible effect on SiC yield. As the α ratio increases, the yield of SiC

increases, but characteristic of the curve remains same. At $\alpha = 80$, the thermodynamic yield is almost 95%, which is the optimum condition to get maximum pure SiC yield. Above $\alpha = 95$, the free Si start appearing, which will be discussed later part of this report. Eventhough α= 80, looks like producing more of SiC, there is not much difference in yield between $\alpha = 20$ and $\alpha = 80$. The free carbon start forming in the deposit for $\alpha < 4$. If the α value decreases further, the carbon yield goes up very fast which surpasses the SiC yield.It decreases with temperature after reaching maximum before stabilizing out. The methane is observed to decrease exponentially almost all the cases and reaches the negligible amount between 1000 - 1200 K. Rest of the species are in very low amount (individually less than 0.5%).Among them CH_3Cl and CH_3SiCl_3(g) are prominent at low α values and SiH_4, C_2H_2, and elemental H are prominent at high α values ($\alpha > 20$). Rest of the component almost remain same in all α values and increase almost linearly (most of the cases) with temperature. The figure 1_b shows the product distribution of other important by-products of the reaction [$SiCl_4$ and HCl]. These almost match with the curves of SiC and CH_4 respectively. This shows that CH_3SiCl_3 dissociates immediately above 500°C to $SiCl_4$ and CH_4 which in turn reacts to form SiC. However, at higher temperature $CH_3, C_2H_2, C_2H_4, SiCl_2, SiCl_3$ species are more predominant.

Similar plot at low pressure (0.3 atm) showed identical phenomenon. There is negligible change in yield of SiC except at low temperature. Compare to that of atmospheric pressure. This is shown in figure $2_{a,b}$.

Here also SiC yield increases linearly at low temperature before stabilizing out above 1100K. The lower pressure helps in decreasing the carbon yield. But the appearance of free carbon region does not change much. Again the SiC yield is higher than at atmospheric pressure at low α values ($\alpha < 5$). The major advantage of low pressure operation is the higher SiC yield at low temperature. This can be clearly seen by comparing two different curves (figure 1 and 2). Above α >55, free Si start appearing in the equilibrium mixture. Higher temperature and lower pressure also decreases the free carbon yield. The HCl, $SiCl_4$ distribution are observing same pattern as discussed earlier for atmospheric pressure results. Rest of the species are in negligible amount and does not affect the purity of the SiC deposit. Hence not plotted in this graph.

Higher the pressure (2 atm), the SiC yield curve is more flat at low temperature. That means yield is lower at low temperature (< 1300 K). Compare to atmospheric pressure curve. However, the maximum yield is not much different than those of low

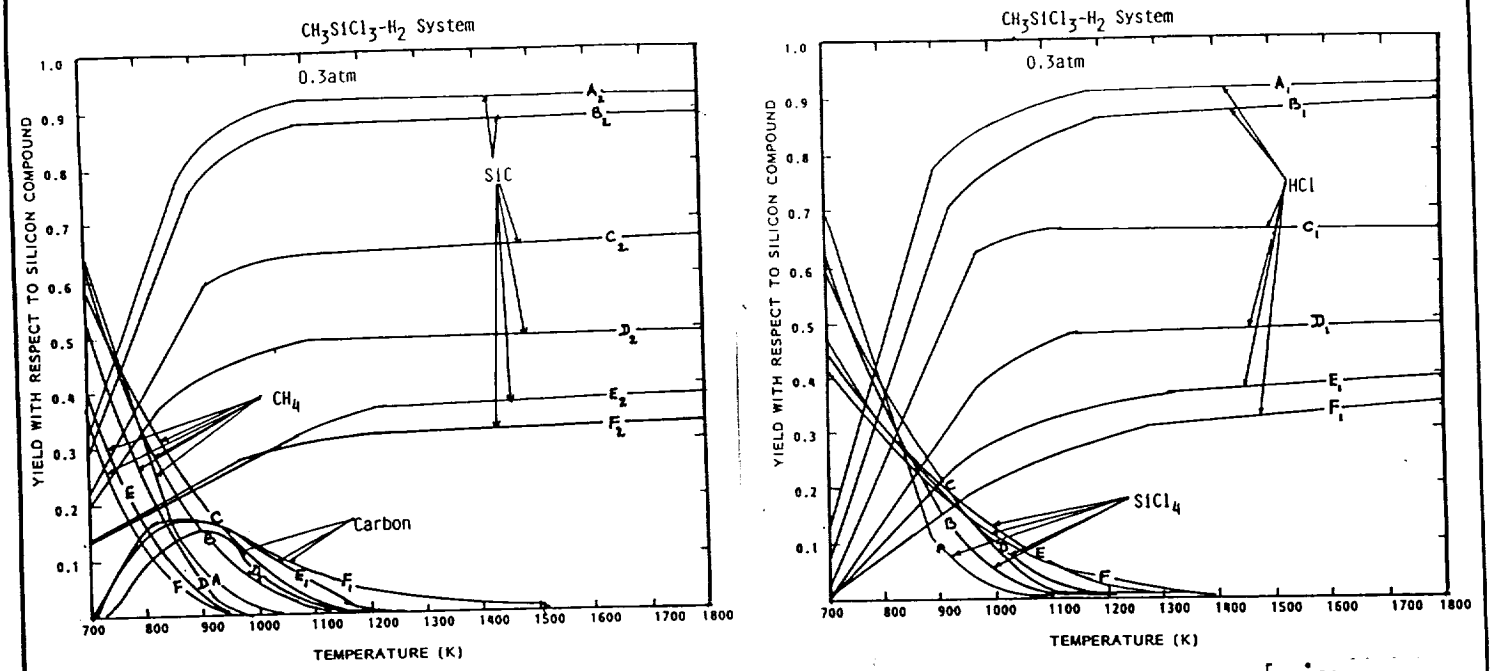

Figure 2: **Product distribution at different α values at 0.3 atm pressure [α is: A=40, B=20, C=5, D=2, E=1, F=0.5]**

pressure curves. This is shown in figure $3_{a,b}$. It is impossible to avoid free carbon in this case except at very high hydrogen input value. ($\alpha > 80$). Free carbon exists in all the temperatures but shows the maximum between 700 - 1100 K, depending on the α ratio. The SiC yield stabilizes between 1100 - 1300 K. The HCl yield curve matches that of SiC curve, shows that Si was generated by reacting silicon halides with hydrogen with very negligible byproduct. The $SiCl_4$ curve shows the slow conversion at low temperature followed by linear decrease with increase in temperature which corresponds to the SiC generated. Figure 4 shows product distribution at 0.7 atm pressure.Curves are showing similar pattern as observed in above cases.The curves exactly lie between 1 atmosphere and 0.3 atmosphere pressure curves.

The effect of temperature on thermodynamic yield of SiC is shown in figure 5.

The carbon and free Si is neglected in the graph. At low temperature, the SiC yield is having linear relationship with α ratio. However, as the temperature increases, the yield initially increases before reaching the stable value. This phenomenon can be clearly seen by comparing the curve at 1200 and 1700 K. There is negligible difference in yield between 1700 K and 1200 K at high α ratio($\alpha > 50$). These results are at atmospheric pressure.

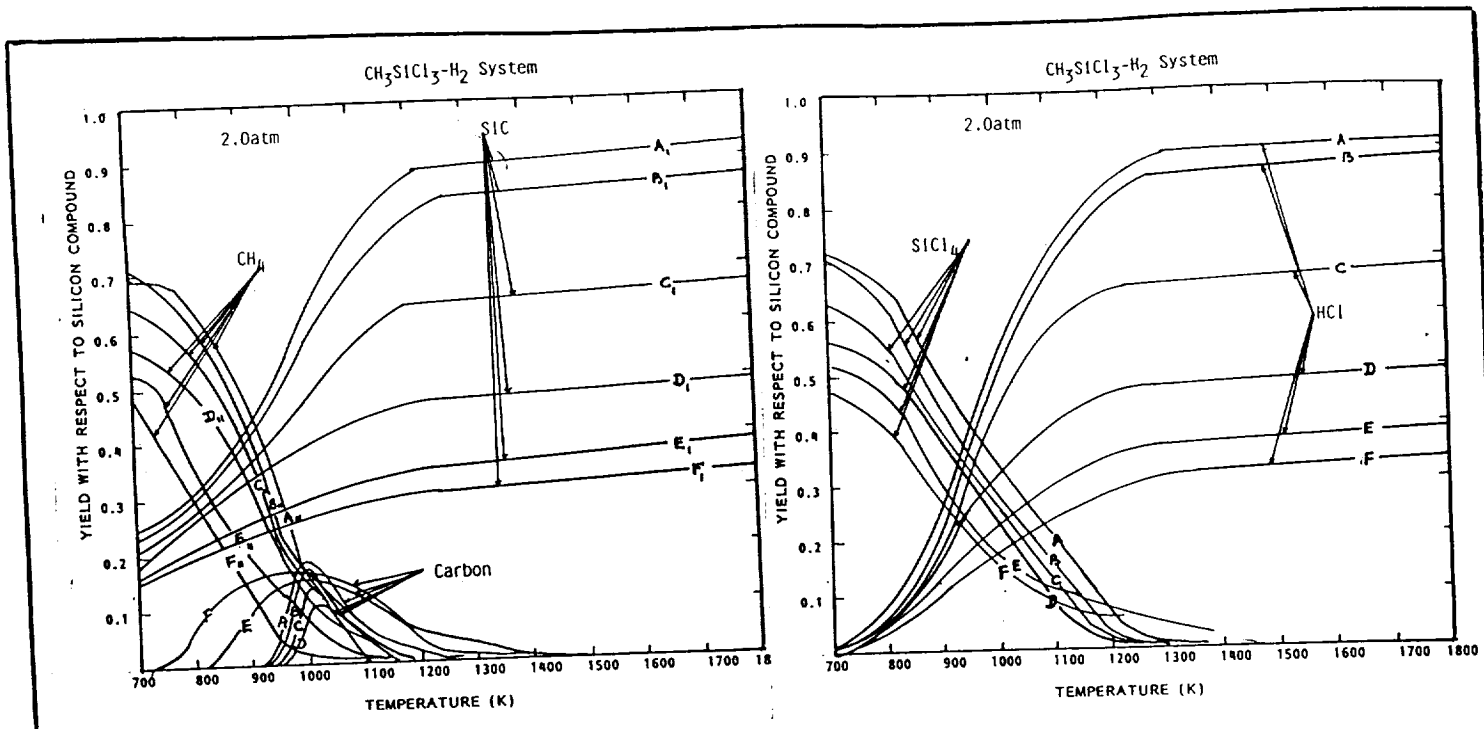

Figure 3: Product distribution profile at different a values at 2 atm pressure [α is: A=40, B=20, C=5, D=2, E=1 and F=0.5]

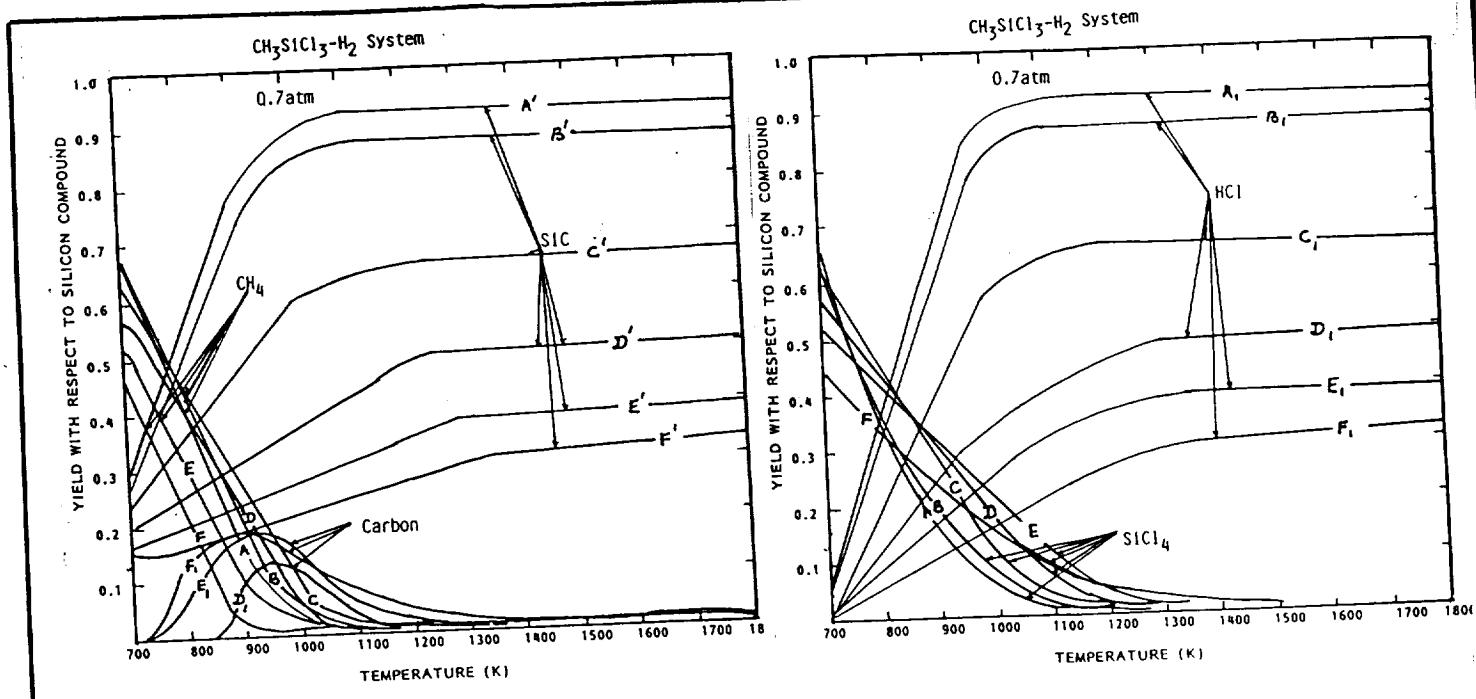

Figure 4: Product distribution profile at different a values at 0.7 atm pressure [a is: A=40, B=20, C=5, D=2, E=1 and F=0.5]

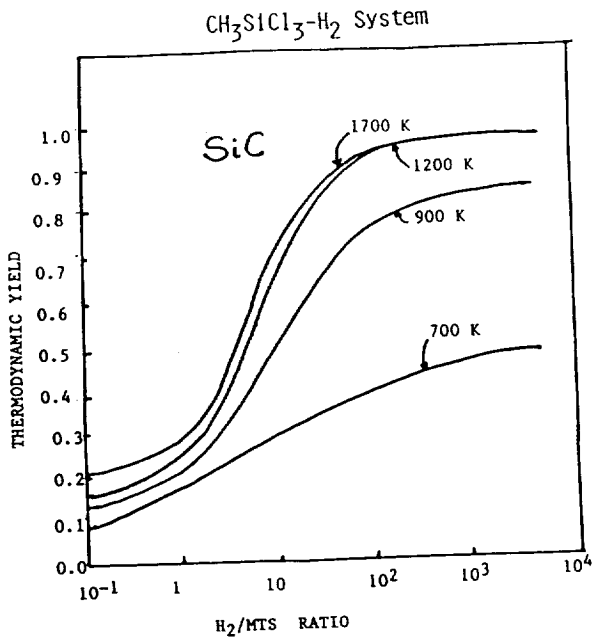

Figure 5: **Product Distribution at Different Temperature, and α ratio at Atmosphere Pressure**

The effect of pressure on thermodynamic yield of methyltrichlorosilane with respect to α ratio is shown in figure $6_{a,b}$. The figure 6_a is at 1100 K. The pressure is having considerable effect at lower ratio of α. At low pressure, (0.03 atm), the SiC yield is considerably higher than at atmospheric pressure at low α ratio. But at high α values, the pressure effect is considerably reduced. Again, higher temperature also reduces the effect of pressure on thermodynamic yield of SiC. This is shown in figure 6_b which is plotted at 1600K for different pressure. At higher temperature, there is decrease in free carbon yield. However, the free Si content does not change much. At 0.003 atm, free silicon appears as low as at $\alpha = 16$. These results showed that higher the temperature of deposition, the pressure of deposition has negligible effect on SiC yield. However, one has to concentrate on crystallinity requirement for the deposit.

These results contradict an earlier published result by various authors [Christin et.al, 1979; Chin et.al, 1977; Chin and Gantzel, 1976; Schlichting, 1980]. Christin et.al [1979] calculated the thermodynamic yield of SiC and reported that it decreases to zero at (α_s) $\alpha_s > 10^4$, which is not true in our case. Where SiC yield remain constant, and steady at higher α ratios. Secondly they reported to observe free carbon at (α_i) α value between 10-15 at or below atmospheric pressure, which is also not true in our case. We observe free C below $\alpha = 4$ only. But at pressure higher than one atmosphere, the free carbon cannot be avoided at low temperatures (T <1500 K). The yield of

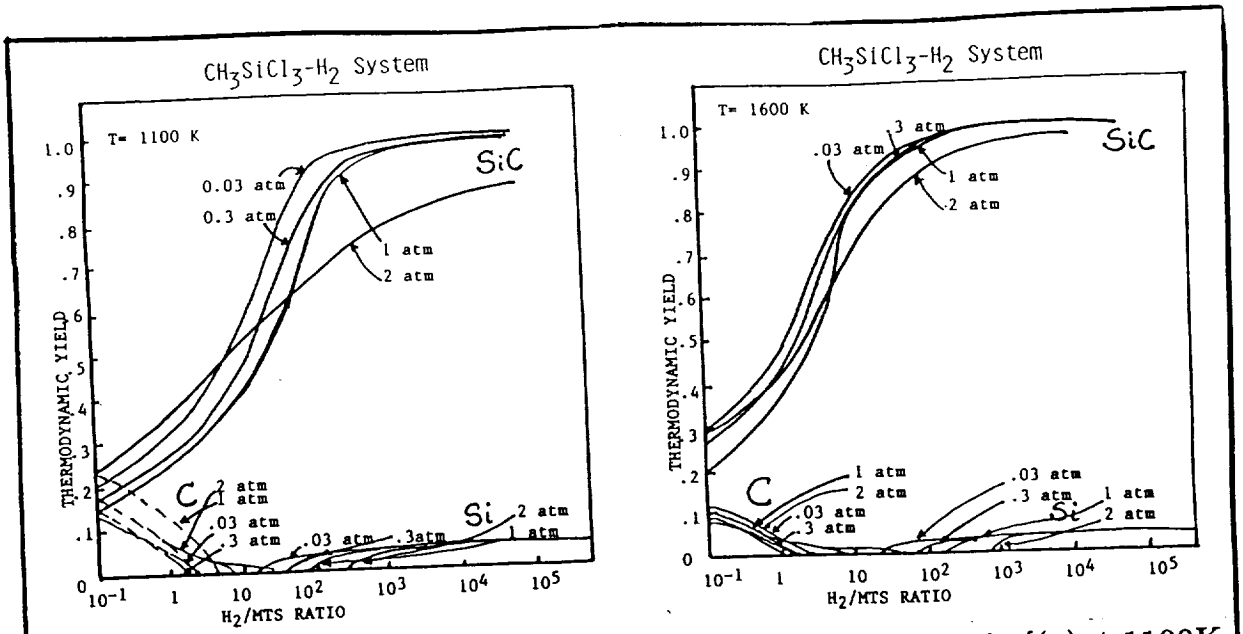

Figure 6: **Product distribution at different pressure and α ratio [(a)at 1100K and (b) at 1600K]**

free Si never exceeds above few percentage in all the cases studied, but it steadily increases with temperature. No free Si is observed, below 600 K, even the α ratio is as high as 10^5. The detailed picture is given in Figure 7 which is a three dimensional graph. This gives an overall conditions to get stoichiometric SiC.Bottom right corner contains free Si+SiC,where as the top left corner always contains free C+SiC. There is the intermediate region where one can get stoichiometric SiC. This is the first time 3-D plot predicted which covers the all general conditions required for SiC deposition for fiber.

The zone in which SiC is deposited is not sharply defined as reported earlier by others [Beutler et al., 1975].Similar results were published by Chin et al.,1977; Chin and Gantzel [1976] and Chin and Ohkawa [1977], but it covers only limited conditions (narrow range of temperature and α ratio and low pressure region). This is only a thermodynamic yield. Further factors such as total gas flow, eddy current in the gas as well as thermal gradient at the gas substrate interface do affect these results. The discrepancies in others results may be basically due to the limited number of species considered in their calculations. For example Christin et.al [1979] have considered only 26 possible chemical species compared to 59 different chemical species considered by us. They did not consider some of the important carbon and carbon halides species. This may be the actual reason for discrepancy in their results.

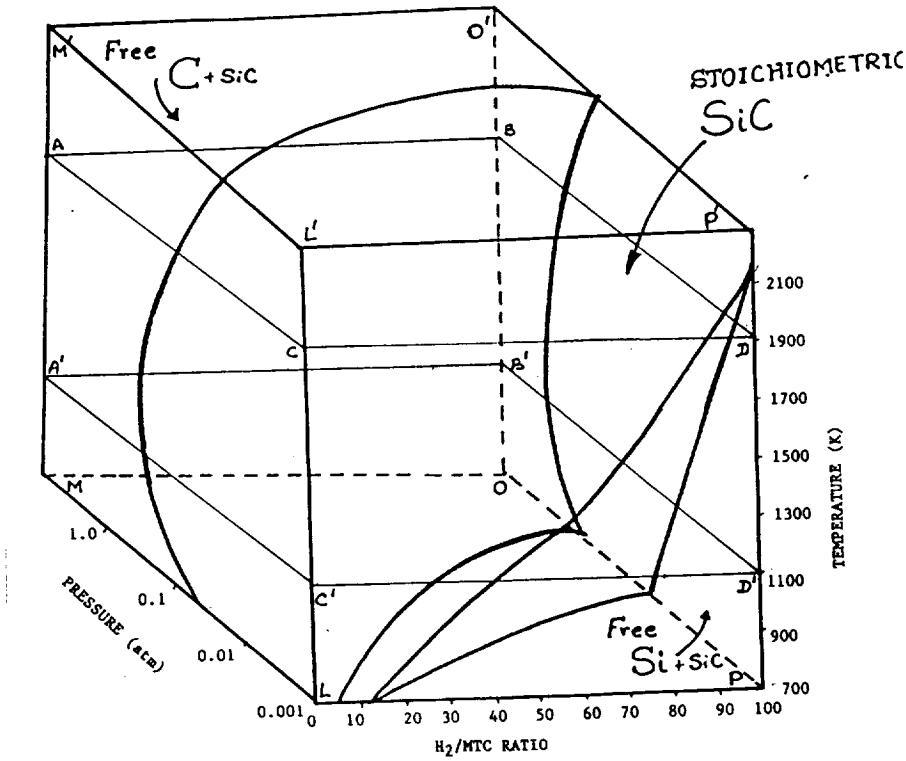

Figure 7: Three dimensional plot to show the variation of temperature, pressure and α ratio on stoichiometry of the product.

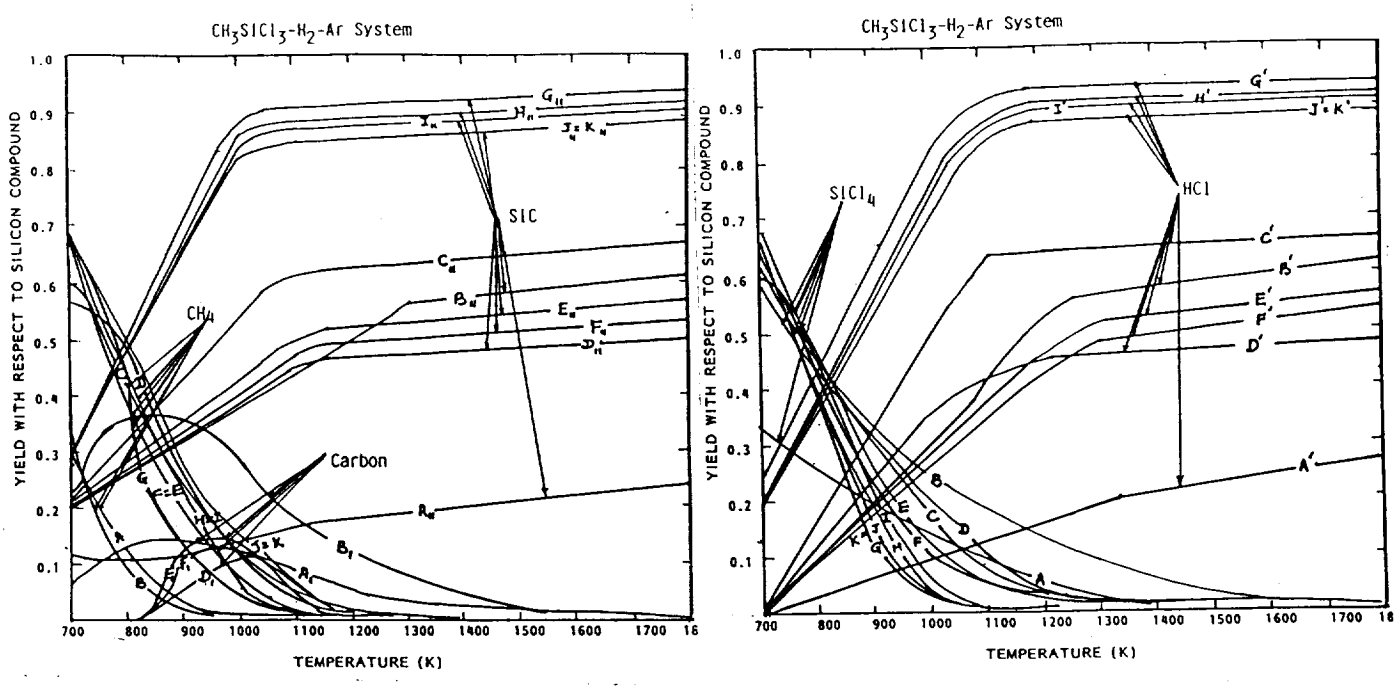

Figure 8: **Effect of addition of argon gas on product distribution. [The ratio CH_3SiCl_3 : H_2 : Ar is: A=1:0:0, B=1:0:5; C=1:5:0; D=1:2:0; E=1:2:1; F=1:2:0.5; G=1:20:40; H=1:20:20; I=1:20:10; J=1:20:1; K=1:20:0]**

Effect of Ar gas on the deposition efficiency is given in figure $8_{a,b}$. The influence of the addition of argon (to the initial vapor phase composition) increases the carbon yield; compare to that with hydrogen. The argon leads to deposit which is mixture of SiC and free carbon. This is due to the existence of multiple silicon chlorides in the vapor phase that remain unreduced due to a lack of hydrogen. At high temperatures (T >1000 K) free carbon concentration in the deposit appear to decrease. Even though, the yield of SiC with argon gas is lower than that with hydrogen, argon gas assist in increasing the yield. Similar predictions were made by Christin et al [1979]. The product distribution profiles of SiC, C, $SiCl_4, CH_4$ and HCl is shown in the figure 8_b. At different α ratio, addition of Ar gas showed reasonable increase in SiC yield. The $SiCl_4$ and HCl curves almost match with that of SiC produced. This result gives an idea that when the experiments were carried out at high α ratio or low pressure and high temperature(T > 1000 K), it is advantageous to add small amount of argon to eliminate the free Si content. Since small amount carbon is not affecting greatly the properties of SiC deposit.

Figure 9 shows the effect of addition of small amount of carbon source in the

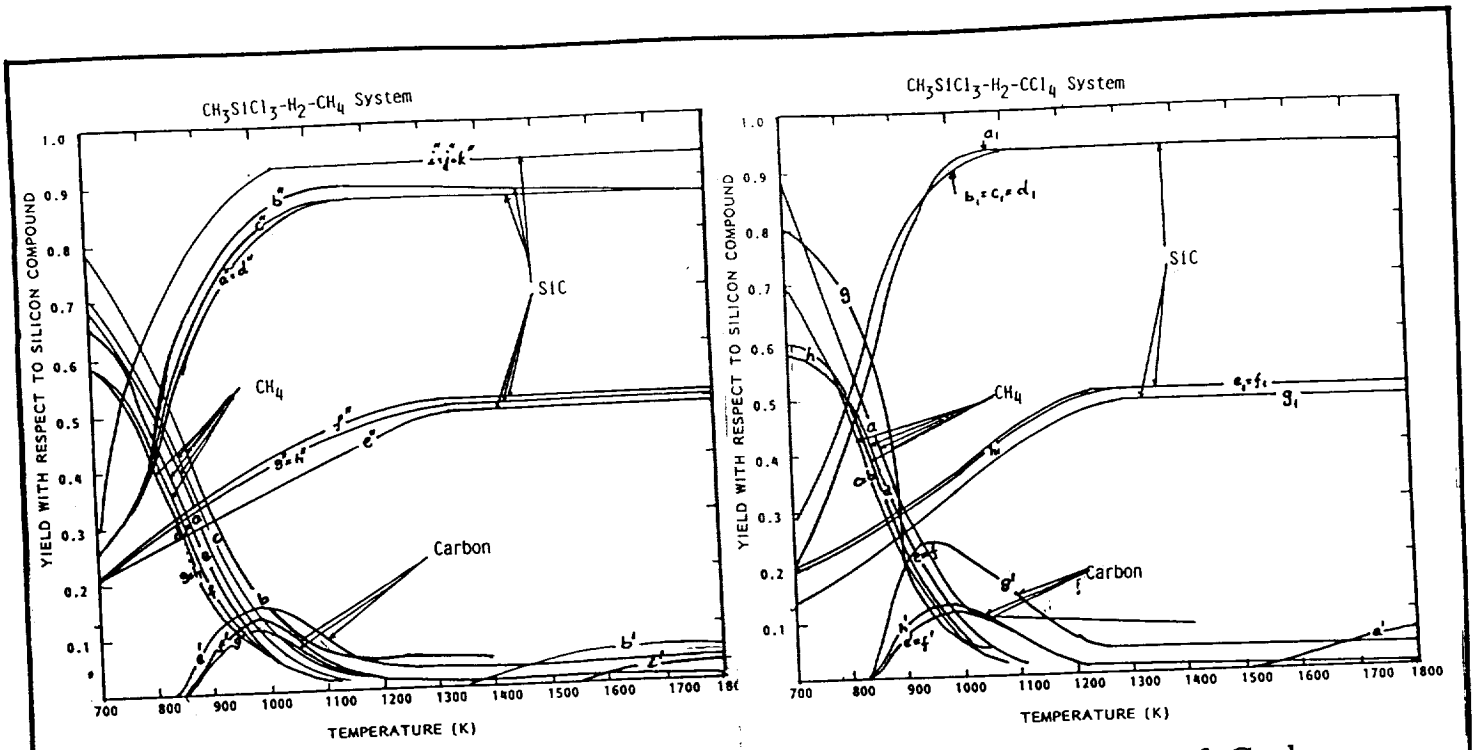

Figure 9: **Product distribution by addition of small amounts of Carbon source in CH_3SiCl_3 system for different α values [ratio $CH_3SiCl_3 : H_2 : CH_4$ is a=1:20:0; b=1:20:0.1; c=1:20:0.01; d=1:20:0.001; e=1:2:0.1; f=1:2:0.01; g=1:2:0.001; h=1:2:0; i=1:50:0.1; j=1:50:0.001; k=1:50:0] and (b) $CH_3SiCl_3 : H_2 : CCl_4$ is.a=1:50:0.1; b=1:50:0.001; c=1:50:0.0; d=1:50:0.01; e=1:2:0.001; g=1:2:0.1; h=1:2:0.01**

system. This result has its own significance because the actual experimental system operates at high flow rate of hydrogen, and free Si cannot be avoided. The following result gives an idea of its effect. Figure 9_a is with the addition of small amount of CH_4 and 9_b is with CCl_4

The CH_4 and CCl_4 were added 0.001, 0.01 and 0.1 mol to one mole of methyltrichlorosilane. The addition of large amount of carbon source, affect the lower temperature yield of SiC. However, at high temperature yield almost remain same. Above 1500 K, free carbon encarporates SiC for all α ratio. Addition of methane gives bigger yield of SiC at low temperature than with CCl_4. But free carbon start forming at higher temperature with $CCl_4 + CH_3SiCl_3 + H_2$ System. On the paper this result does not look to have any importance. But in actual experimentation, to get stoichiometric microcrystalline deposit of SiC between α values 40-80, one has to pass 0.1 to 1%(of CH_3SiCl_3) of extra carbon source.

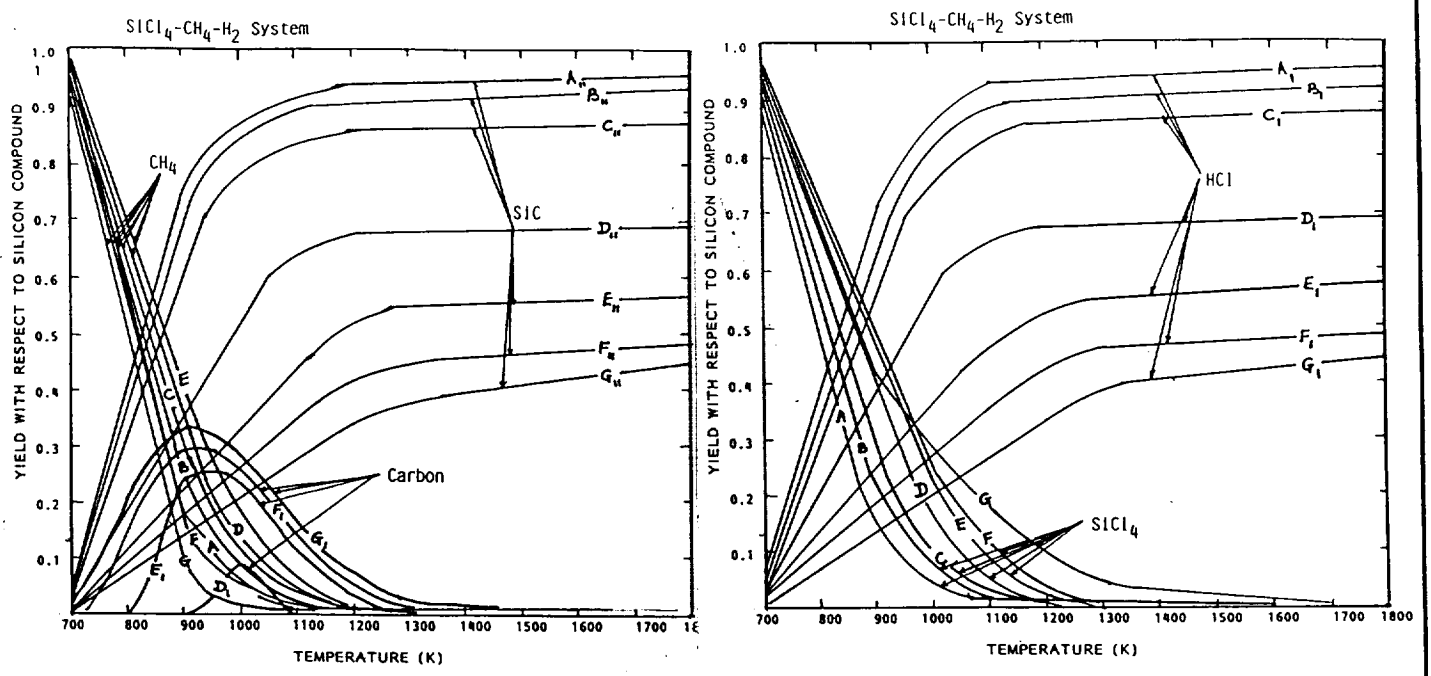

Figure 10: **Product distribution profile for $SiCl_4+H_2+CH_4$ system [$SiCl_4 : CH_4$ ratio is 1:1] α values are A=80, B=40, C=20, D=10,E=5, F=2, G=1.**

Other simple, not so expensive precursor is silicon halide and carbon source with hydrogen system. We decided to test the same parameter including the dependence of Si/C ratio for the deposition of SiC. This has been reviewed by Pampuch [1977] and also reported by Doherty [1976]; Spruiell [1968]; Tukovic and Suznjevic [1970] Yajima and Hirai [1969]. However, detailed thermodynamic data is lacking in their reports. That is why we tried to analyze thermodynamically $SiCl_4$ with CH_4 and CCl_4 in hydrogen atmosphere system. Figure 10_a and 10_b gives the variation of SiC, C, $CH_4, SiCl_4$, HCl yield with temperature at atmospheric pressure for various α ratios [hydrogen to silicon tetrachloride ratio]. The carbon source is CH_4, which is kept 1:1 ratio with $SiCl_4$. At low temperature [T<1300 K], carbon is the predominant species which passes through the maximum around 800-1000 K depending upon the α ratio. The α ratio > 20, the free carbon disappears, and SiC yield increases rapidly. The SiC yield reaches saturation level after around 1200-1300 K, above which the change in yield is negligible, whatever may be the α. The HCl and $SiCl_4$ curves almost match the conversion profile requirement of SiC which suggests that HCl is formed directly from the dissociation silicon chloride. Small amount of Cl_2 and atomic chlorine also found in our analysis which is not considered here. The yield curves almost matched that

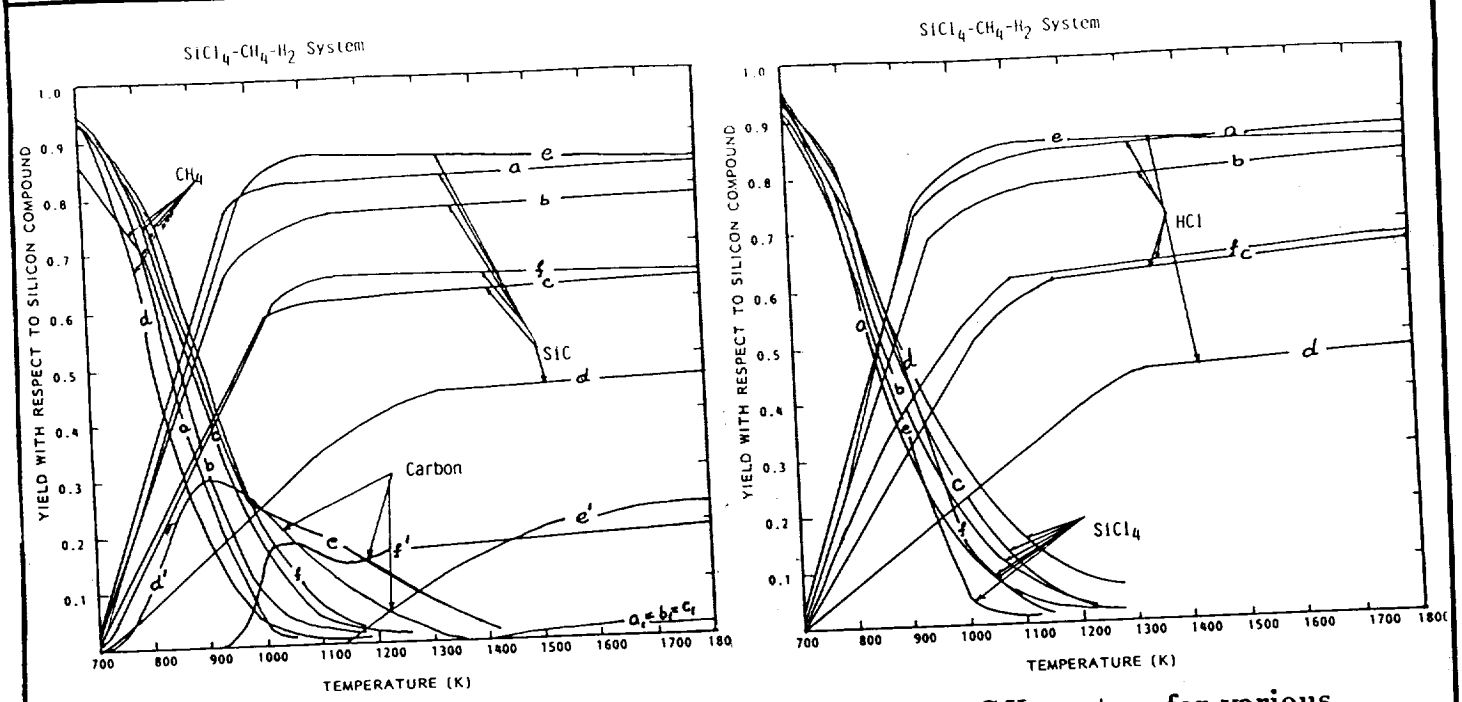

Figure 11: **Product distribution profile for $SiCl_4 + H_2 + CH_4$ system for various amounts of CH_4 [a=1:40:0.9; b=1:20:0.9; c=1:5:0.9; d=1:1:0.9; e=1:20:1.3; f=1:5:1.3]**

of CH_3SiCl_3 system curves at high temperature which suggest that CH_3SiCl_3 system also goes through silicon halide methane reaction system. We changed the ratio of CH_4 to $SiCl_4$ ratio from 0.8 to 1.3, to locate the effect of carbon source on SiC yield and overall species conversion. This is shown in figure 11 and 12. If the carbon to Si ratio is less than one, free Si incorporates the SiC. If it is less than 0.8, the free Si is seen at all conditions. Again at low α ratio (< 20) free carbon start appearing, even though C to Si ratio is less than one. If carbon to Si ratio, greater than 1%, free carbon cannot be avoided in the deposit, but the appearance depends on temperature and α ratio. These results suggest that $SiCl_4 + CH_4 + H_2$ behaves similar to $CH_3SiCl_3 + H_2$ system at high temperature. In actual practice one has to keep carbon to silicon ratio slightly greater than one at α ratio > 20, to get the stoichiometric deposit. We changed the carbon source to CCl_4 and varied the mole ratio of carbon to silicon source from 0.8 to 1.3. The product distribution profiles are slightly different from that from CH_4. The free carbon is larger than that from CH_4 at all conditions. This is shown in figure 13 and 14. At low temperature (T$<$ 900 K) there is absolutely no SiC formation at all α values where as carbon values increases linearly at low α values and high carbon to Si ratio. At high

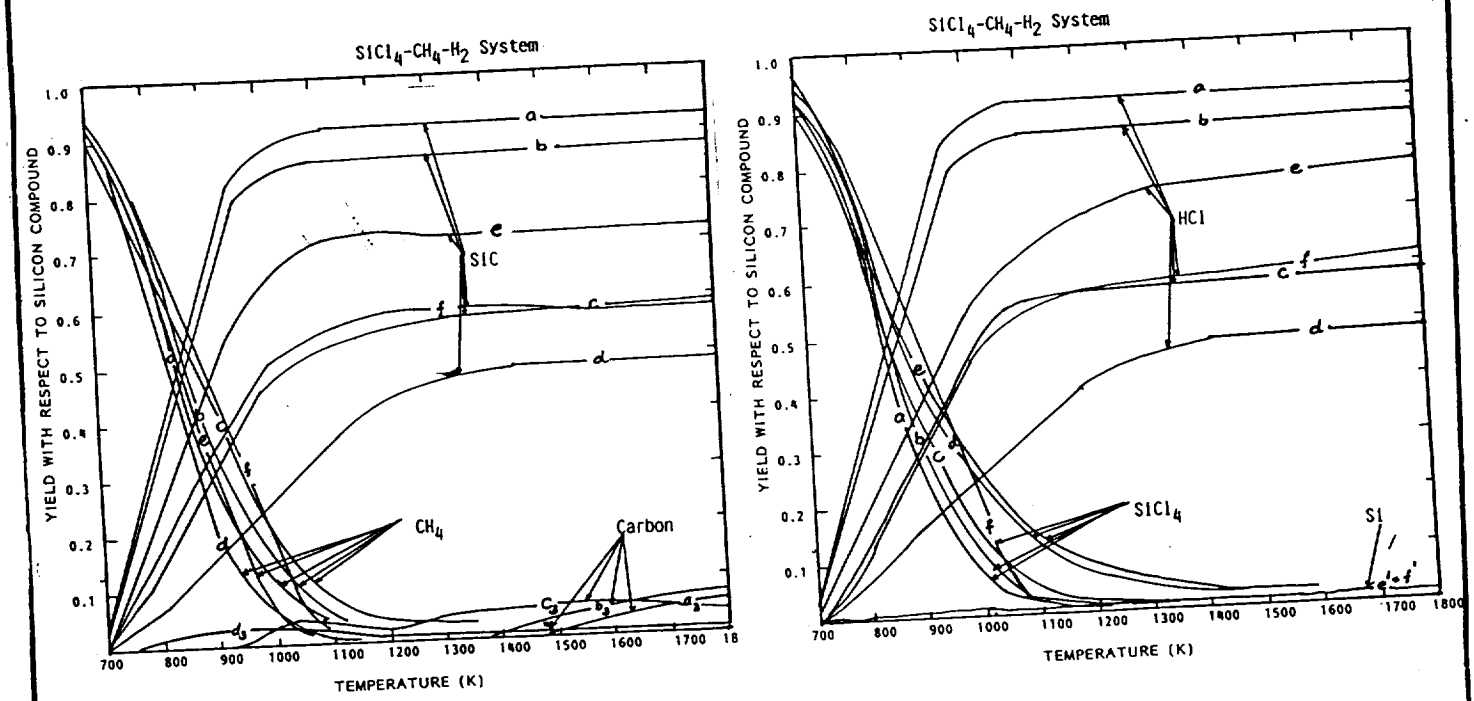

Figure 12: **Product distribution profile for $SiCl_4 + H_2 + CH_4$ system for various amount of CH_4 [a=1:40:1.1; b=1:20:1.1; c=1:5:1.1; d=1:1:1.1; e=1:20:0.8; f=1:5:0.8]**

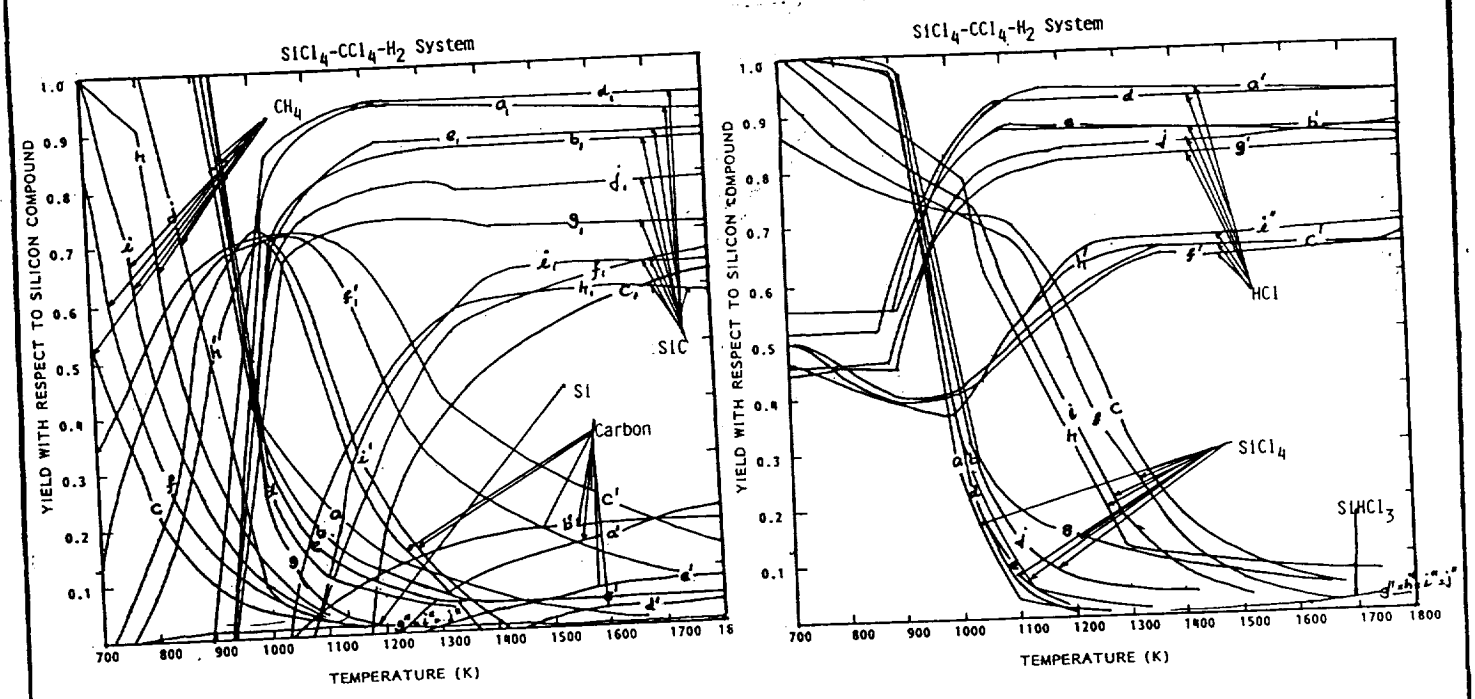

Figure 13: **Product distribution profile for $SiCl_4+H_2+CCl_4$ system for various amount of CCl_4 [a=1:40:1.3; b=1:20:1.3; c=1:5:1.3; d=1:40:1.1;e=1:20:1.1; f=1:5:1.1; g=1:20:0.8; h=1:5:0.8; i=1:5:0.9; j=1:20:0.9]**

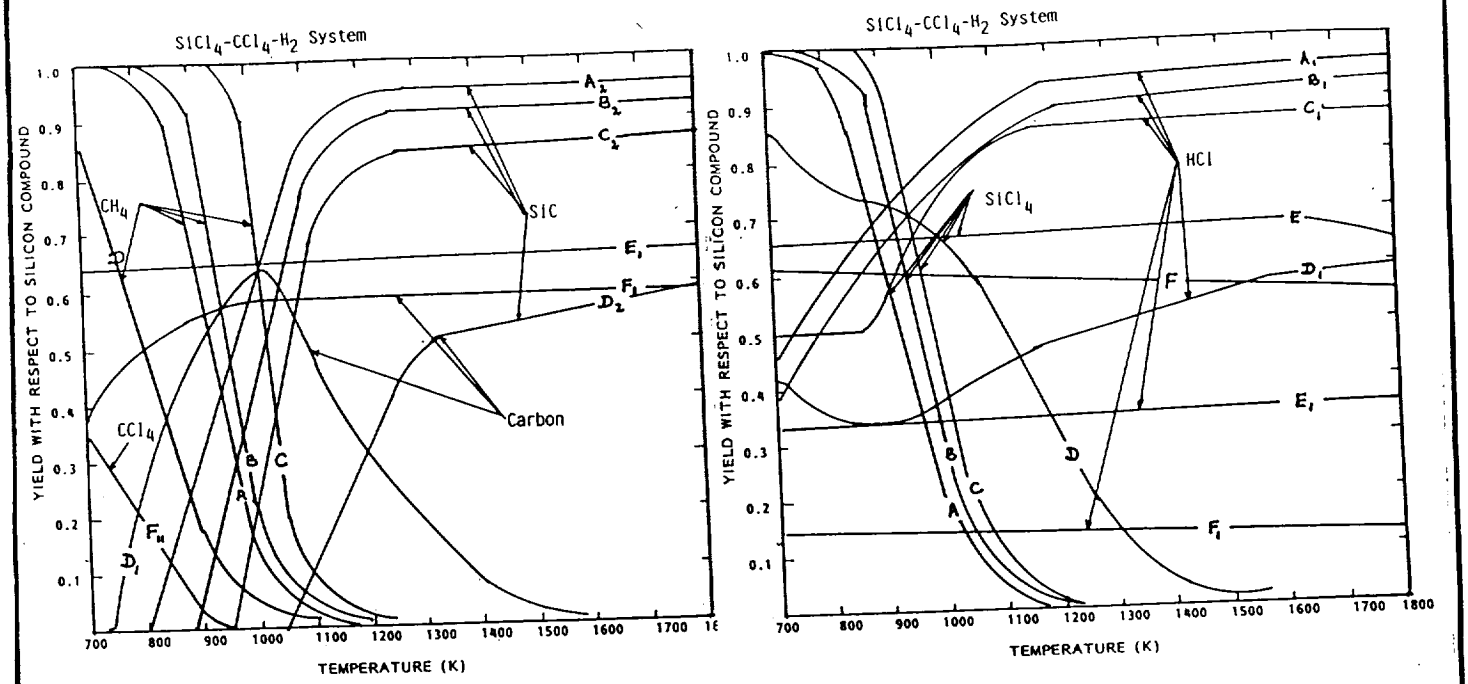

Figure 14: **Product distribution profile for $SiCl_4+H_2+CCl_4$ system by keeping $SiCl_4$ to CCl_4 at1:1 [α value: A=80, B=40, C=20, D=5, E=2, F=1]**

temperature SiC yield is not much different than that of CH_4 + $SiCl_4$ or CH_3SiCl_3 system. By decreasing the α values and lowering the C to Si ratio, the SiC formation (appearance) can be shifted to higher temperature. Again free Si cannot be avoided, if the operation is below one, carbon to silicon ratio. This gives an fair idea for an operational conditions. In actual experimentation CCl_4 system is more advantageous than CH_4 because CCl_4 system can effectively eliminate free Si at high α values and gas phase nucleation as in the case of CH_4 of carbon can be avoided. The $SiCl_4$ and HCl curves show different pattern which is not observed in other results. We can see two set of curves. Below 900 to 1100 K, the $SiCl_4$ and HCl curve becomes flat and above this temperature, there is sharp decrease and increase in these values respectively. Another prominent species here is $SiHCl_3$ which appears at silicon to carbon ratio less than one. These curves gives an idea of actual reaction. At low temperature CCl_4 dissociates to give CH_4 and HCl followed by reaction with $SiCl_4$. That is why one can see very high HCl value at initial stage. Again, the large amount of HCl also hinders(controls) the rate by shifting the equilibrium.

Effect of pressure on the yields of SiC, C,CH_4, Si, HCl and $SiCl_4$ is shown in figure $15_{a,b}$.

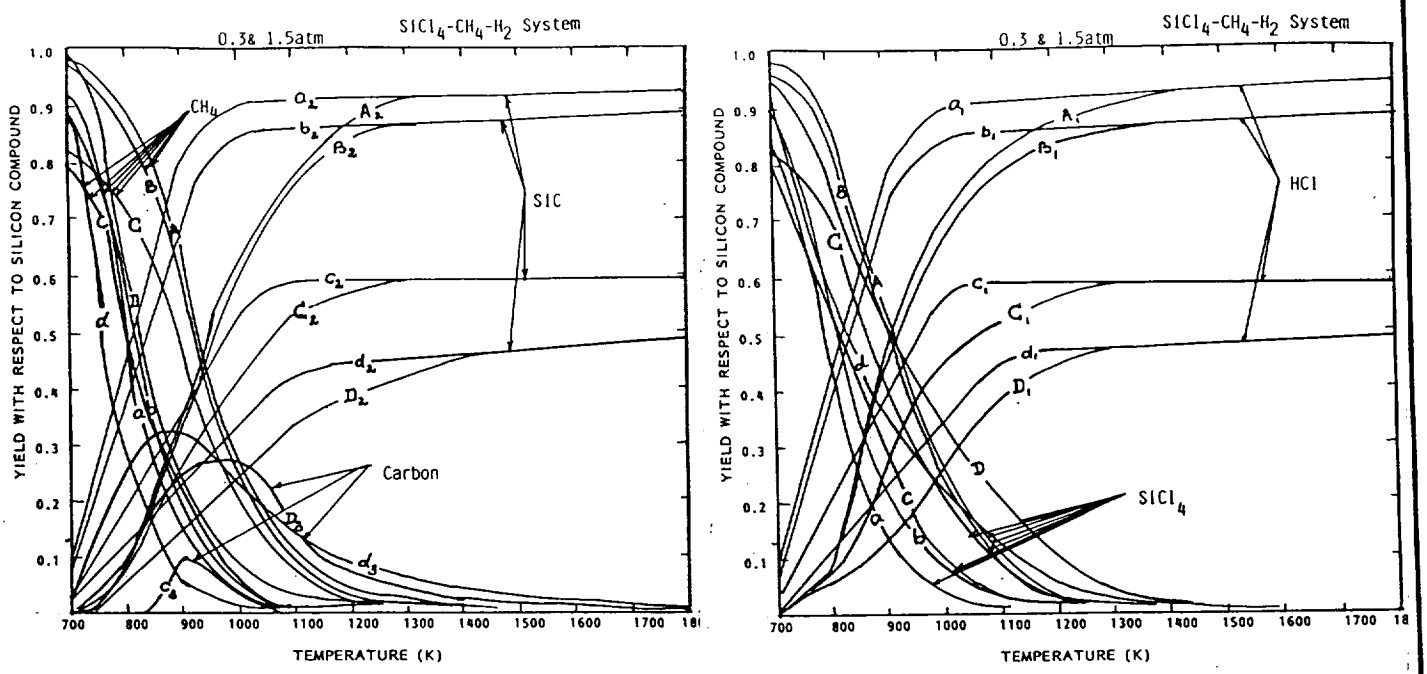

Figure 15: **Product distribution profile for $SiCl_4+H_2+CH_4$ system at different pressure [$SiCl_4 : CH_4$ is 1:1 and a is A=40, B=20, C=5, D=1]**

The values were plotted for 0.3 atm and 1.5 atm for different values of α, keeping carbon to silicon ratio one. Here CH_4 is the carbon source. This also behaves similar to that of CH_3SiCl_3 system except the yields are low at low temperatures. As the pressure decreases, the SiC yield increases at low temperature for $SiCl_4$: CH_4 ratio 1 but at high temperature (T> 1200 K), effect of pressure is negligible. Again, at low pressure, the free carbon yield increases and it is difficult to avoid free carbon at low α values.Hence greater than 20 α value is more suitable for operation. The CH_4 and HCl curves matched that of $SiCl_4$ conversion patterns with small variation.

Figure 16 shows the calculated equilibrium molar fraction of different species at different temperature for α ratio of 20.

This is a typical example of distribution of equilibrium species. Even though similar result was published earlier by Doherty, (1976); Lewis et. al, 1969, Harris et.al (1971) and others, they never considered these many number of species in their calculation. That created some discrepancies in their result. This figure summarizes all those species. It can be seen, that at low temperatures (T< 1000 K) CH_4, $SiCl_4$, $SiHCl_3$ are the most stable compounds. However, with increasing temperatures, their equilibrium composition decreases. At such temperature chlorine combines with

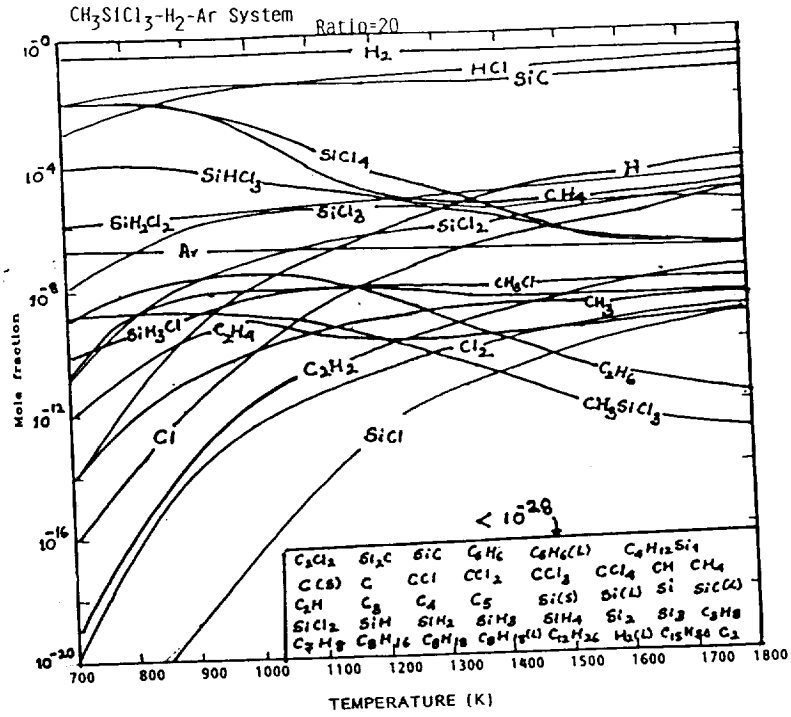

Figure 16: **Typical equilibrium chemical species distribution [Example here is CH_3SiCl_3 with $\alpha = 20$ and 1 atm pressure]**

hydrogen to form HCl and Si combines with carbon to form SiC. At high temperature (T wire> 1300 K) C_2H_2, $SiCl_2$, $SiCl_4$, H, Cl_2 are more stable and become somewhat predominant Si and C containing species in the gas phase. At these temperatures the chlorine is present in basically in HCl and partially divided between Cl_2 and atomic Cl. Rest of the species are shown in figure. Remainder are in very small amount ($< 10^{-28}$ mole fraction individually). They are shown in the bottom of the graph.

Finally we decided to compare different silicon precursor thermodynamically at different (0.3 atm, 1 atm) pressure at two different α values ($\alpha = 5$, $\alpha = 20$) given the figure 17.

These precursors are most commonly used for SiC deposit. $(CH_3)_4Si$, CH_3SiCl_3 , $(CH_3)_2SiCl_2$, SiH_4 + hydrocarbon and $SiCl_4$ + hydrocarbon. 42 different species were considered for $(CH_3)_4Si$, $SiH_4 + CH_4$ analysis and 59 different species were considered for rest of the precursor analysis. The order of maximum yield for SiC in presence of H_2 is $SiH_4 + CH_4 > SiCl_4 + CH_4 = CH_3SiCl_3 > (CH_3)_2SiCl_2 > (CH_3)_4Si$ for $\alpha >$ 20 and below this value the order is $SiH_4 + CH_4 > CH_3SiCl_3 > SiCl_4 + CH_4 > (CH_3)_2SiCl_2 > (CH_3)_4Si$. Last two precursor always generate free carbon except at very high α values ($\alpha > 80$). Free Si cannot be avoided with SiH_4 system at carbon

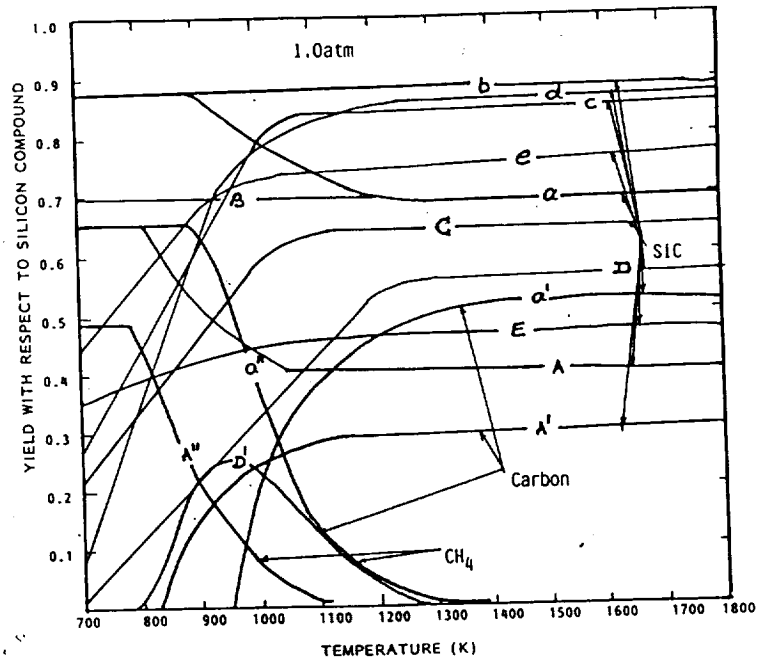

Figure 17: **Comparison of various silicon precursors** [**a**=$(CH3)_4Si$; **b**=SiH_4:CH_4 **c**=CH_3SiCl_3 , **d**=$SiCl_4$: CH_4; **e**=$(CH_3)_2SiCl_2$; α=**20 for capitals** α=**5 at 1 atmospheric press.**]

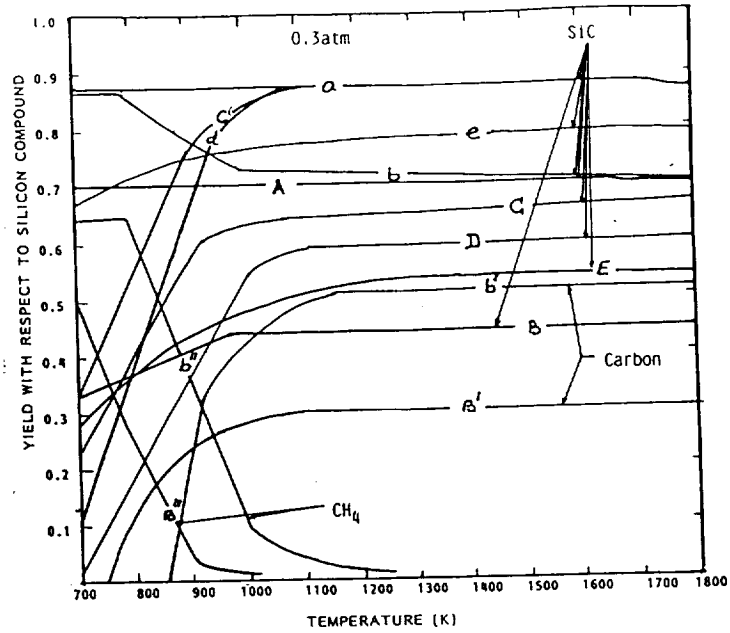

Figure 18: **Comparison of various silicon precursors at 0.3 atm pressure** [a=SiH_4 + CH_4, b=$(CH_3)_4Si$, c=CH_3SiCl_3 , d=$SiCl_4$+ CH_4 and e=$(CH_3)_2SiCl_2$ **with** α**=20. For capitals** α**=5]**

to silicon ratio one or below, at low temperature. At lower pressure (0.3 atm), it shows the similar patterns.This is shown in figure 18.

However, above 1800 K, there is no difference yield with SiH_4, $SiCl_4$ and CH_3SiCl_3 systems for α values greater than 20. The $(CH_3)_2SiCl_2$ produced more SiC than $(CH_3)_4Si$. At lower α ($\alpha = 5$), the order of activity is different. The order is: SiH_4 + CH_4 > CH_3SiCl_3 > $SiCl_4$ + CH_4 > $(CH_3)_2SiCl_2$ > $(CH_3)_4Si$. Again free Si was always present with SiH_4 system for carbon to silicon ratio one. Even though, SiH_4 system looks interesting and promising, it is not recommended as one of the system because of its

(1) high volatility and poisonous nature

(2) very difficult to handle

(3) free silicon content in the deposit

(4) difficult to control deposition rate

(5) Difficult to control morphology of the deposit

(6) price of the materials/equipments

Hence, we decided to pursue $SiCl_4$ + hydrocarbon and CH_3SiCl_3 systems. Even

though we did some preliminary runs with other precursors, they were not successful in implementing for fiber deposition process.

7 Theoretical Consideration in Reactor Design

7.1 Modeling and Analysis of CVD Reactors

A CVD system is simply a chemical reactor. As such, flow rates and flow patterns of reactant vapors along with substrate temperature must be carefully controlled if uniform film layers are to be obtained. Certainly, the reactor design plays a decisive role on the properties of the materials deposited. The control and/or elimination of recirculating gas patterns over the substrate as well as the improvement in the species transport to the reaction surface are essential goals pursued when designing the chambers to carry out CVD processes.

In simple geometries, as the horizontal planar channel reactor, one way to attain an homogeneous distribution of the reactant concentration gradients has been to tilt the susceptor in order to obtain a constant mass transfer driving force. In vertical reactors used in the microelectronic industry the substrate is commonly rotated to expose the substrate wafer uniformly to the reacting gas stream. In more complex configurations, or applications other than microelectronics, the alternatives are not so apparent.

In contrast to catalytic reactions, in which natural convection effects can be sometimes neglected, buoyancy-induced flows play a major role in determining the flow, temperature and concentration fields in CVD reactors. In cold wall reactors in particular, the main driving force for natural convection is the large temperature gradients existing between the substrate and the reactor wall.

The intensity of natural convection effects can be quantified through a dimensionless number: the Grashof number. The magnitude of this number will depend on several operating variables, i.e. $Gr = Gr(p,T,M,\mu,g,r_2)$. However, among these variables is perhaps the pressure in the reactor chamber the one that can be varied over several orders of magnitude. Thus, only the effect of pressure will be discussed in detail in this section. We can see in Table 1 how the pressure affects the magnitude of the Grashof number.

Table 1: Effect of Pressure on the Grashof number

Pressure,kPa	1	10	100
Grashof$\times 10^{-3}$	0.030	3.04	304

7.2 Vertical Configuration

In vertical configurations free convection manifested itself in the form of a large "cell" filling the entire reactor length (cf. Figure 19(a)). We can see in Figure 19 that at low pressures (1 kPa), the contribution of forced and natural convection affect equally the flow field in the reactor. Similarly, the effect of natural convection on the temperature field is negligible and, with exception of the end effects, the temperature remains constant all through the reactor. The concentration field is characterized by a thin boundary layer close to the fiber while away from the fiber a linear profile can be observed. As pressure is increased natural convection begins to overshadow forced convection, the temperature field is distorted by the recirculating flows (cf. Figure 19(b)) and a "fingering/mixing" effect becomes significant in the concentration field.

Different modes of transport from and to the fiber exist, i.e. conduction, radiation and interface convective transfer, for energy; and interface transfer for mass. The transport at the interfacial boundary layer is, however, the most affected by natural convection phenomena. The interaction between natural convection and mass diffusion can be accounted for from a dimensionless number: the Nusselt number, defined as:

$$Nu_h(z) = \frac{r-1[\frac{\partial T}{\partial r}]_{r_1,z}}{< T > -T(r_1,z)} \quad and, \quad Nu_m(z) = \frac{r_1[\frac{\partial x}{\partial r}]_{r_1,z}}{< x > -x(r_1,z)} \tag{8}$$

The heat Nusselt number can reach its minimum value for the situation of completely developed flow and temperature fields. In Table 2 we can see that the effect of natural convection on the thermal boundary layer is negligible. On the other hand, it can be seen how the interfacial mass transfer is enhanced drastically as a result of natural convection phenomena.

7.3 Horizontal Configuration

Unlike in the case of vertically arranged reactors, in horizontal configurations the model equations cannot be reduced to two-dimensional formulations. In order to make the

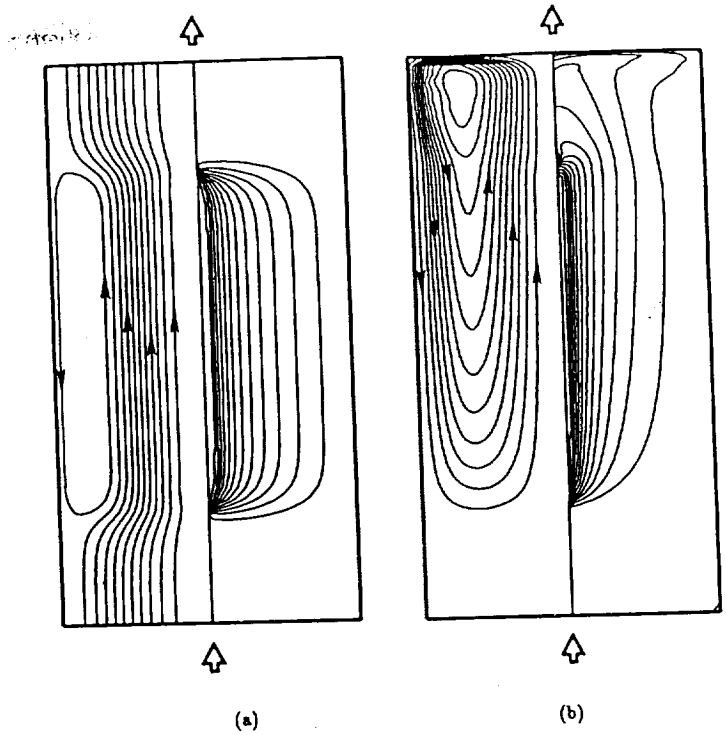

Figure 19: **Streamlines (left) and temperature fields (right) for (a) low (1 kPa) and (b) high (100 kPa) pressures.**

Table 2: **Average Nusselt Number for Different Pressures.**

Pressure,kPa	1	10	100
$< Nu_h >$	0.216	0.216	0.233
$< Nu_m >$	0.372	0.436	0.539

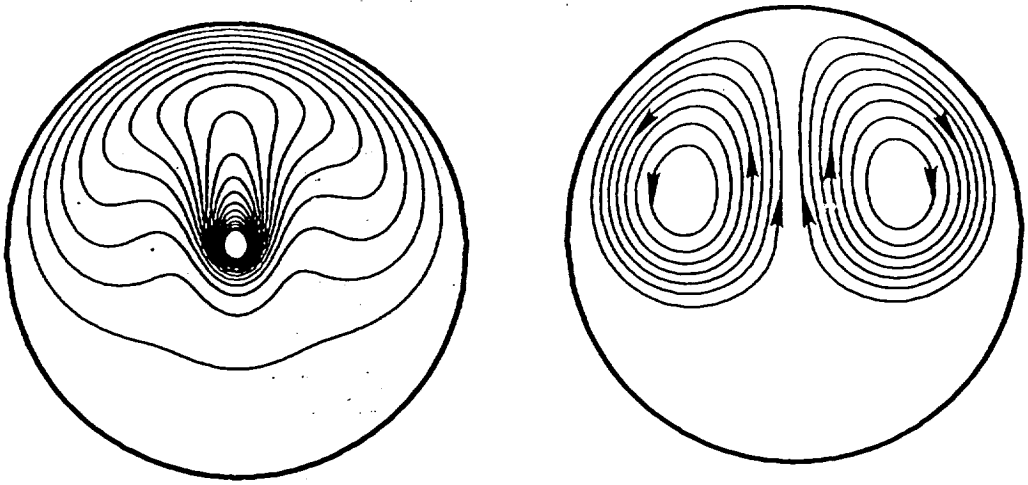

Figure 20: **Streamlines (right) and temperature field (left) for a horizontal reactor.**

problem more tractable the flow and temperature field are considered completely developed. These assumptions will overlook two major phenomena: the development of longitudinal "rolls" and the transversal "rolls" present in the entrance region of these reactors. As these phenomena will be confined to the entrance region (Chiu and Rosenberger, 1987; Scholtz, 1991) the results reported next will be considered as a qualitative picture for long reactors.

The results presented in Figure 20, show that both temperature and concentration boundary layers lose their angular symmetry as a result of the longitudinal rolls.

7.4 Comparison with Experimental Results

At this stage our laboratory does not posses an experimental setup that permits to run flow visualization experiments. However, if certain reactions are carried out under non-optimum conditions homogeneous reactions can be observed in a large extent and deposition on the reactor walls results. Using those experiments the authors believe that it is possible to obtain a preliminary estimation of the flow fields. These results are reported in figure 21. It can be seen clearly that in the vertical reactor the deposition distributes evenly around the reactor wall; however, the deposition at the top of the reactor differs significantly from that observed on the bottom section. This would suggest that the products of homogeneous reactions are being swept upwards through

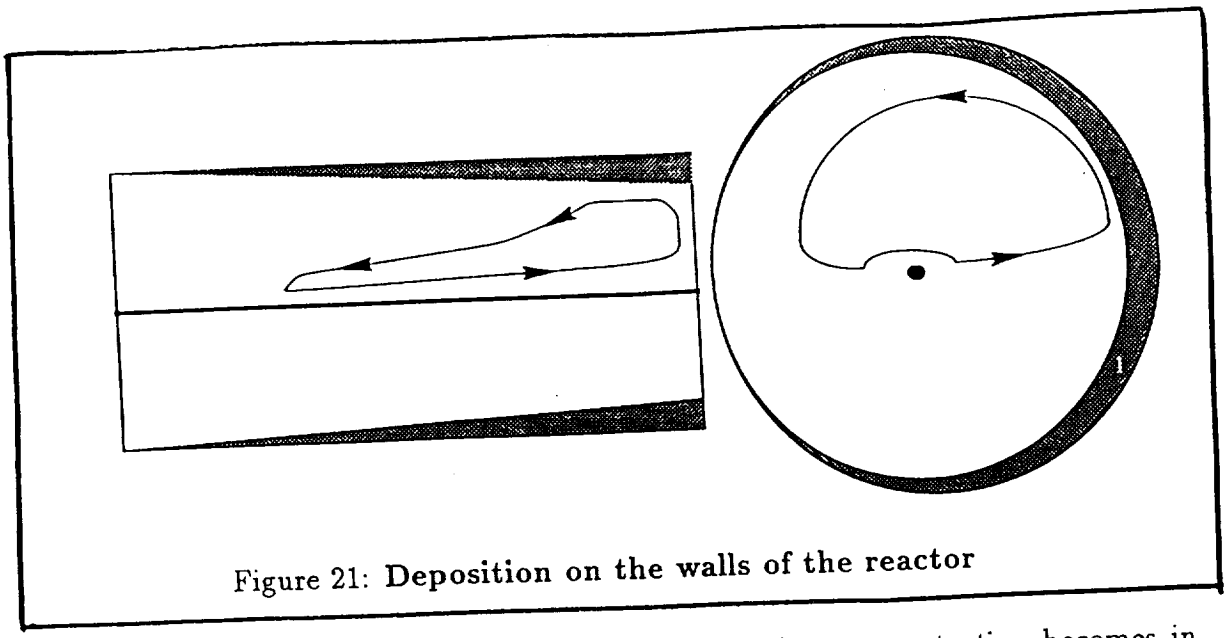

Figure 21: **Deposition on the walls of the reactor**

the center of the reactor and the gas with higher product concentration becomes in contact with the wall at the top of the reactor. Similarly the results for the horizontal arrangement suggest that the products are being swept through the center of the reactor and impinging on the top part of the reactor wall; the lower half of the reactor almost does not get in contact with high product concentration gas. Besides, although the gas remain stationary at the bottom of the reactor, the low temperature precludes any homogeneous reaction to occur. These results, however, should only serve as an indication and further conclusions can only be drawn from additional experimental observations.

7.5 Thermal Stress in the Deposition Process

To conclude this discussion it is interesting to note a problem detected for some fibers. The fibers and their coating are being exposed to three different stresses: thermal expansion mismatch, thermal stresses and blistering. These three stresses induce microcracks in the coating with the subsequent weakening of the final product. The question to answer is which one of these stresses crosses the resistance threshold for the cracks in the coating to appear. For most situations, a slow cooling process after reaction is completed will suppress thermal stresses. On the other hand blistering most likely will appear when coating and core interact to form a tertiary intermediate layer. The solution to mismatching thermal expansion coefficients has been to deposit an intermediate pyrolytic carbon layer; this "spongy" layer acts as a "cushion" and "absorbs" stresses

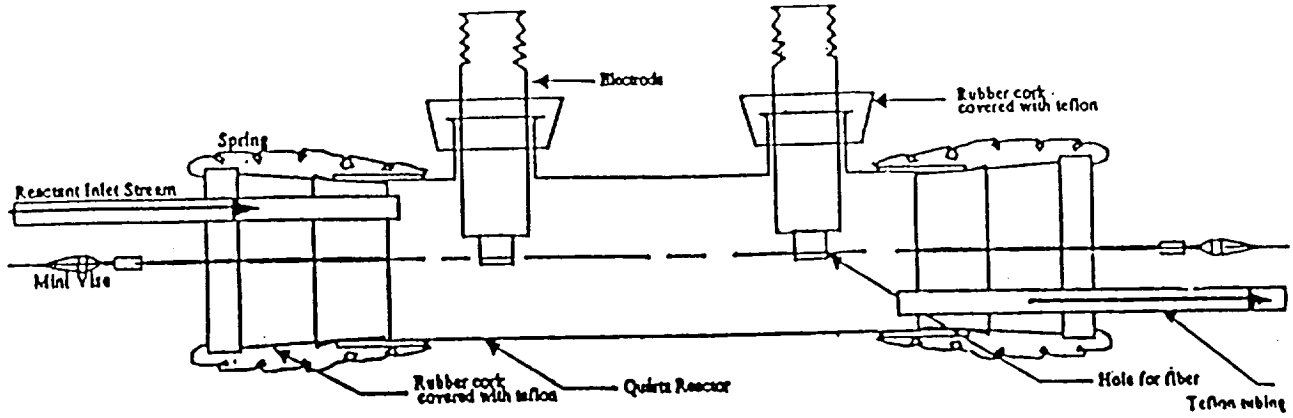

Figure 22: CVD System Lay-out

on the coating. However, the pyrolytic carbon layer may have a deleterious effect on the fiber strength.

This brings us to a second problem involved in the modelling analysis of this process: the fiber evolution. The results obtained for the reactor chamber suggest that a model can be formulated to study the fiber evolution problem. This model would be based on a boundary layer approach and it would consist of the electrical potential balance, energy balances for the solid and fluid phases, mass balance for the gas phase, and "moving boundary" (interfaces core - corrosion product - ceramic coating) equations. The moving boundary problem can be formulated by describing the problem through the shrinking core model. These equations will ensure mass conservation for the solid phase.

8 Experimental Set-up and Operations

The various applications of CVD have resulted in the development of various kinds of reactors, heating systems and feeding systems. The manner in which the substrate is heated is the primary factor in the design of the deposition chamber. The design will be influenced by the geometry, shape, and the composition of the substrate, the type of deposition process used, the nature of the coating desired and by the economic and personal preference factors. The most important criteria among all these should be the performance and cost. The CVD system used is illustrated in Figure 22. The main components of the system are: the CVD chamber, the vapor precursor feed system, the

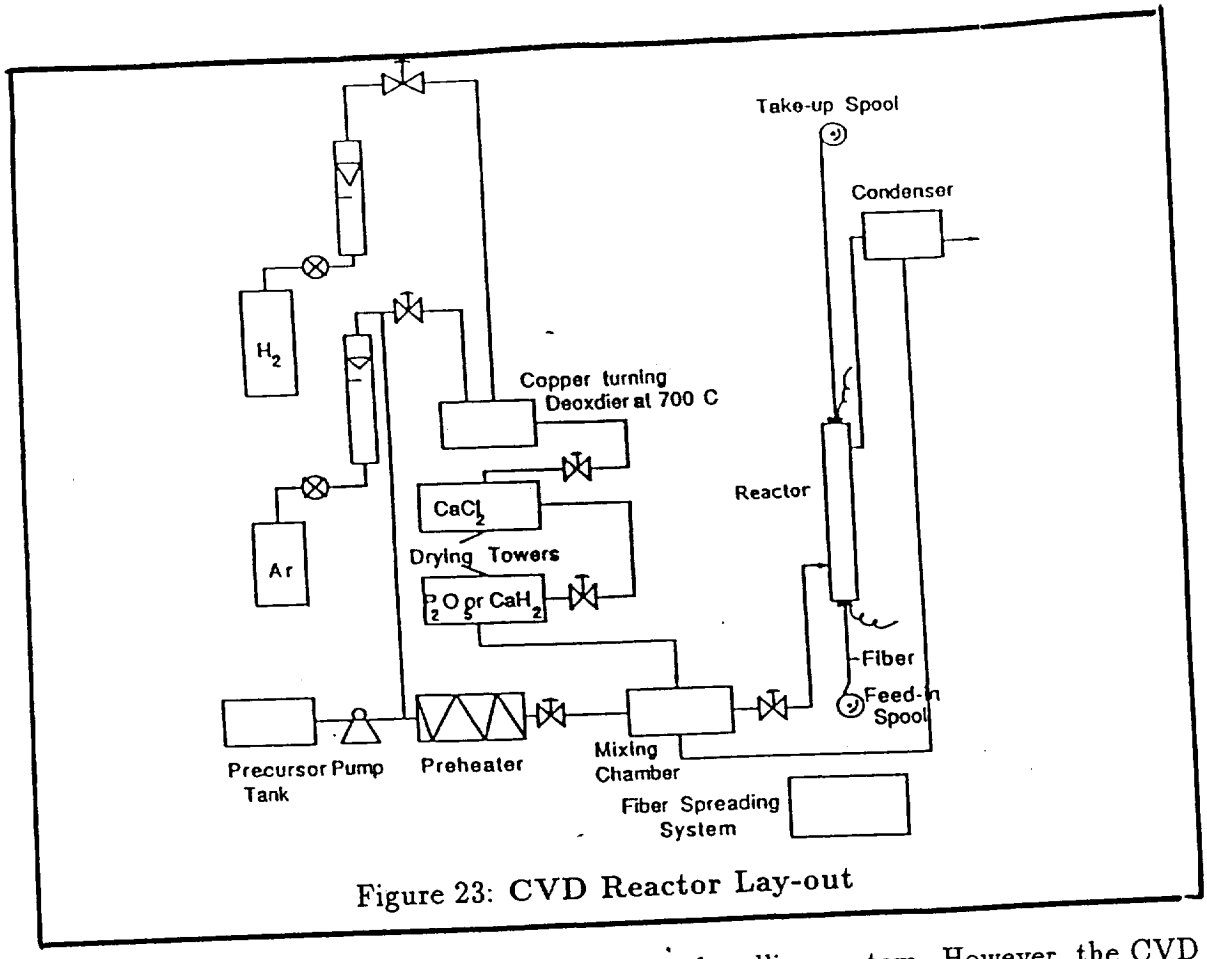

Figure 23: CVD Reactor Lay-out

temperature monitoring unit and the effluent gas handling system. However, the CVD reactor is the most important part of the process. Our batch system basically consists of a quartz reactor of 1.5 inch diameter with projections for electrode insertion. The distance between the electrode is 15 inch (i.e. sample fiber length). The electrodes are of cylindrical shape with a small hole to mount the substrate fiber. The bulkiness of the electrodes was necessary to avoid overheating of the electrodes. The extra heating coil was wound around the reactor to avoid the condensation of sub-metal chlorides on the walls of the reactor. The typical wall temperature was varied from 200-600°C. The reactor is shown in Figure 23.

The vaporizer was maintained at 250°C. This also serves as a mixing chamber for the reactants and the carrier gases, which is critical for uniform deposit. The temperature of the substrate was measured by an optical thermometer ($\pm$5°C accuracy) and controlled by monitoring the applied voltage. The de-oxo system contains activated copper turnings maintained at 500°C to remove traces of oxygen from the carrier gases. The traces of moisture were eliminated by passing through Dehydration unit (anhydrous calcium oxide). The liquid reactants were pumped through a graduated peristatic pump.

In a typical operation, the fiber was mounted between the two electrodes and

system was made air-tight. The reactor surface and preheater were brought to the required temperature. Meanwhile, the reactor was continuously flushed with extra pure argon gas which was pre-purified by passing through de-oxo and dehydrating units. After making sure that there is no more oxygen inside, the hydrogen flow was started at 1.5 lit/min., again passing through the pre-purifying unit. The purity of reactants and carrier gases is extremely important because the trace amount of impurities has a deleterious effect on the physico-chemical properties of the fiber [Powell et al., 1955]. The fiber was brought to required temperature (1000- 1300°C) under hydrogen atmosphere. Once the temperature was stabilized, reactants were pumped into the vaporizer/mixing chamber, for a fixed amount of time. Once the deposition was over, the fiber had been cooled to room temperature slowly under hydrogen atmosphere to avoid the thermal stresses.

8.1 CVD - Continuous Process

The synthesis of ceramic fibers by CVD technique will be carried out in continuous manner. The set-up is shown in Figure 24.

The metallic or graphite filament to be coated enters the apparatus through a mercury seal and is heated in an inert gas atmosphere in the inlet chamber. The hot fiber enters the main plating chamber through a small hole in the inlet chamber and finally leaves the apparatus through a similar arrangement at the exit end. The procedure is the same as that of batch operation.

The fibers are heated resistively. The reacting gaseous mixture enters the reactor at different axial and angular positions to increase accessibility and uniformity of reactants on the filament surface. A motor- driven reel draws the fiber through the apparatus at a steady, controlled rate.The fiber spreading techniques employed to the system is explained in the later part.The results were average to good in avoiding gluing in the continuous process.

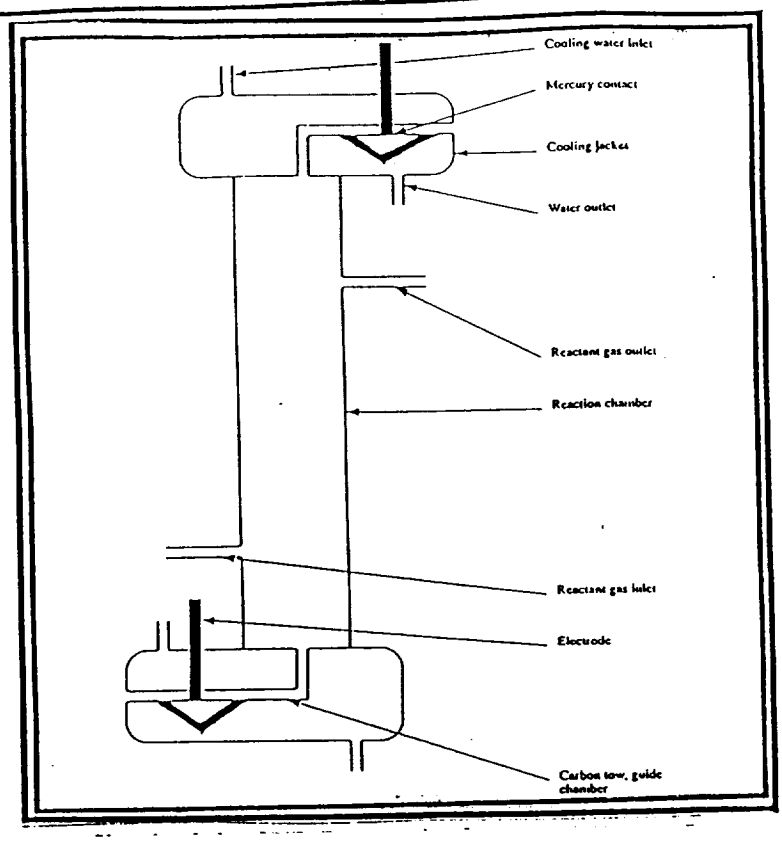

Figure 24: **CVD Continuous Reactor**

9 Materials and Chemicals

9.1 Substrate selection:

The final properties of the CVD fiber are dependent on the substrate fiber used. Several substrate uses are reported in the literature [Pierson and Randich, 1978; Pierson et. al., 1979; Bryant and Meier, 1974]. Basic criteria for a satisfactory substrate selection are as follows:

- Ability to withstand the temperature of deposition.
- Chemical inertness to the deposition atmosphere.
- Thermal expansion is close to that of the deposit.

Several materials were tested for our substrate. Among them Ti, W, Mo, Cu, Ni and C. showed good potential. In all of the experiments, hydrogen is the carrier gas. At the deposition temperature, all the material except W and C, absorbs hydrogen to various

degree to form a metal hydride leading to embrittlement. Even though most of the above mentioned material are resistant to HCl, only W and C can withstand prolong attack at deposition temperature. Finally, ductile materials like Ni, Cu are having high thermal expansion mismatches with the ceramic deposit compared to W, Mo and C, creating a larger residual stresses in the deposit. After analyzing all these results, we selected W, C, Mo as the substrate materials for the synthesis of fibers. The properties of the commercial fibers/wires used are given below.

C (Thornel, From AMCO) Fibers:

- PAN based: Dia. = 5-10 μm, Surface area = 0.5 m^2/g, Strength = 100-300 KSI, 2000-5000 filaments in a bundle.
- Pitch based: Dia. = 6-10 μm, Surface area = 0.3 m^2/g, Strength = 300-400 KSI, 2000-5000 filaments in a bundle.

W (Wire Johnson Matthey and GE):

- Johnson-Matthey fiber - dia. = 100 μm, tolerance $\pm$8%, Surface area = 0.07 m^2/g
- Johnson-Matthey fiber - dia. = 75 μm, tolerance $\pm$8%, Surface area = 0.07 m^2/g.
- **GE fiber**, Electro polished and Electro etched (customized),
  - Electro etched - Dia. = 40 μm; tolerance $\pm$3%, Surface area = 0.5 m^2/g
  - Electro etched - Dia. = 100 μm, tolerance $\pm$3%, Surface area = 0.5m^2/g
  - Electro polished - Dia. = 70 μm, tolerance $\pm$3%, Surface area = 0.3m^2/g
  - Electro polished - Dia. = 70 μm and 100 μm, tolerance $\pm$8%

9.2 Chemicals:

The quality of the film is directly dependent on the purity of the reagents used. It is of utmost importance in CVD to use extra pure material [Powell et al., 1955] to avoid poor physico-chemical properties to the film. Following chemicals are used:

- H_2 and Ar obtained from CS Gas Products, Linde Div. of Union Carbide (electronic grade, extra dry, 99.99% pure). The gases were further purified by passing through de-oxo and dehydration units.

Table 3: **Reactant Analysis**

Reactants	Impurities at Parts Per Million(PPM)
H_2	O_2=0.5, Cl_2=0.1
Ar	H_2=0.1, O_2=0.1
CH_3SiCl_3	Cl_2=60, Si=20, C=80
$SiCl_4$	SiC=200, Si=100, Cl_2=400, C=110
CH_4	Cl_2=40, C=40, O_2=20, H_2O=40
CCl_4	Cl_2=340, C=75, O_2=20, S=10

- $SiCl_4$, CH_3SiCl_3, SiH_4, $(CH_3)_4Si$,CH_4 and CCl_4 obtained from Johnson Matthey Co. are of commercial grades,generally above 99% pure. Wherever possible, these materials were redistilled to improve the purity.

The typical chemical analysis is given in Table 3.

10 Factors Affecting the Deposition

10.1 Pretreatment of the Substrate

One of the main requirements of the deposited films is that it should adhere to the core at all operating temperatures and capable of withstanding severe deformation without spalling. Hence surface cleanliness of the substrate is of utmost importance. This was done three different ways:

1. treatment with boiling concentrated nitric acid for 10 mins.
2. treatment with steam at 250°C for 10 mins.
3. treatment with H at 500°C for 5 mins.

These treatments not only clean the surface of the substrate material but also increase the surface area. The best results were obtained with hydrogen treatment where surface area of W was increased by 10% and that of carbon was by 25%. This method was used in most of our sample runs; if otherwise, mentioned.

10.2 Factors Affecting Grain Structure and Deposit Uniformity:

The main process variables in CVD reactor are pressure, temperature, composition of the gases, flow rates and reactor geometry. The pressure at which a CVD reactor is operated influences first the concentration of reactants in the gas phase and secondly the diffusivity of reactants. However, increased diffusivity due to decreased pressure, increases the surface uniformity. The substrate temperature not only influences the rate of deposition but also the structure of the deposit, mainly because of its effect on the surface diffusion and bulk diffusion that is on grain growth mechanism. The effect of temperature and supersaturation on the structure of the deposited material is explained by Blocher(1974,1984) as follow:

With increasing temperature, the structure changes in this sequence from gas phase nucleated snow, amorphous deposit, fine grain polycrystalline, polycrystalline, dendrites, whiskers, platelets to epitaxial growth.

In order to obtain deposit uniformity and a particular grain structure, one needs to consider the various mechanisms that can be operative at various deposition conditions. In the simplest case involving adsorption of the reactant, desorption of the by- product, and migration of the deposited atom to an active site, if the temperature is sufficiently high to sustain bulk diffusion, one can obtain epitaxial deposition which is important for solid state electronics. Epitaxials growth is carried out at low supersaturation(excess of reactant/by-products relative to equilibrium). At somewhat higher supersaturation, and particularly if the substrate does not influence orientation, or at lower temperature where bulk diffusion is restricted, a randomly oriented grain growth can occur initially, followed by growth in a preferred crystallographic direction which engulfs disoriented grains and develops a textured structure consisting of parallel bundles of those grains that initially had the optimum orientation.

At still higher supersaturation, the supply of reaction product at the surface may be high enough to renucleate randomly oriented grains, resulting in a fine-grained equi-axed structure. The range of conditions over which these types of growth occur obviously depends on the anisotropy of the growth mechanism.

By raising the supersaturation at the surface, the supersaturation in the adjacent gas phase exceeds some critical value leads to the gas-phase precipitated material.This can incorporate in the deposit. Depending on the size of the gas phase precipitated

particles and their relative amount, the net result may be

- grain refinement due to interruption of growth, leading to re-nucleation,
- the development of greater or lesser porosity in the deposit, depending on the gas phase mass transport conditions.

The important point here is that the advent of gas phase precipitation represents a secondary growth mechanism and that the introduction of any such competing growth mechanism in a CVD process offers the opportunity for grain refinement.

The competing growth mechanism may be purely mechanical distortion of the growth pattern causing re-nucleation, as employed by Holman and Huegel(1967) in producing fine grained, high strength CVD tungsten. A deliberate chemical addition to feed stream to co-deposit a second phase material to interrupt the grain growth of the major phase.The example is the suppression of grain growth in BeO coatings by co-depositing carbon. Where the interfacial tension between the two phases is low, e.g. as in the case of silicon and silicon carbide, this approach is particularly effective in yielding a fine grained dense deposit.

In the chemical vapor deposition of ceramic materials, oxides, nitrides, carbides, borides, and silicides, the competing growth mechanism(s) may be inherent in the CVD reaction used. Thus, from the reaction system $SiCl_4 + CH_4$(g) + H_2 (g), it is possible to deposit silicon, silicon carbide, and carbon, including the two phase silicon/silicon carbide, and carbon/silicon carbide mixtures, depending on the conditions of temperature, pressure, and composition chosen. Since a surface phenomenon is involved, this simple mechanism of grain refinement in multi-component systems should be possible with small quantities of second phase material, e.g. below the level of its detection by X-ray diffraction.

10.3 Deposit Uniformity

The requirements for obtaining uniformity of deposition in CVD and avoiding the development of surface protuberance can be appreciated by considering the effects of the two impedances that are present in series in a CVD system. These are:

- Mass transport from the bulk stream through gas film which is increasingly stagnant in the direction of the substrate surface, and

- Surface reaction kinetics.

At some point, as the substrate temperature is further increased, mass transport through the boundary layer can no longer keep up with the more rapid reaction kinetics at the surface. The gas composition at the surface almost reaches an equilibrium value.This develops an appreciable concentration gradient in the boundary layer, and the rate of deposition becomes less temperature dependent.

As mentioned before, the deposition rate tends to drop off downstream owing to decreased reactant concentration. But in practice, the object to be vapor coated or formed can be rotated on its axis to average out the exposure and enhance deposition uniformity. When this is not practical, for example in the vapor forming of nickel molds for plastics, conditions can be chosen to give low conversion of the reactants per pass, thus minimizing the effect of reactant depletion. In many cases, the effect of reactant depletion can be offset by increasing the substrate temperature downstream to achieve the same rate of deposition for the lower reactant concentration. This technique is

- Rotation or translation of substrate relative to gas stream
- Limited reactant conversion per pass
- Compensating temperature gradient
- Increased gas velocity downstream by narrowing of tube.

Avoidance of surface protrusions in CVD and attainment of surface uniformity:

- Operate in kinetically controlling regime
- Avoid gas phase precipitation by
  Reducing pressure
  Decreasing temperature
  Decreasing reactant concentration
- Eliminate dust particles
- Minimize substrate surface irregularities

Grain refinement in CVD by providing competition to grain growth:

- Allow controlled gas-phase precipitation
- Mechanically distort surface structure (brushing)
- Add competing CVD reaction to precipitate second phase
- Utilize inherent competing processes by co-deposition of second phase.

11 Product Analysis:

The reaction product obtained by CVD reaction was coated fiber which was analyzed for deposition thickness, shape and surface morphology, strength and composition. The deposition thickness and shape and surface morphology were analyzed using scanning electron microscope, JEOL Model JSMU3. The tensile strength and Young's modulus of the fibers were measured on the Instron testing machine, model #1000. Measurements were made at a cross head speed (strain rate) of 1.75 mm/min. Specimen load was sensed by a 500 g capacity Instron type-A load cell. This cell was mechanically calibrated by precision standard weights prior to testing. Only 10% of the load sensor's range was utilized in obtaining load versus crosshead displacement curve to determine fiber specimen failure load and extension.

The strength observed were sufficient to allow tensile testing by the standard technique for monofilaments, namely ASTM D-3379-75. The ends of the fiber were cemented by red wax to two arms of the $\sqcap$ piece of card that were subsequently held in the machines' pneumatic grips. To reduce the stresses involved in mounting the fiber and to improve their alignment during the test, a hot wire was used to cut off the central portion of the card, instead of the sharpe blades. This did not change any alignment of the grips. The tensile properties were measured with a gauge length of 2.5 centimeters and slenderness ration, L/D ratio, of the specimen varied between 1400 and 4400.

Phase analysis was carried out with GE diffractometer using CuK_α radiation at intensities ranging from 1000 and 3° slit width. Norelco- Phillips powder cameras of type 52570/O was also used for phase analysis at λ=1.5418 mm. Carbide fibers were tested for free carbon and chlorine content by chemical analysis.

12 Silicon Carbide Fiber Synthesis

We thermodynamically discussed the several possible routes for the production of SiC by CVD. However, the initial stages we carried out experiments with each of these (CH_3SiCl_3, $SiCl_4$+CCl_4/CH_4, SiH_4+CH_4, $(CH_3)_2SiCl_2$, and $(CH_3)_4Si$) precursor. Among these only CH_3SiCl_3 and $SiCl_4$+ hydrocarbon system produce more acceptable result. Dimethyldichlo Silane(DDS) and tetramethyl Silane precursors always produced large amount of free carbon in the deposit on tungsten substrate (10-40%, between 1000-1300°C, α ratio = 20-40) and it is difficult to deposit microcrystalline film. Again it is not practicable to use large excess of H_2 to get SiC with Silane system. We had real problem of handling this material in addition to the problem mentioned earlier. The rate of deposition is so fast that there is no control on the rate of deposit. A small amount of Oxygen present in the system also reacts violently to produce silica in the deposit. Eventhough, thermodynamically stoichiometric SiC possible, it is impossible to get it at our condition [i.e. 1000-1300°C,α ratio =20-40, 1 atm pressure]. Many cases co-deposition of C and Si, layer by layer is observed.Hence we abandoned these precursors. This leaves us with other two precursors processes:

- Silicon halide with hydrocarbon (CH_4 or CCl_4)
- Methyl trichloro silane (some time carbon source is balanced by hydrocarbon at high α values)

In the first case, we varied the α ratio from 20 to 60 by keeping the Si to C ratio in the reactant 1, using CH_4 as the carbon source. At 1350°C and 1 atm pressure, we saw small amount of free silicon in the deposit. The fiber was brittle and irregular, had a very poor strength. This irregularity of deposit may be due to fast gas phase nucleation of carbon compare to SiC. Hence we changed the source of carbon to CCl_4(extra-pure). The operation with this precursor at 1350°C, with same α ratio gave much better result. However, analysis showed small amount of free silicon in the deposit. Hence we varied the Si to C ratio by changing the CCl_4 input in the reactants. Final optimum molar ratio was $SiCl_4$+ CCl_4 = 1:1.01. The deposition rate was varied from 150-400 μm/hr. The fiber obtained was smooth, microcrystalline deposit, and good enough to measure the strength and modulus. The fiber obtained through this process is shown in Figure 21. The average strength was 1.59GPa and modulus of 201 GPa on carbon substrate fiber. This process is fairly successful to get stoichiometric SiC. But the following reasons made us to look for other precursor:

- the temperature of deposition is relatively high.
- rate of deposition is too slow at our conditions.
- conversion per pass is very low.

This led us to our last and best process for deposition of SiC, Methyltrichloro silane and hydrogen system. Our initial scanning runs were carried out at thermodynamically optimum conditions i.e. 1200°C and α ratio of 20. Total flow rate was kept around 0.5 to 2.5 lit/min in the reaction mentioned earlier. At this temperature, deposition appeared to be smooth and almost stoichiometric. This process gave us the following advantages:

- mixing problem of the different gases were eliminated.
- very easy to control the flow rate.
- for tungsten substrate, etching action of HCl is limited compared to $SiCl_4$ system.
- chlorine content in the deposit is also limited.
- deposition rate is fairly good to generate fiber. i.e. good enough to control the deposition rate.
- lower deposition temperature and lower price.

This led us to explore this system in more detail.

12.1 Detailed Studies on SiC System:

The following deposition parameters (independent variables) were studied, include temperature, inlet gas stream composition and inlet gas flow rates for methyltrichloro silane system. The special importance was given to

- deposition rate
- morphology
- tensile strength of the fibers.

The structure of the deposit obtained was studied for selected samples. The kinetic parameters were analyzed. And based on the above study, optimum operating conditions for the experimentation were established.

Experimental apparatus and procedure has been discussed in earlier. To this apparatus, a new feature was added to record the power input and voltage across the electrodes as a function of time. This information would be utilized in future modelling and control studies. The temperature in the study range from 950 to 1800°C. The amount of MTS supplied to the reaction vessel varied from 0.0637 g/min to 0.6365 g/min. The hydrogen flow was varied from 0 to 4000 cc/min. to get the H_2/MTS, i.e., α, ratios from 0 to 100. The total gas flow rates ranged from 16 cc/min to 4500 cc/min.

A compilation of the experimental variables used for tungsten core (100 μm) is presented in Table 4 and 5. Similar studies were also carried on the carbon yarn substrate. The only difference here was that the optimization studies were carried out on multifilament substrate of small diameter (5-8 μm) instead of monofilament as in the case of W-substrate. Experiments and deposition rates are presented in Table 6, for carbon substrate.These are typical runs carried out only for kinetic analysis and optimization.

12.2 Deposition Rate

The chemical vapor deposition process is mainly controlled by kinetic, diffusion and thermodynamic factors. Under real conditions, these factors manifest themselves simultaneously and determine the feasibility and direction of the deposition process as a whole. The various parameters studied include total gas flow rate, temperature of the substrate and concentration of the reactants. The operating pressure was maintained at 1 atm.

The rate of growth can be measured by the change of weight, provided the surface area available for deposition is fixed. Therefore, deposition rate must be defined as the weight or volume change per unit surface area. Hence overall deposition rate is expressed as r_2 - r_1/t where r_1 and r_2 are initial and final radius of the fiber and t is the deposition time, (i.e.in terms of thickness) μm/hr.. The plot of growth versus deposition time at 1200°C showed the linear dependence of time (Figure 26).

Table 4: **Compilation of SiC deposition experiments on W substrate.**

Substrate Temperature, ^oC	MTS flow rate at STP $cm^3.min^{-1}$	α Ratio	Total flow rate $cm^3.min^{-1}$ at STP	Deposition μm.hr^{-1}
1200	104.2	0.0	2200	600.0
1200	20.8	0.0	137	11.9
1200	75.0	20	1600	120.0
1200	10.4	20	240	44.0
1200	20.8	20	450	84.2
1027	104.2	20	2200	171.0
1127	104.2	20	2200	377.0
1200	104.2	20	2200	610.0
1300	104.2	20	2200	716.0
1350	104.2	20	2200	965.0
1450	104.2	20	2200	1501.0
1450	104.2	80	8350	1614.0
1450	104.2	40	4210	1608.5
1550	104.2	20	2200	1645.0
1200	41.6	10	470	128.0
1200	20.8	10	240	64.0
1200	25.5	20	550	60.6
1200	46.0	20	1110	98.0
1200	75.0	25	1900	145.5
1200	85.1	20	1800	142.0
1200	75.0	9.5	788	63.3
1200	104.2	9.5	1100	98.3
1200	88.1	25	2200	600.0
1200	145.0	14	2200	561.0
1200	350.0	5	2200	383.0
1200	710.0	2	2200	365.0
1200	19.3	100	2200	1447.0
1140	104.2	20	2200	460.0
1265	104.2	20	2200	701.0
1310	104.2	20	2200	867.0
1380	104.2	20	2200	1121.0
1405	104.2	5920	2200	1561.0

*Differential flow rates are due to argon.

Table 5: Compilation of SiC deposition experiments on W substrate.

Substrate Temperature °C	MTS flow rate at STP $cm^3.min^{-1}$	α Ratio	Total flow rate $cm^3.min^{-1}$	Time (sec.)	Deposition $\mu m.hr^{-1}$
1200	104.2	20	2200	60	14.5
1200	104.2	20	2200	180	40.5
1200	104.2	20	2200	240	62.0
1200	104.2	20	2200	300	71.0
1200	104.2	20	2200	360	92.0
1200	104.2	20	2200	420	105.0

12.2.1 Factors Influencing Deposition Rate

In CVD of SiC, many factors affect the deposition. These are the starting precursor, the base material (possible reaction at its surface), the shape of the specimen and its position inside the reactor, the reactor dimensions, flow geometry, temperature of the specimen, temperature distribution inside the furnace, pressure, gas composition i.e., C/Si ratio in the vapor as well as its concentration. Information given in the literature fails to characterize these parameters in this process. In our experiments, deposition rate is varied between 0 - 1450μm/hr at 1200°C and very high rates were observed at and above 1450°C ($\approx$2000μm/hr) and further increase in temperature has negligible effect on the rate.

12.2.2 Effect of Total Flow Rate on Deposition Rate

The effect of total flow rate for different composition on deposition rate at 1200°C for tungsten and carbon yarn is shown in Figure 25. It is seen that with an increase in total flow rate of the reacting mixture, there is an increase in deposition rate and a point is reached sooner or later when the rate of deposition ceases to be a function of the rate of flow. For higher α ratios, this plateau is reached earlier. This is discussed in next section. Here one can assume that in such a case, the deposition rate is determined solely by the kinetic and thermodynamic factors involved in the process and the mass transfer limitation could be ignored.

Table 6: **Compilation of SiC deposition experiments on C substrate.**

Substrate Temperature, ^oC	MTS flow rate at STP $cm^3.min^{-1}$	α Ratio	Total flow rate $cm^3.min^{-1}$ at STP	Deposition μm.hr^{-1}
1100	10.4	0.0	137	14.4
1100	20.8	0.0	137	9.5
1450	104.2	0.0	2200	875.0
1200	104.2	25	2700	624.0
1350	75.0	20	1650	781.0
1200	75.0	5	550	362.0
1200	10.4	20	275	63.5
1200	20.8	20	485	156.0
1200	75.0	20	1650	465.0
1200	20.8	10	270	80.2
1200	41.6	10	500	110.0
1550	104.2	20	2200	1210.0
1450	104.2	40	4210	1235.0
1450	104.2	80	8360	1215.0
1450	104.2	20	2200	1250.0
1350	104.2	20	2200	815.0
1300	104.2	20	2200	717.5
1200	104.2	20	2200	605.7
1127	104.2	20	2200	375.0
1027	104.2	20	2200	165.5
1100	104.2	9.5	1100	140.1
1150	104.2	9.5	1100	238.4
1200	104.2	9.5	1100	328.4
1275	104.2	9.5	1100	445.1
1350	104.2	9.5	1100	623.6
1400	104.2	9.5	1100	608.6

*Differential flow rates are due to argon.

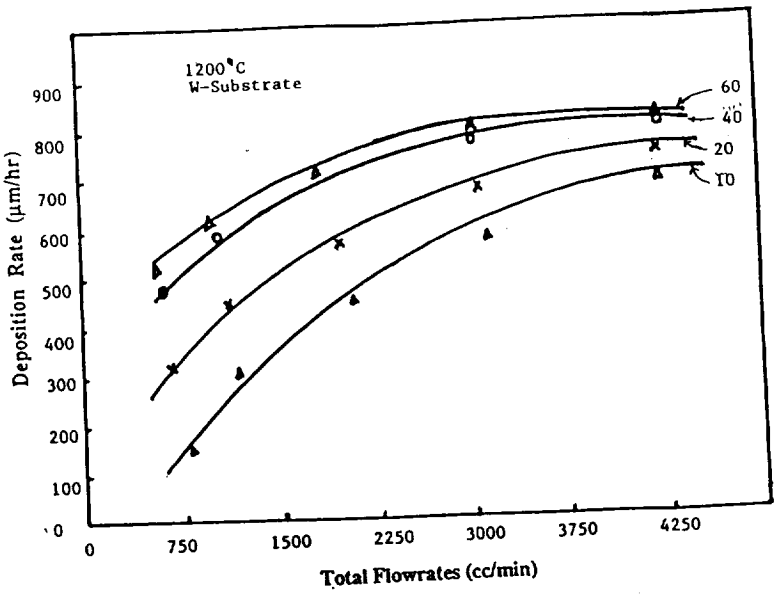

Figure 25: **Effect of Total Flow Rate on Deposition**

The time dependence of deposition was studied by keeping the rest of the parameters constant.The results, seen in Figure 26, show linear increase in deposition thickness with time. This observation is quite consistent with literature and justifies our definition of rate of deposition and the rate expression in the kinetic studies. In the Table 4 and 5, the deposition rates with as argon as carrier gas, in absence of hydrogen showed reasonable rates. They are lower than that with hydrogen alone for same amount of total flow. But the rate at initial time was negligible giving an idea of incubation period as explained by Brennfleck et al.(1984). We did not analyze for free C content.Brennfleck et al.(1984) observed this kind of incubation period and reported to observe 3-times higher activation energy.Their incubation period was 1 minute for SiC deposit to start.

12.2.3 Effect of Composition on Deposition Rate

We varied the α ratio to find out its effect on the deposition rate for various flow rates. This can be seen in Figure 27. It is seen that the deposition rate increases with increase in hydrogen content. This can also be interpreted as decrease in deposition rate with increasing MTS concentration. At high α ratio(>20) and high total flow rates(>1000cc/min),the rate of increase of deposition rate is minimum.Interestingly, this α >20 is the thermodynamic optimum condition to get stoichiometric deposit. So the experimental result matches that of the theory. But at low total flow rates, the

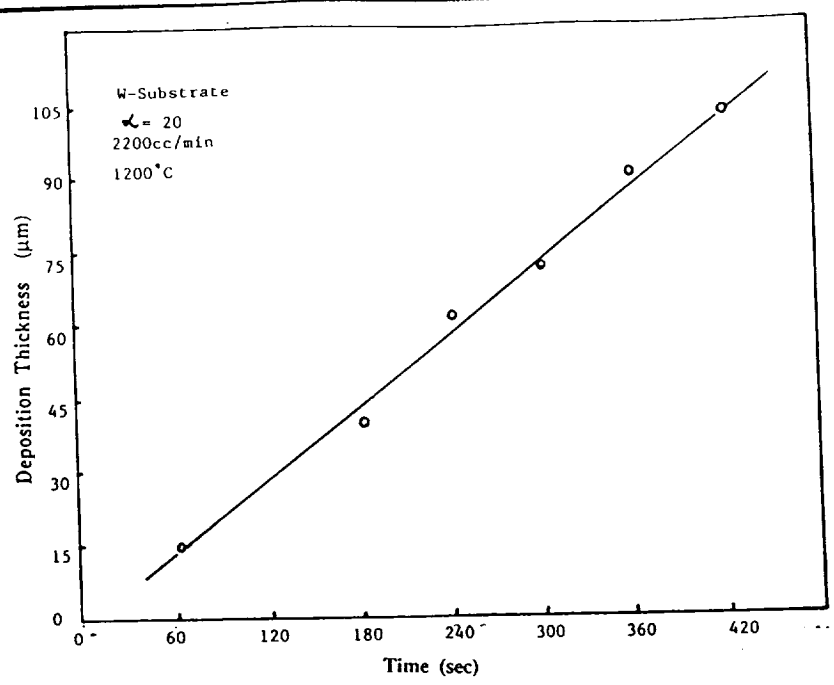

Figure 26: **Time Dependence of Deposition Rate**

deposition rate does not vary much with α ratio. Hence, there exist a experimental optimum which goinsides with the thermodynamic optimum. Similar trend was also observed by Motojima et al.(1986). The study done by them at 1050°C, the silicon decreased gradually as MTS concentration increased for any value above 0.60%. Though contrary to this, linear coating rate with respect to MTS partial pressure has also been reported, however, it may be at lower total flow rate.

The decrease in SiC deposition rate with increase in concentration of MTS can be explained by increased in gas phase nucleation in the boundary layer for the fixed total flow rate. At this layer, the temperature varies linearly from the bulk gas to the substrate, as explained in our theoretical studies, and the equilibrium partial pressure of various gas components also varies with temperature. This temperature gradient practically insures that the gas is supersaturated with respect to the final product over the portion of the laminar zone. This is due to the temperature dependence of equilibrium partial pressures of the molecular species in the gas phase. If this cluster formation occurs, the deposition rate decreases. These small particles diffuse down the thermal gradient and are carried away in the downstream. The increasing in MTS concentration at a fixed total flow rate insures this supersaturation farther away from the deposition surface resulting in decreasing deposition rates. Several methods can be utilize to suppress these cluster formation. The general method is by increasing the gas diffusivity by reducing the total pressure (this also reduces Re). A second solution is by

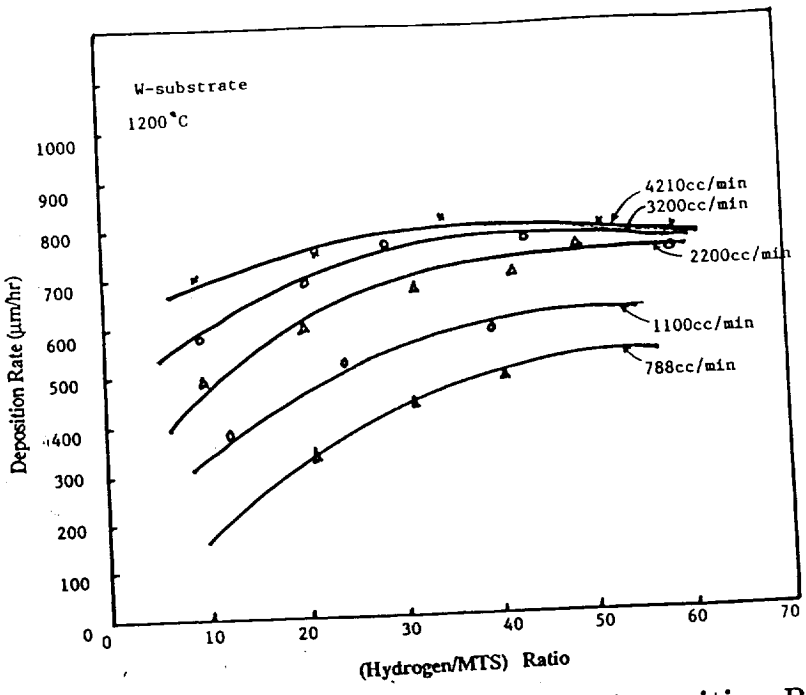

Figure 27: **Effect of MTS Concentration on Deposition Rate**

decreasing the temperature, so that the supersaturation of gas species occurs exactly at the surface. This would of course results in lower deposition rate but loss of material could be prevented. The third solution could reduce the time available for premature nucleation by reducing laminar zone thickness i.e., by sharply increasing the total flow rate. Ideally, one would want to arrange the time temperature life of gas species as they move through the boundary layer so that particle nucleation will occur just at the substrate surface. The increase in flow rate is doubly effective since it not only prevents loss of material by particle gas phase nucleation by reducing the diffusion distance. Hence,high flow rate with high α values are more suitable for operation.

12.3 Effect of Temperature on Deposition Rate and Evaluation of Kinetic Parameters

The deposition rate of SiC for fiber the coating produced are controlled mainly by kinetic, diffusional and thermodynamic factors. Under real conditions, these factors manifest themselves simultaneously and determine the feasibility and direction of the deposition process as whole. Therefore,there is considerable practical interest not only in the actual results obtained but also in the values of the rate and kinetic characteris-

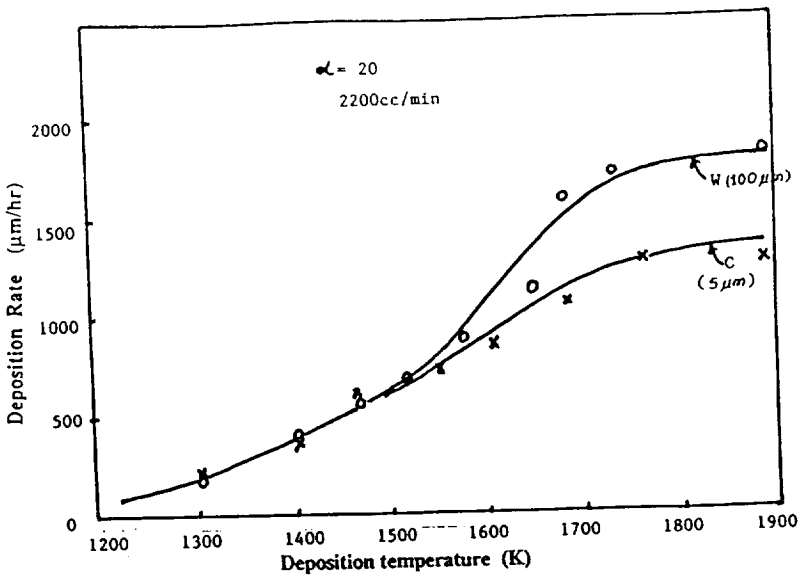

Figure 28: **Dependence of Deposition Rate on Temperature**

tics (k_o and E) of SiC deposition as a function of the principal process parameters. The following analysis is based on the same approach as followed by Mamete'ev et al.(1974). In this study, very high flow rates of 2200 cc/min were maintained so as to overcome mass transfer limitations. The α ratio, [H_2 /MTS], was kept constant at 20 and temperature was varied from 1000 to 1450°C because this is the deposition temperature range of interest.

At this high value of α ratio and total flow rate, one can assume that only thermodynamic and surface reaction kinetics are controlling the rate of deposition. The typical dependence of deposition rate on temperature for tungsten and carbon substrate is shown in Figure 28. Here the α value was kept at 20 at total flow rate of 2.2 lit/min. At lower temperature both tungsten and carbon substrate behaves in similar manner. However, at higher temperature (T> 1350°C), tungsten 100μm monofilament has higher deposition rate than that of the carbon multifilament of small(5-8 μm) diameter. This may due to the mass transfer limitation involved in the process. In the case of multifilaments, there is an interaction between the neighbouring filaments and also exist a large temperature gradient over the length and the width, leads to the earlier jump to mass transfer control regime. This region has been discussed in our Arrhenius plot where both these substrates have different shift but almost same activation energy at this region. The rate of deposition of SiC deposition can be described by a kinetic

equation of the type:

$$R = \epsilon^*.k^1.f(C) \tag{9}$$

where $k^1 = 1/(1/\beta + 1/k)$ and $k = k_o \exp(-E/RT)$

R = rate of deposition of coating in μm/hr

f(C) is some function of specific concentration of the reacting component responsible for the formation of the solid phase.

ϵ^* is the thermodynamically possible degree of transformation of the reactant component in to the solid phase for a given temperature and starting mixture composition.

β is the coefficient gas exchange between the deposition surface and the gas stream.

The assumptions involved in eqn. (9) are that the deposition rate constant k obeys Arrhenius law; the rate of deposition is some function of the concentration of reacting component (MTS), the deposition process takes place under isothermal conditions, and the solid phase is formed only on the deposition surface.

The quantity in eqn. (9) is determined on the basis of compositions of reaction products in thermodynamic equilibrium. In a general case for the deposition of silicon carbide, ϵ^* is a function of :

$$\epsilon^* = f(T, P, (H_2)/(CH_3SiCl_3)) \tag{10}$$

Under any given deposition process, ϵ is determined by the ratio of mole fraction of the silicon present in condensed SiC phase in equilibrium reaction products to the total mole fraction of SiC in Si-containing reaction products. The temperature dependence of the quantity, established on the basis of thermodynamic calculations of the equilibrium composition of reaction products was done by executing NASA code for α=2 to 80, at temperatures between 950 and 1450°C. In these calculation, 59 species were considered. Equilibrium mole fractions can be seen in Figure 1 to 6.

In this study, we shall limit ourselves to curve pertaining to $\alpha = 20$. ϵ^* varies from 0.911 to 0.949 at this temperature range for $\alpha = 20$. This means that at these temperature SiC is thermodynamically the most stable and concentration of other intermediate species is extremely low. Therefore can be assumed unity for all purposes.

Mechanism of pyrolysis of MTS to SiC is not very well understood. The low equilibrium concentrations of intermediates suggest that these intermediates are formed very fast and hence concentration of MTS affects the rate of deposition linearly(Doherty,1976). Thus the function of specific concentration can be taken as C^1_{MTS} and is the MTS concentration in the starting (H_2+ MTS) mixture. It should be noted that this is also true

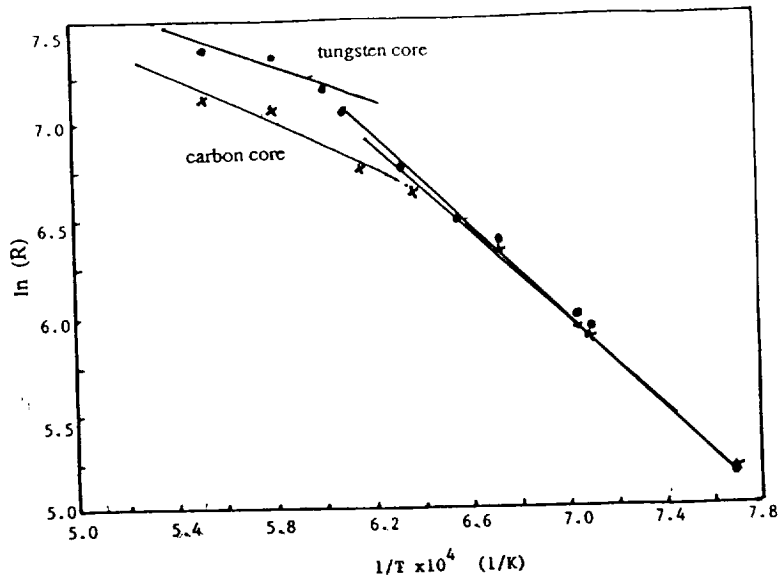

Figure 29: **Arrhenius Plot**

for higher values α of and lower temperatures.

The kinetic characteristics (k_o and E) of SiC deposition process can be determined by plotting semi-logarithmic coordinates ln R vs. 1/T. This is shown in Figure 29.

Several critical observations can be made here. From the change in slope, one can say that the reaction mechanism changes from reaction control regime to diffusion control regime at temperature of around 1623 K for the total flow rate of 2200 cc/min flow for tungsten monofilament substrate. For carbon yarn, since the mass transport is more intense, this transition occurs at a lower temperature of 1573 K. For SiC on tungsten core; the activation energy calculated is 101.3KJ/mol and k_o has the value of 2.05 x $l0^6$ (μm./hr)x$(gm/cm^3)^{-1}$ at kinetic control region. Activation energy calculated on carbon core is slightly different. The value obtained is 98.9KJ/mol(k_o=1.66 x 10^6)and is shown by Figure 29. The apparent activation energy in diffusion regime is 33.5KJ/mol(k_o=2.7 x 10^3) for tungsten core and 49.4KJ/mol(k_o=3.5 x 10^4) for carbon substrate.

Hence, the kinetic expression for the deposition of SiC from gaseous phase containing Si-Cl_2-C-H_2 system can be expressed as:

$$R = \epsilon^* kC exp(-E/RT)(\mu m/hr) \tag{11}$$

Table 7: Debye-Scherrer pattern obtained for CVD SiC on W filament

d	intensity	h k l	comments
2.76	2		Unidentified
2.57	10		SiC (8H)
2.50	10	1 1 1	Cubic b-SiC
2.22	1		W
2.02	BV		alpha-SiC
1.89	BV		alpha-SiC
1.58	BV		W
1.55	5	2 2 0	Cubic beta-SiC
1.41	0.5		?
1.31	BV		?
1.32	5	3 1 1	Cubic beta-SiC
1.29	2		W
1.26	2		Cubic beta-SiC

12.4 Composition of the Coating

SiC deposition of produced at $\alpha = 20$ was characterized for crystal structure on Norelco-Phillips X-ray powder diffraction camera of type 52057/0. The filament was directly exposed to a X-ray source without grinding and was rotated around axial axis. The Debye-Scherrer pattern is shown in Table 7.

The SiC investigated consisted primarily of cubic β-form with occasional diffraction lines corresponding to some α inclusions or caused most likely by stacking faults as reported(Gulden,1971). The specific polytype could not be recognized. The occurrence of small amount of α-SiC in β-SiC deposits obtained at 1100 to 1400°C seems to be common and have already been reported by several authors. Free silicon or carbon were not seen at all. The chemical analysis of SiC fiber obtained at 1300°C in exploratory studies at α=10 showed 0.51% free carbon and α=40 showed 0.4% of free Si. The composition analysis of SiC fiber, along with commercial fibers, is shown in Table 8. Also, it has previously shown that at this temperature and composition β-SiC is the only stable product.

Table 8: **Composition of the Coating (Wt.%)**

Composition	NICALON	TEXTRON	EXPERIMENTAL
ELEMENTAL			
Si	55.5	70	70
C	28.4	30	30
O	14.9	trace	nil
H	0.13	–	–
MOLECULAR			
SiC	61	99	99
SiO_2	28	–	–
Free C	10	trace	0.51
Density(gms/cc)	2.547	3.045	2.950
Tensile Strength(GPa)	2.4-4.3	2.4-4.1	2.8-4.5
Modulus(GPa X10^{-2})	1.7-2.0	4.0-4.1	3.4-4.1
Filament Diameter(μm)	10-15	125-175	$\approx$20
Filaments	500		500-5000(batch)

12.5 Morphological Observations and Analysis

The effect of temperature and supersaturation and total flow rate on the morphology and microstructure of the deposit. This study is of interest because of sensitive dependence of properties on microstructure. Several observations were made and are discussed qualitatively.

Smooth featureless, rounded columnar, angular crystalline,long whiskers, to platelet kind structures were obtained in the deposits by varying the process parameters.

At low supersaturation(α=20), it is observed that at lower temperature of 950°C, the deposit is fairly smooth and that the surface of the substrate is not completely covered. The deposited material is amorphous in nature. Referring to the micrographs in figure 30, as the temperatures increase, the deposition gets very smooth and the structure consists of equisized grains. The grain size increases from less than 0.0l μm at 1l40°C to 0.04- 0.08 μm at 1200 C to 2-3 μm at 1450°C. This can be seen in Figure 31. The material deposited at the conditions(T=1200°C, α=20, and Total flow rate= 2.2lit/min), showed best surface morphology. The increasing grain size may be result of increasing surface mobility of the product with the temperature. At this temperature, the structure starts changing to nodular and smooth rounded columnar growth appears. As temperature increases bigger nodules with deep crevices between them start forming. At 1450°C, these rounded large columnar grains evolve from faceted columnar grains of preferred orientation near the substrate surface. Above this temperature, these grains grow like a platelets as shown in the photograph. These large columnar grains are themselves composed of smaller grains. The transition from equiaxed granular microstructure to columnar can be attributed to the rate limiting mechanism of process to diffusion controlled. The whiskers slowly start appearing in this region and in these conditions.This region is explained in our Arrhenius plot. In this region, high concentration gradients are observed, thus resulting in unstable growth process. On carbon substrate, morphology varied from smooth to ripples on surface at higher temperature. This can be seen in Figure 32. These ripples are instabilities on the depositing surface which don't continue to grow.This finally generates platelets of around 3 - 5 μm size.

At temperature 1200°C, fiber showed perfect microcrystallinity.Eventhough, it is very difficult to describe the grain size requirement for this, one can assume that it should be around 0.04-0.08 μm.

The change in concentration of MTS also affected the surface morphology. This

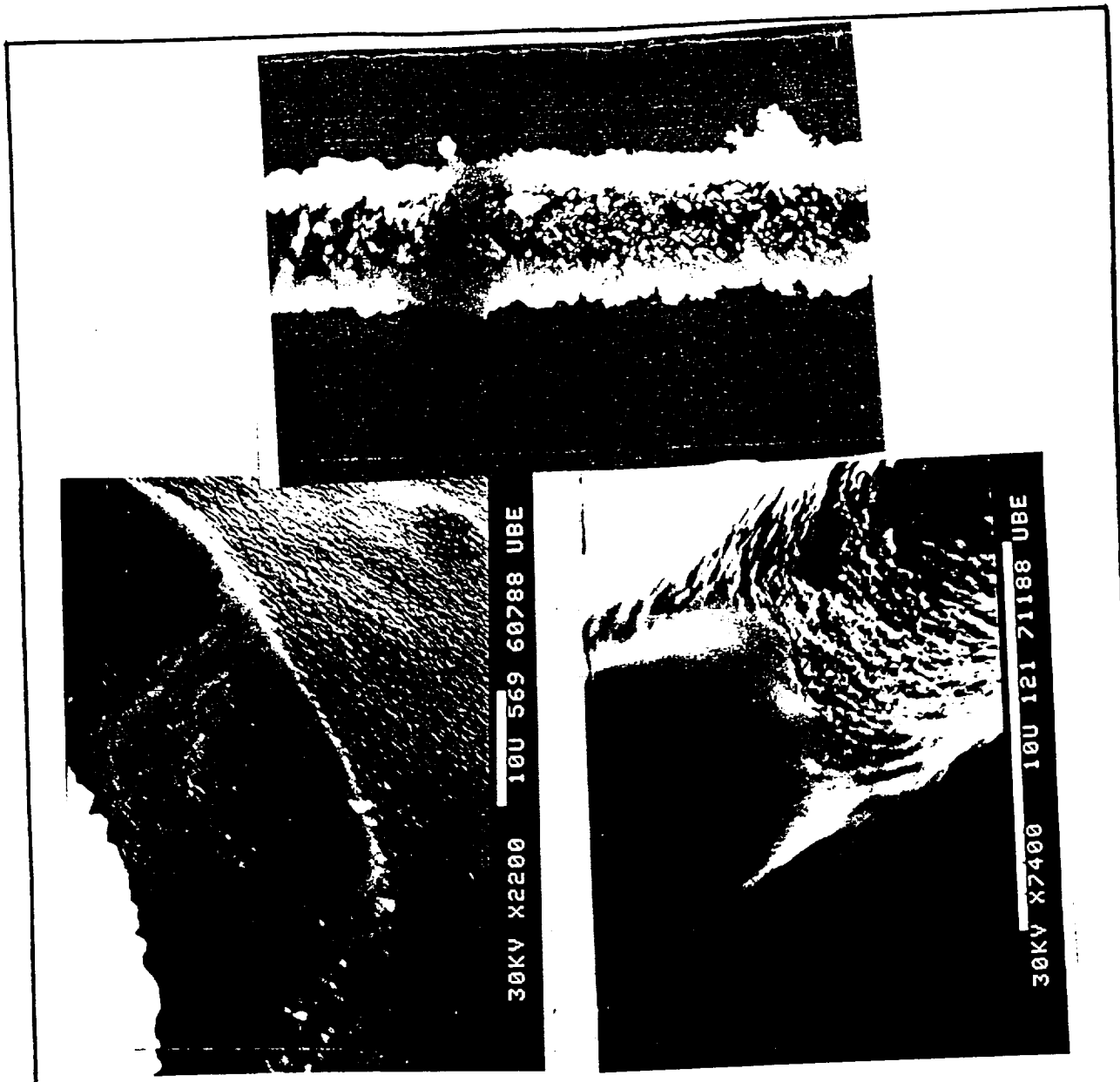

Figure 30: **Unstable Amorphous Growth,(at 950°C,α=20 and Flow rate= 2.2lit/min)**

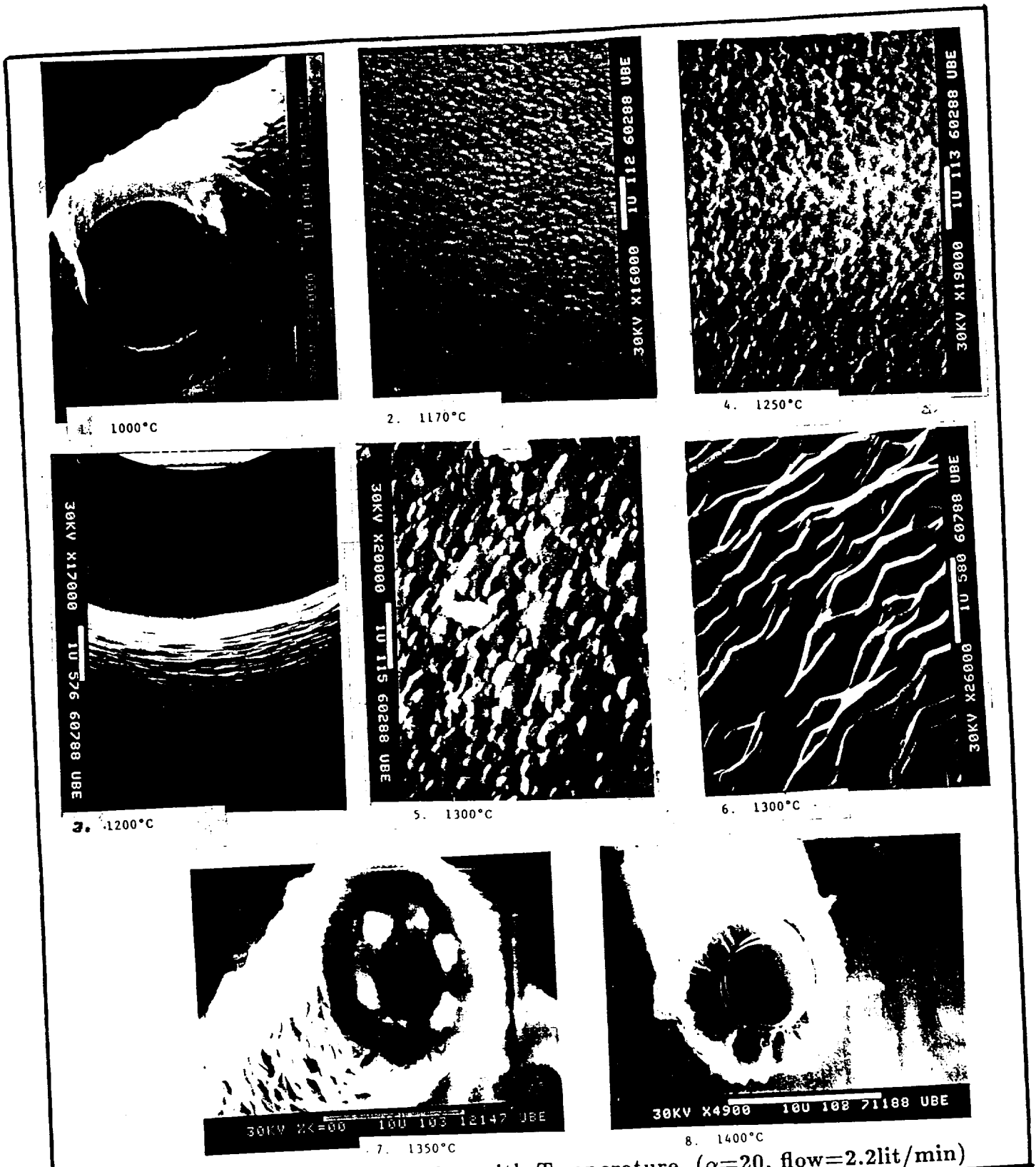

Figure 31: Grain size Variation with Temperature, (α=20, flow=2.2lit/min)

can be seen in figure 33. The micrograin structure of the deposited surface changes to faceted structure with randomly oriented crystals as H_2 flow is increased at same MTS flow. Further increase in H_2 flow, i.e. with increase in total flow rate but decrease in concentration, the deposition becomes highly crystalline. This can be explained by decrease in saturation which decreases the rate of nucleation of a new grain. The increase in surface mobility of the atom, increases the crystal size.

The increase in flow rate at any composition smoothen the surface, as can be seen in figure 34.

The resulting morphologies of this study correlate quite well with the morphology-process relationships as described by Chin et al(1977). A 3D plot of their process parameter vs. resulting morphologies is presented in Figure 35. Our plot covers the overall picture to describe the experimental phenomenon, which covers all the possible(general) conditions for deposition compare to the limited conditions presented by others including Chin et al.(1977). The process parameters of this plot are the H_2/MTS ratio, total pressure, and temperature.

Figure 35 gives the overall picture as to what happens to the deposition morphology when different conditions were maintained. In this diagram, a ratio, pressure and temperature are the three different parameters. Below the plane ABCD, the deposit is smooth/microcrystalline or snowy deposit. This is the desirable condition for the deposition. However, one has to select the microcrystalline, stoichiometric SiC to get excellent deposit which is shown by planes covering II^1 and AA^1. This was the experimentally located region. As the temperature increases, the deposit starts showing nodular or columnar characteristics. This can be clearly located if one knows the input conditions. This region covers a broad range of crystallinity which is difficult to define in words. These nodules or columnar deposits are nothing but the clusters of small microcrystalline deposits. As the temperature increases and α ratio varies, we start forming angular or whisker kind of growth, which is shown in the figure. At high temperature (T>1800k) whatever may be the conditions, faceted or platelet kind of deposit is observed. These results were approximated with experimentation.

Some of the fibers generated in our laboratory are shown in Figure 36.

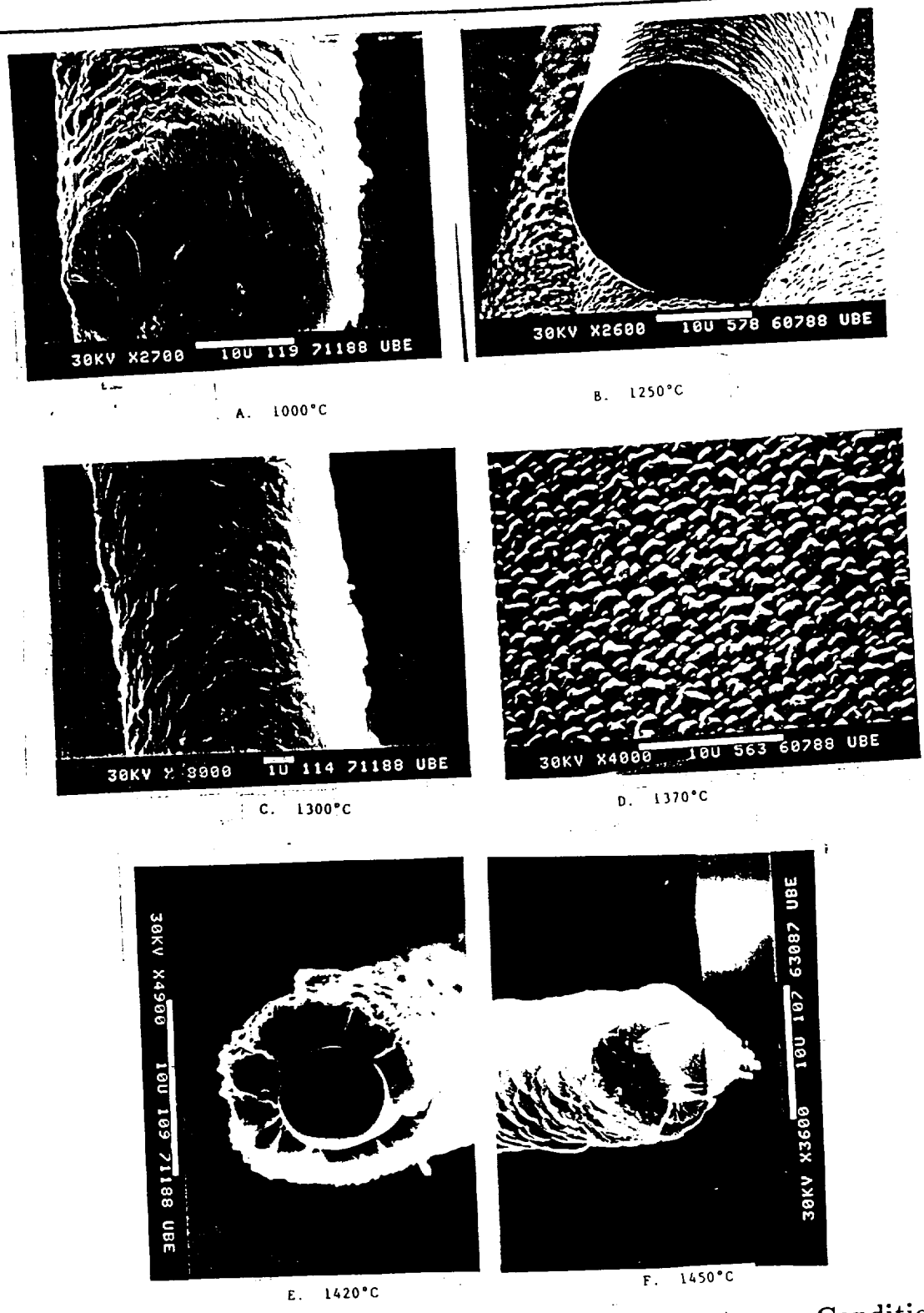

Figure 32: Morphology at Different Temperature Conditions, (α=20,Flow=2.2lit/min)

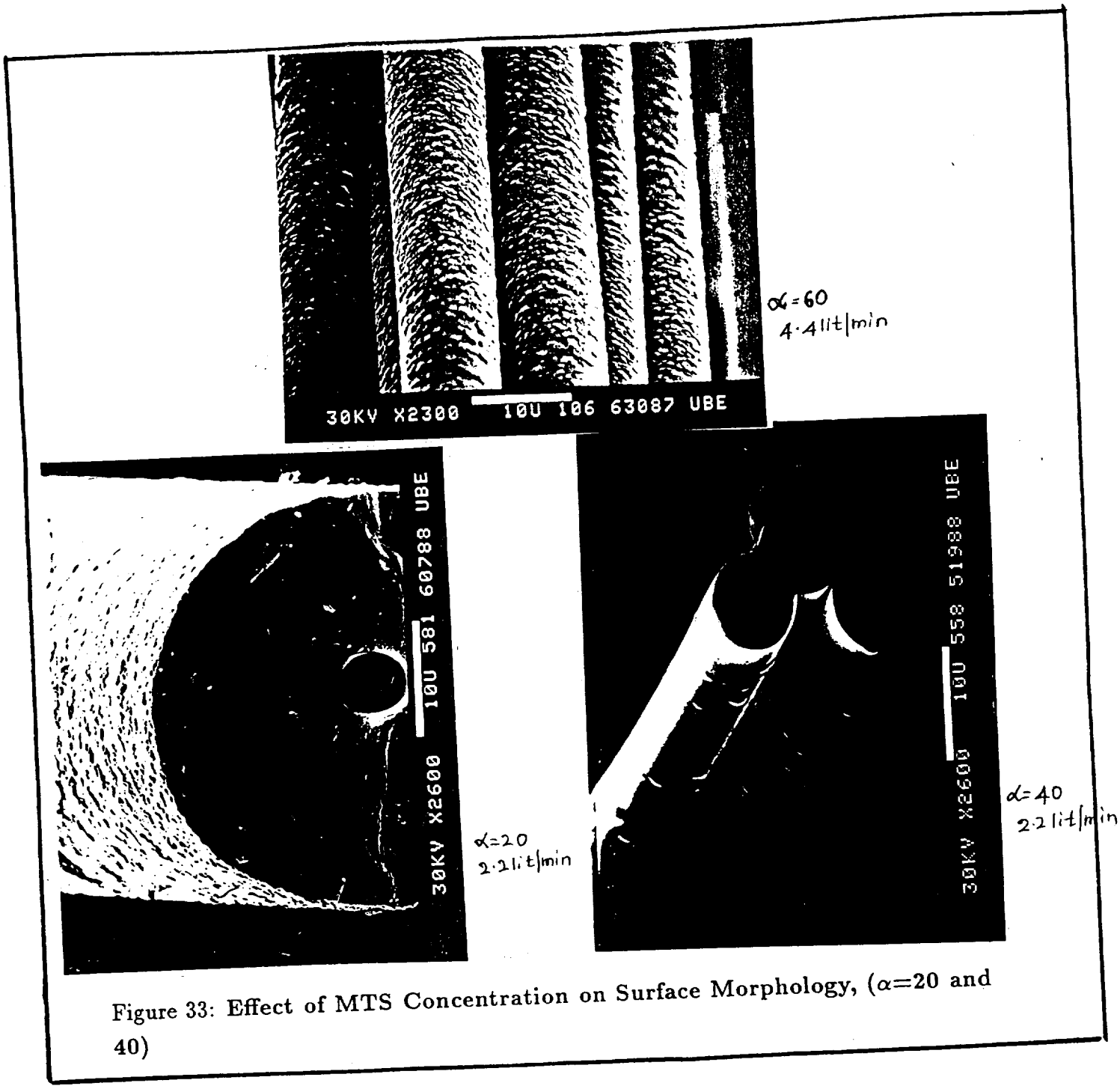

Figure 33: Effect of MTS Concentration on Surface Morphology, (α=20 and 40)

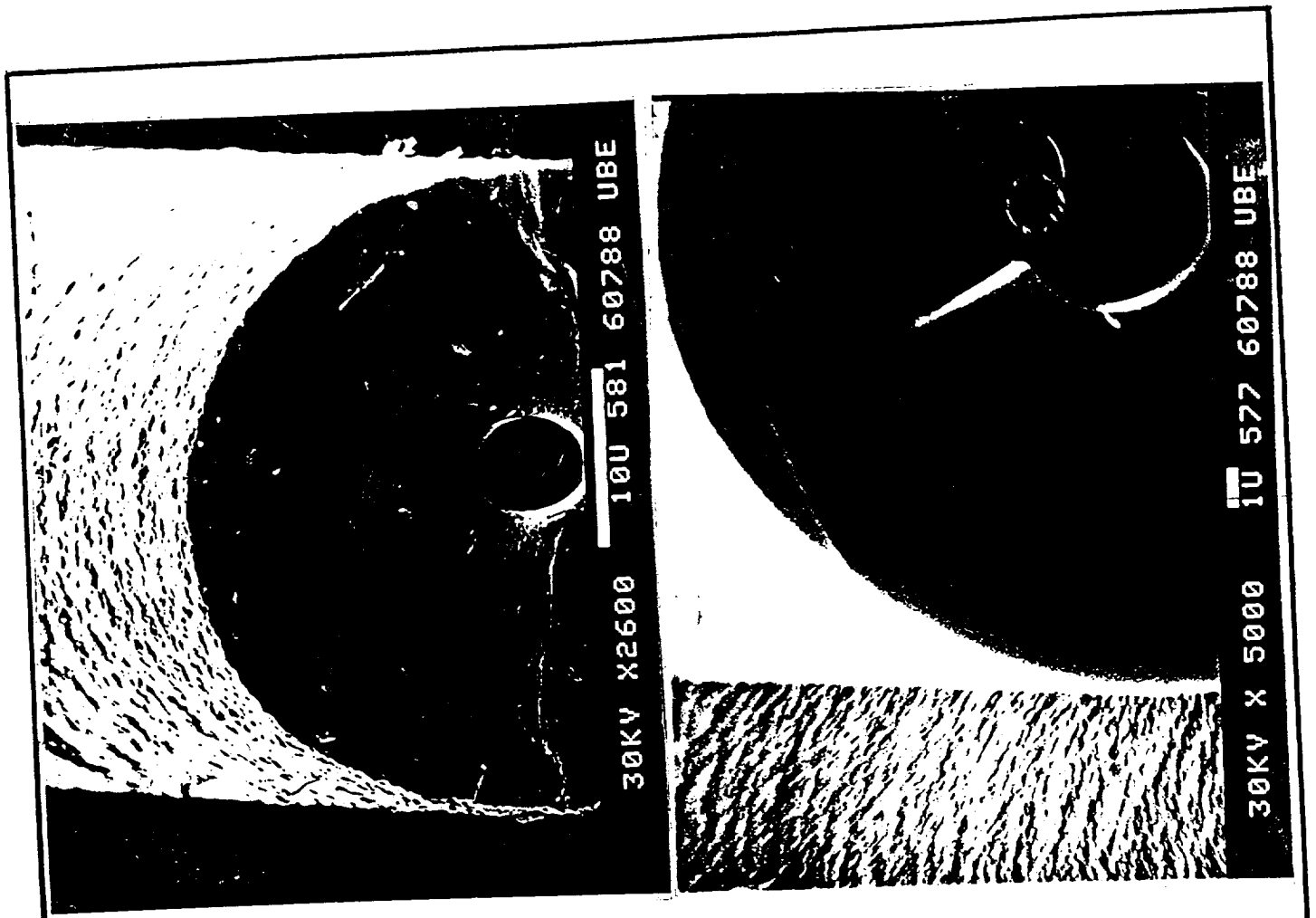

Figure 34: Effect of Flow Rate on Surface Morphology(α=20,Flow= 1.1; 2.2 ; and 4.2 lit/min)

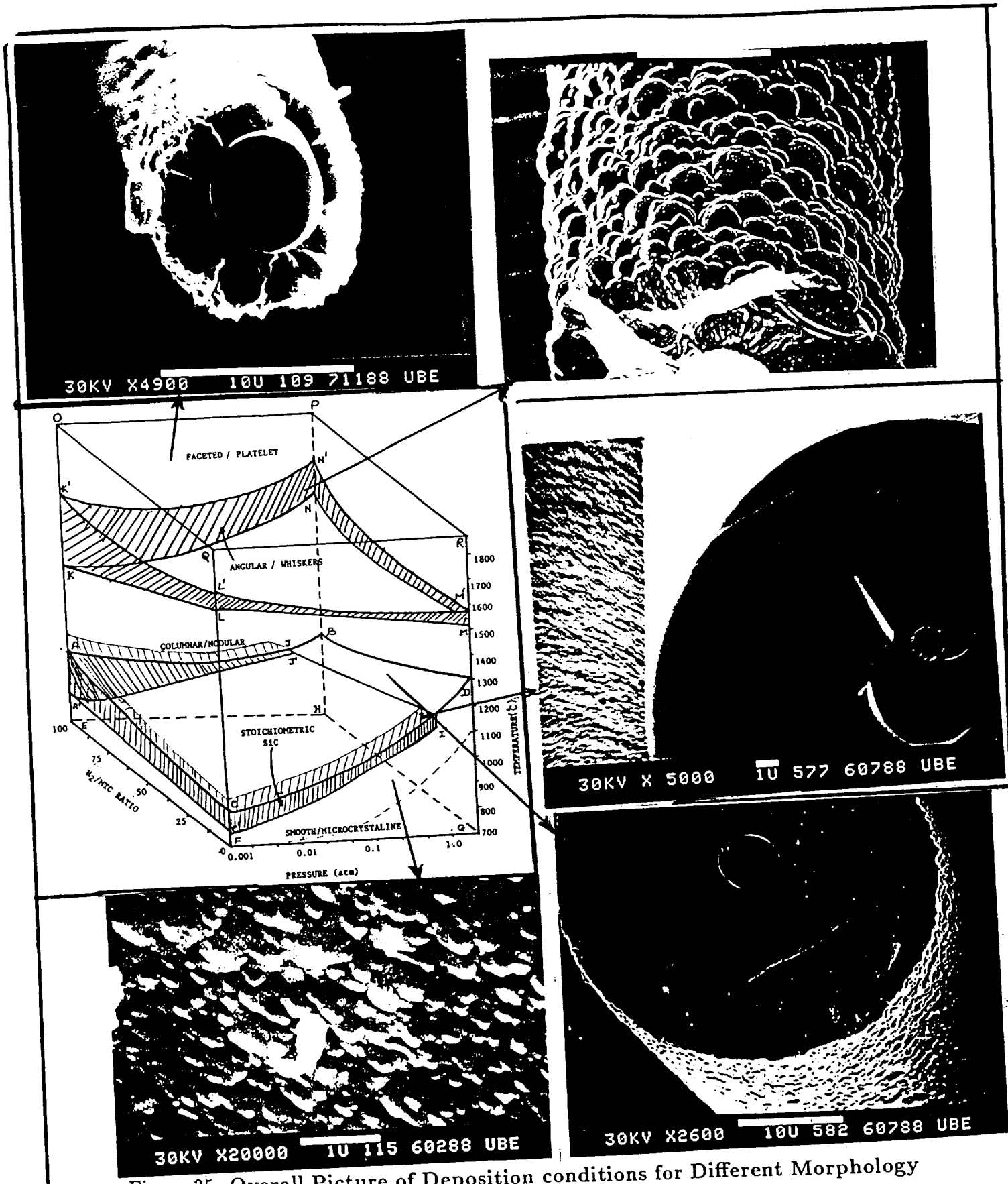

Figure 35: Overall Picture of Deposition conditions for Different Morphology

FIG (a).

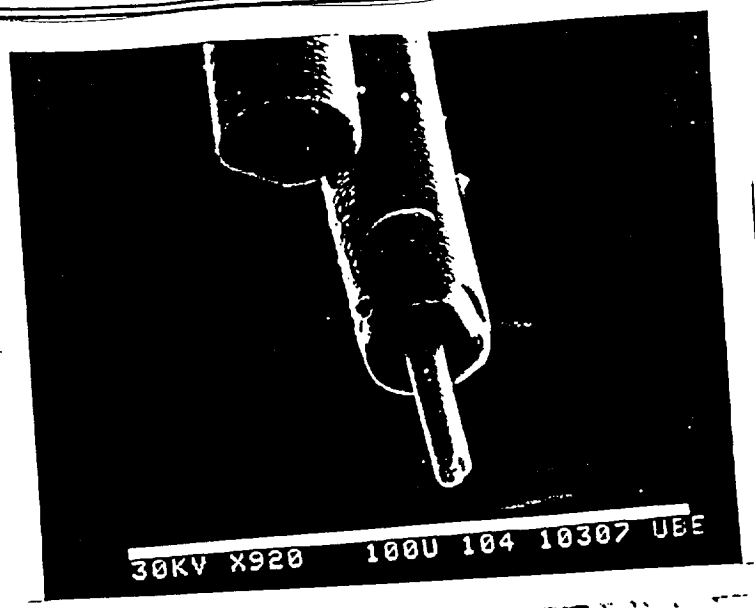

FIG (b).

FIG (c)..

Open channel in the tow

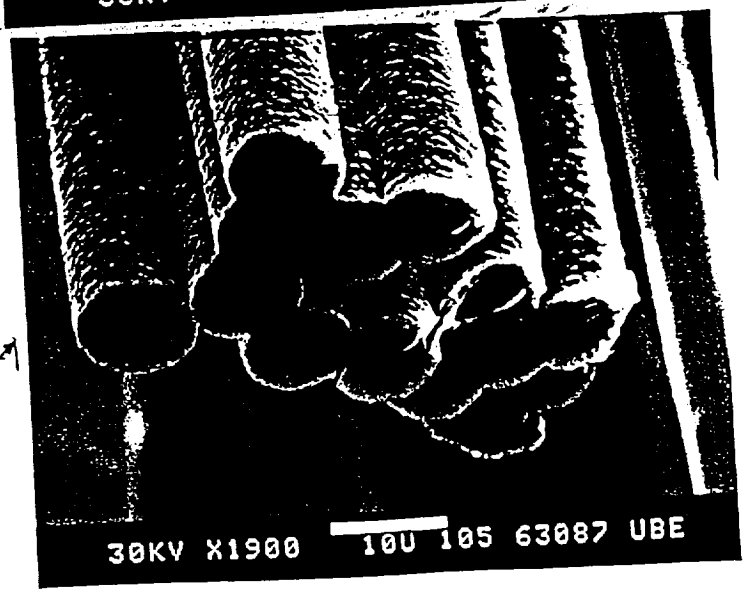

Figure 36: Some of the Fibers Synthesized in our Laboratory

12.6 Mechanical Properties of the Coated Fibers

The tensile properties of the different fibers obtained are presented in Table 9. It can be seen from Table 9 that there is considerable reduction in strength and modulus once a ceramic coating has been deposited. Similar observation are also reported in literature. There are several reasons for this behaviour. One of them is the weakening of the substrate fiber as a result of coating process. Warren et al.,(1978) measured tensile strength of the substrate fiber after removal of the coating and observed the reduction in the strength. Since there was not apparent change in the internal structure and since the elastic modulus is not effected correspondingly, it seems likely that, the weakening results from some form of surface deterioration or by introduction of cracks. This main damage is due to the difference in thermal expansions of coating and fiber. The axial thermal expansion of carbon fibers is much lower than the coatings studied here. Therefore, upon cooling from deposition temperature, the carbon fiber is expected to be under axial compressive stress which can produce circumferential cracks in carbon fibers. This problem of differential thermal expansions has been partially removed by introduction of an intermediate layer of pyrolytic carbon. The other advantages of this layer have been discussed earlier. Application of this layer resulted in 40-60% increase in strength of SiC fibers as can be seen from Table 9. Another reason for decrease in strength of substrate fiber is due to the rough substrate surface. Though no unusual geometric features were seen on the C fibers and tungsten wire as obtained from the supplier, the chemical treatment with boiling nitric acid and then steam increased the strength of the deposited fiber by 20%. This means that the substrate fiber initially had some surface flaws which were etched away by the chemical treatment and smoothening out the defects as shown in table 9.

The strength of the coating decreased markedly with increasing coating thickness due to a stress concentration on the carbon fiber. This leads to the premature fracture of the coating. The critical coating thickness above which carbon fiber can not bear the stress created when coating fractures is approximately 1 - 1.6 μm for carbon fibers of strength between 2 - 5 GPa. Fracture at the low stress is linked mainly with surface defects and impurities in the coating. The grains are separated generally by 0.25 - 0.75 μm deep intergranular grooves. There are also so called secondary grains, which increase the sharpness of the grooves at these sites. Also, heterogeneous fiber surface promotes the fracture by inducing crack nucleation and their growth from the surface in to the fiber. Apart from this the coating is already under tension as a result of higher

Table 9: Tensile Properties of the Fibers

Coating	Tensile Strength σ(GPa)	Modulus γ(GPa)	Strain to failure ε(%)
C (substrate)	4.34 - 4.68	326	1.33
SiC^1	1.65	285.6	0.47
SiC^2	1.52	126.3	1.21
SiC^3	1.59	117.3	1.36
SiC^4	2.17	134.7	1.61
SiC^5	3.31	241	1.40

[1] -using $SiCl_4$ and CCl_4

[2]-using MTS.

[3]-with intermediate layer

[4]-with intermediate layer on chemically treated substrate.

coefficient of thermal expansion. These stress concentrators can be removed by:

- Electrochemical polishing, which removes surface layers of the fibers up to 3 μm thick by electrolytic pickling.
- Plasticizing coating, in which selective dissolution of the fiber surface along the intergranular grooves or at stress concentrators. This increases the strength by smoothening out the defects.

The basic requirements of a plasticizing coating are as follows:

- The fiber must readily dissolve in the coating without forming a brittle chemical compound with the later.
- The coating application technique and performance characteristics (or subsequent heat treatment conditions) must provide for sufficient diffusion mobility of the coating material on the fiber surface to ensure the necessary conditions for healing the stress concentrators. These conditions involve leveling off the geometric features, i.e., extending the radius of curvature of the crack apexes, jogs, microseparation etc. and decreasing their height.

- In addition, the coating material must exhibit sufficient relaxation capacity to inhibit the nucleation of cracks near the surface stress concentrators and to check the propagation of already existing microcracks.

The tensile strength SiC fiber produced commercially by AVCO is 3.43 GPa with modulus of 422 GPa, which is very nearly the same as the SiC fiber produced during this studies. In this fiber, the strength is stabilized by plasticizing effect of carbon rich outer layer. It has been shown that Ni coating of 1 μm thickness of SiC enhances the strength and the wettability (Shorshorov et al.,1978). This can be used to further improve the strength of our fiber.

One can improve the properties of the fibers by eliminating the residual stresses on the deposit. These are basically due to a thermal expansion mismatch between the core and the deposit, inherent growth strain, influence from substrate and cooling rate. We decreased this by having secondary spongy pyrolytic carbon deposit of around 0.5-1.0μm between the substrate and the SiC deposit by decomposition of methane. Figure 37 indicates the strength of the 20μm SiC fiber with 5μm carbon core as a function of between layer of pyrolytic carbon in a batch process. The dependence displays a maximum. This optimum secondary coating is around 0.6-1.0μm. There is some relationship exist between intermediate coating thickness and total deposition thickness.The approximate ratio in this case around 15 to 20. The secondary coating is seen in Figure 38. Further, secondary coating of the carbon on the substrate is important in separating the SiC deposit from the substrate. If the substrate should fracture on being oxidized, the SiC deposit would not fracture and would still be able to carry a mechanical load. This secondary coating also 'heals' the surface flaws of the the substrate and makes the deposit uniform.

13 Scale Up

To maintain economies of scale, it is understood that using carbon fiber tow is the best answer to lowering of the production cost. The costs run high because of the expensive precursor materials, low conversion per pass required to obtain uniform composition and stringent process control. Moreover, tow or yarn is the only commercially available form. Unfortunately, using carbon tow as a core material generates a critical welding problem.The main purpose is to physically separate these fibers in the untwisted tow so that the bridging can be avoided during the CVD reaction. Several designs are

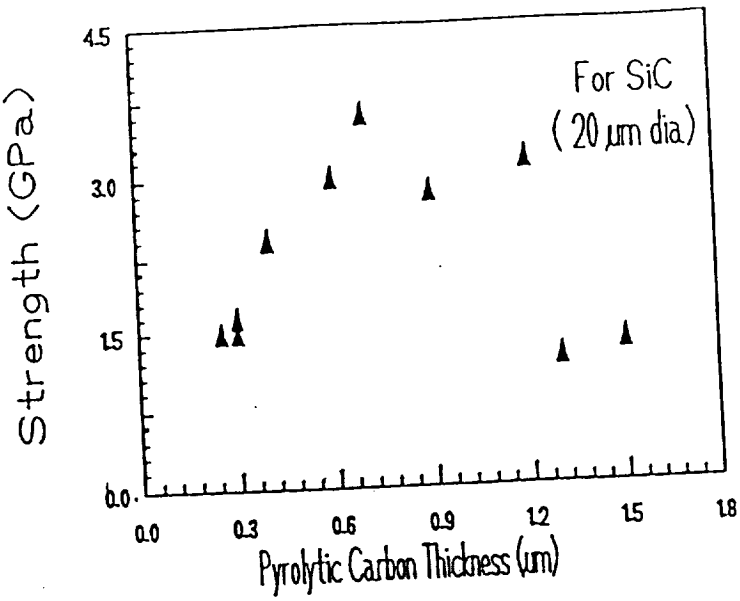

Figure 37: Variation of Fiber Strength with Intermediate Layer Thickness

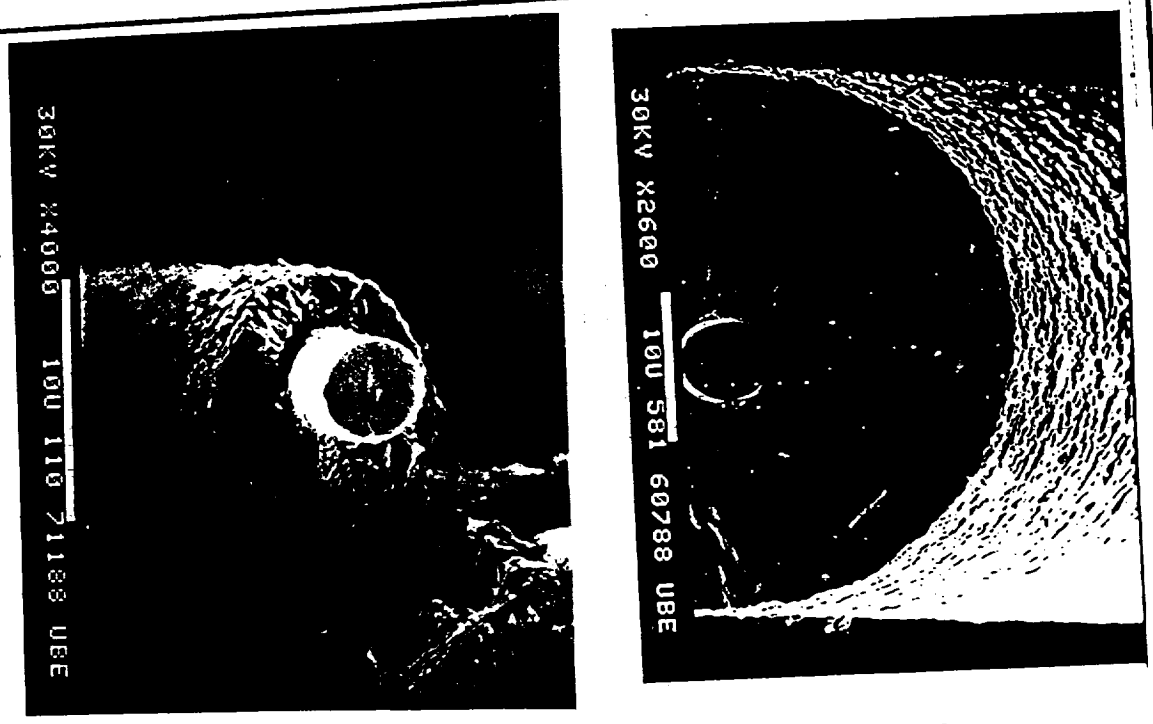

Figure 38: SiC Fiber Showing Intermediate Layer of Carbon

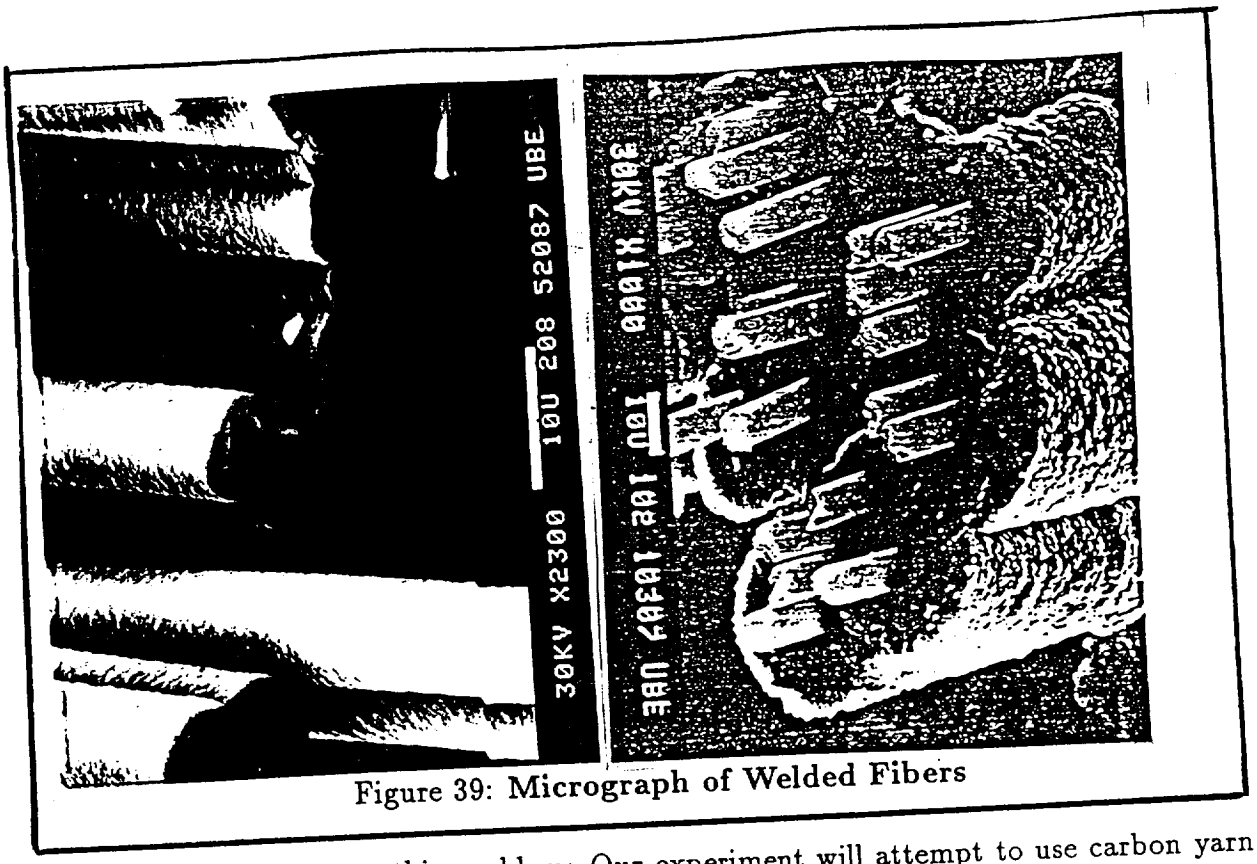

Figure 39: Micrograph of Welded Fibers

suggested to overcome this problem: Our experiment will attempt to use carbon yarn of 500-2000 fibers (5-7μm in dia.) as a substrate, thereby producing SiC fibers of 10-20μm in diameter. Unfortunately, using carbon tow as a core material generates a critical welding problem in our continuous system.

We used the batch system experience to obtain the same 20 μm SiC fiber by performing CVD on a multifilament commercial 6-9μm carbon tow that moves continuously through a reactor. Unfortunately, using electrical current to heat the carbon tow as a core material generates a critical welding problem shown in the Figure 39.

Here carbon fibers are interconnected by SiC bridges and their individual existence is lost. Nevertheless, these fibers showed good flexibility. To eliminate the bridging problem, the separation of these fibers is necessary before entering the deposition chamber. However, several problems are encountered in thermochemical separation. The initial problem is removing the small twist on the tow and separating intermingled fibers within the tow. The second problem encountered is the large number of discontinuous fibers in the tow which behave like unbound springs. Several designs were tried to separate these fibers before passing through the main reactor. We will try to eliminate the welding effect (i.e., individual fibers are glued together by the CVD process) by using the following fiber spreading system:

- The technology developed in West Germany(Brennfleck et al.,1984) has

avoided the bridge formation between the monofilaments by moving the bundle of yarn perpendicular to its axis with a vibration device. This suppresses the bridge formation even at thicker layers of deposition.This is effective only for small deposition(1-5 μm).

- The setup for spreading the fibers by **Venturi effect** is fairly simple. Fibers are passed through the aperture with forced gas flow in the opposite direction. Due to the pressure gradient and diverging gas flow at the threshold, the fibers are bound to spread. Restrictor action controls it. Providing the tension roller, the bundle of fibers can be directly passed through the CVD reactor. The schematic diagram is shown in Figure 40. This arrangement is similar to that advocated by others(Sandy,1987).

- **Pneumatic fiber spreading techniques:** The pneumatic fiber spreader type is shown in Figure 41. Most spreading action takes place in the left nozzle according to the Venturi effect.

The method tested was the Venturi effect where fibers and airflow are moving in countercurrent direction and are thereby separated. However,there is always blockage of Venturi due to unbound fibers, and control of fiber spreading is difficult.The pneumatic spreader by vacuum effect spread the fibers uniformly but not completely.Sketches are shown in the figure.The electrostatic effect separation is also not successful in spreading the fibers completely. Finally, we spread the fibers mechanically and wind them over the spool before passing through the reactor. The deposition was carried out with the spread fibers. The gluing effect was approximately 25-30% for 10-15μm deposit and 15% for 5μm thick deposit. The resultant fibers showed good properties but inferior to those from the batch process. Independent studies are underway to understand the contribution of the core and the deposit to the strength properties. The main aim is to allow the SiC deposit provide the fibers structural properties rather than the carbon substrate. In this way, oxidation problems with the substrate would be minimized. Greater thickness of SiC is necessary to achieve this requirement. We should focus on achieving a thick deposit (20μm in total diameter) without gluing in a continuous system. This is the very difficult task to do but may not be impossible.

Technique was tried in the laboratory and we were able to separate fibers partially. None of these techniques by itself seem to be capable of solving the problem completely. Therefore these have to be tried together in sequence with another such

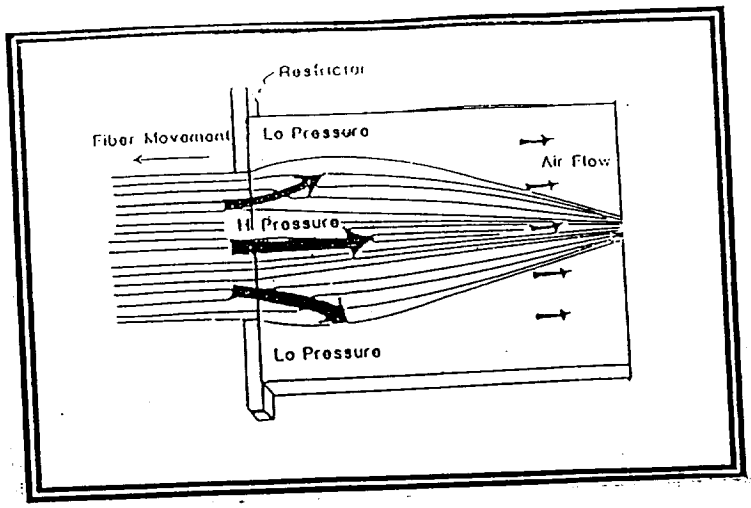

Figure 40: **Fiber Spreading by Venturi Effect**

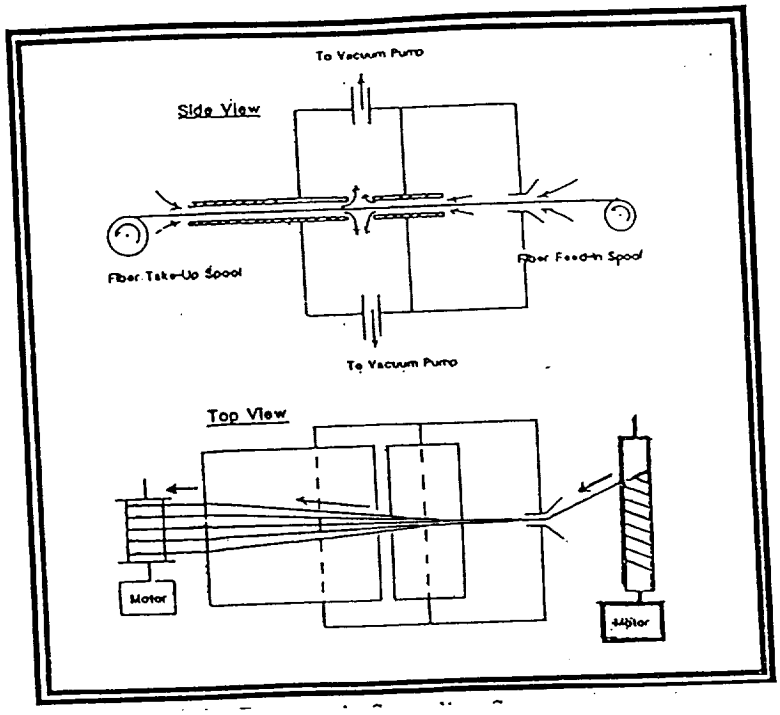

Figure 41: **Schematics of pneumatic fiber spreader**

that the spreading action produced by one is enhanced by the next.

The nature of applications of the fibers require, fibers to be produced in a controlled diameter range with high strength, modulus and theoretical density of the material. This required CVD to be carried out in a very controlled environment. This has been achieved by electronic mass flow controllers and custom made temperature measurement and control unit (optical) obtained from Mikron Corp. These units along with the Teflon pump and motors driving the spools will be controlled by the computer through an interphase. Software for the process control is being developed in collaboration with Dr. Sun of Electrical Engineering Department.

13.1 Deposition with Carbon Monofilament [5-8μm diameter)

One of the aims was to get monofilament of small diameter (10-20μm) with consistent deposit on it for vigorous testing and analysis. This requires large numbers of the same diameter deposited SiC fibers. That means one has to control the deposition rate up to the fraction of a second. The initial problems were many. Because fibers itself have different diameter along their length. This leads to an uneven deposit. The problems will be discussed later with our remedies. That is why we decided to separate the fibers from the deposited bundle of fibers. However, since the fibers were very brittle and very small in diameter, it was difficult to get enough fibers of the same diameter and length for testing. Secondly, interconnection between the fibers makes the problem even worse. Therefore, this process of separation was abandoned after the initial attempt.

Our result with partially separated fibers was good in a continuous mercury electrode reactor process; the incorporation of 1-3μm carbon layer on initial layer was not consistent enough to claim it a success. Secondly, separation of individual filaments was so difficult, the bundle had broken during separation.

In short, we can summarize our problems as follows:

- First of all, getting the monofilament of carbon of 5-8μm diameter was very difficult. Since these fibers are 2000-5000 in number in a tow, which are twisted together. Most of the fibers are broken in a tow. So one can imagine the difficulty of getting monofilament. Our attempt to get separated monofilament from the supplies was not successful.

- Separated fibers showed uneven diameter along the length. In some cases, the tolerance level in the diameter was $\pm 15\%$, which created uneven deposit.

- Since fibers are small in diameter, this has created a heating problem. Resistance heating requires large power, so alternate methods of heating were tried i.e.-heating in a quartz tube, alumina tube and carbon tube. This always led to uneven heating along the length. Hence, fiber was not having consistent diameter.

- When using hot wall arrangement created oxidation of the fiber, since alumina tube reduced to release oxygen resulting in degradation of the fiber. Therefore, we replaced alumina heating tube with carbon and quartz.

- Fixing the fiber (single) was the most difficult task since the fixing agent should withstand high temperature of deposition. Keeping the intact up to the end was our most concern.

- Since we were using hot wall arrangement, the time we maintain was hypothetical (approx.) and randomly generated a lot of errors.

- Finding a suitable fixing agent took some of our efforts. Since we have to locate the compounds which does not imparts any impurities and hold the fiber at the condition of deposition.

- Fibers are in bundles of 2000-5000 in number. They are likely to get damaged while separating out. Further, the damage to these fiber can occur during any one of this handling operation. These were two main problems along with flow conditions, concentration gradients, etc.

13.2 Fixers

Different kinds of fibers were tried to hold the fibers together. These should hold the fibers together at deposition temperature and flow conditions. The following types of fixers were used:

1. Silicone rubber

2. Epoxy and polyamide resins

3. Acrylic acid and methyl acrylate ester paste

4. Methyl cellulose tape

5. double plate contact

Basic idea about first four paste is that they will decompose initially and carrier gas will carry away all the impurities leading to carboneous fix for the fibers. Finally, methyl cellulose tape gave easy and viable results. Once fibers were mounted on plate, the tape was decomposed at 260-400°C and carboneous fix was obtained.

13.3 Electrodes

As we discussed earlier, hot-wall arrangement led to major problem in heat transfer and deposition. Hence we decided to go with resistance heating. These fine fibers require enormous amounts of current to heat them up. Hence ordinary electrode contact is not enough. Following are different kinds of electrodes were tried:

- Solid copper electrode (1.2mm dia., 8mm length)
- Air cooled electrodes (1.8mm dia.)
- Water cooled electrodes (1.8mm dia.)
- Side penetrated electrodes

The water cooled electrode solved the overheating of the electrode problem.

13.4 Systems/Processes:

A few different systems were tried to generate single monofilaments

1. **Mo, W were resistance heating:** Here the wires were mounted on to an insulated material connected plates, above which carbon fibers were mounted. However, heat is not enough to generate uniform coating.

2. **Nichrome, Canthol wire heaters:** Here we made the mesh of nichrome wires and it is mounted on contact plates. The fibers mounted on it showed uneven deposition due to the gap between the mesh wire. Distance between the electrodes and contact breakdown was also a problem.

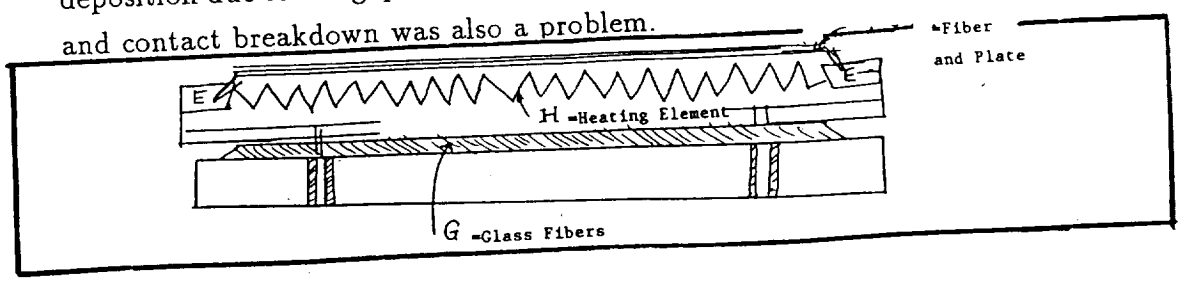

3. **Coiled Wire Heating:** Coiled wire heating generated uniform temperature along the length. Here coils/strip were coiled keeping uniform distance between each ring and more concentrated rings at the edge. However mounting the fibers and controlling the system conditions were the major problems.

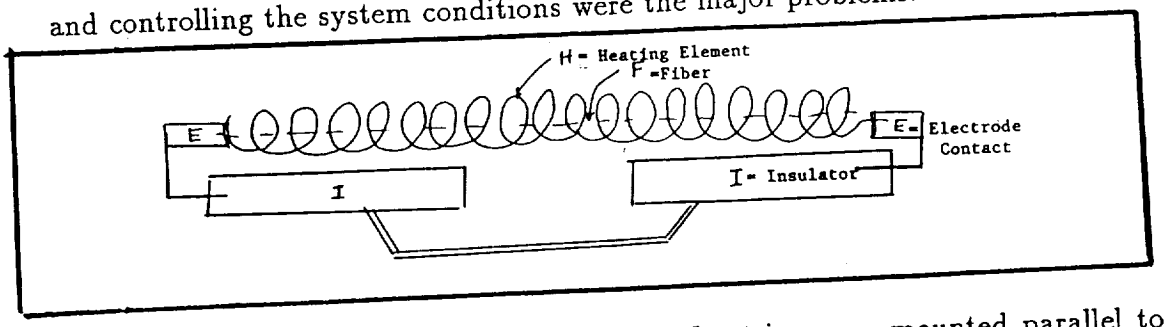

4. **Parallel Strip Resistance Heating** The Mo strips were mounted parallel to each other on electrode contact plates. The substrate fiber was mounted between it. This led to more uniform deposit than the above three.

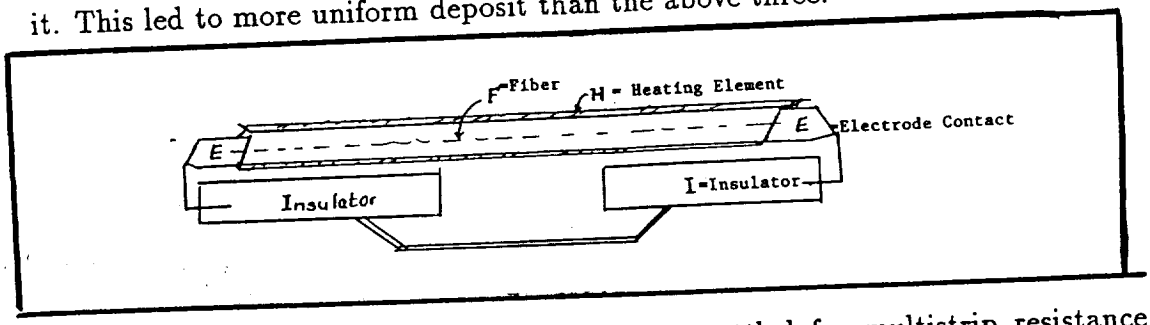

5. **Multistrip Resistance Heating** Finally we settled for multistrip resistance heating where strips were mounted around the plate of contact and fibers were mounted on it. These resistance heated strips created uniform temperature except at the end. The only major drawback is that one can generate a single fiber at a time of short length. Quality control was also a major problem. Finally, temperature control was not accurate. In this system we generated enough fibers for our testing. The best results are tabulated in the table.

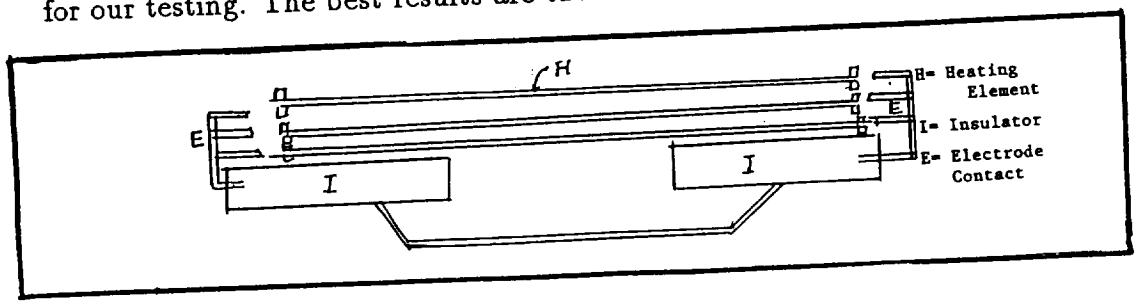

14 Siliconizing of Carbon Yarn by Reaction with SiO

Gaseous silicon monoxide, SiO, reacts with carbonaceous materials to generate silicon carbide. The reaction is not accompanied by any volume change in the system and after a time the carbonaceous material is converted to ceramic material. The reaction was originally proposed by Prof. Fitzer from Karlsruhe and later studied also in our Laboratory. Even though the physical and mechanical properties of the resulting silicon carbide filaments are rather satisfactory, the amount of information accumulated in Karlsruhe and Buffalo is not satisfactory.

14.1 Reaction Between Carbon and Silicon Monoxide

The reaction between carbon and silicon monoxide is strongly endothermic. Experimental investigation performed in Karlsruhe and here indicated that the process is strongly temperature dependent and that the activation energy for the rate controlling rection is 466kJ/mole.While a direct reaction between carbon fibers and liquid silicon results in silicon carbide fibers which are very brittle,the more gentle way of siliconizing the carbon fibers through SiO can convert the core carbon fibers to silicon carbide with much better mechanical properties.Under certain circumstances silicon carbide whiskers can grow on carbon support but there are ways to avoid the whisker formation.The reaction front in an individual carbon filament propagates in a radial way and a parabolic law can be applied to describe the propagation. The activation energy of the reaction depends strongly on type of the carbon material.The value presented above is typical very fine graphite particles. On the other hand, the value of activation energy for PAN based fibers is only 120kJ/mol.The carbon fibers which have initial porosity can be converted much faster to silicon carbide fibers than the fibers which have glassy surface.Typically THORNEL M40 fiber can be converted to silicon carbide by SiO gas in 30 min.,at 1450°C.Few photographs of these fibers is shown in figure 42. Thornel(poly acrylo nitrile based) carbon fibers with high porosity showed the highest conversion compared to pitch based fibers with lower porosity and surface area.These fibers showed the moderate strength(60-200KSI).In order to improve the mechanical properties of the silicon carbide fibers, CO gas can be used in the carrier gas.Typically the argon stream is diluted by 5-15% of CO.The rate of counter diffusion of SiO and

FIG (a).
Graphitic

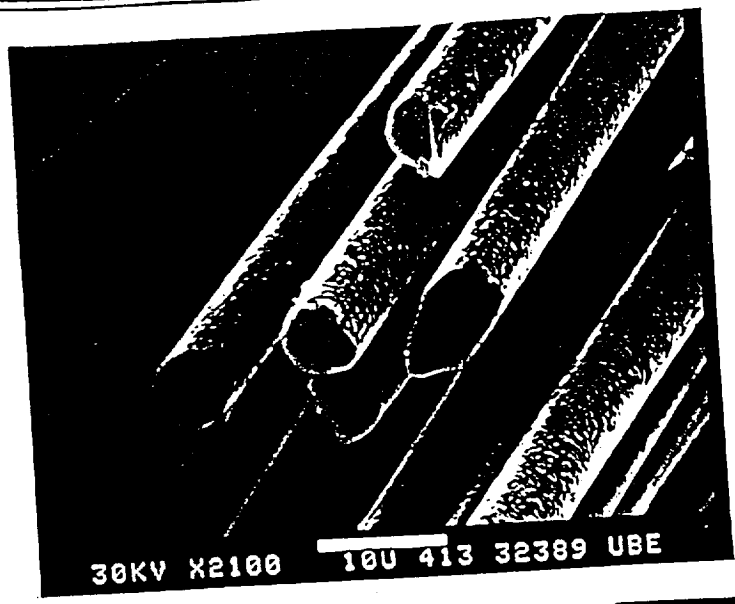

FIG (b).
PAN based

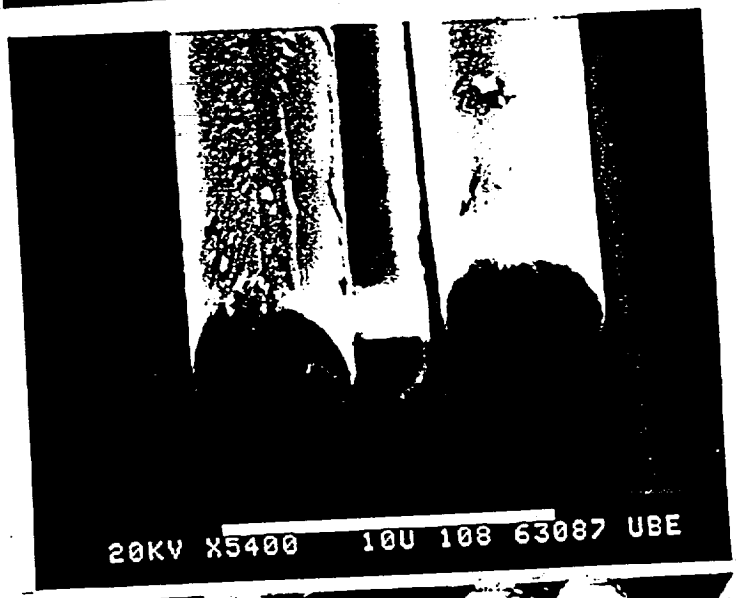

FIG (c).
PAN based

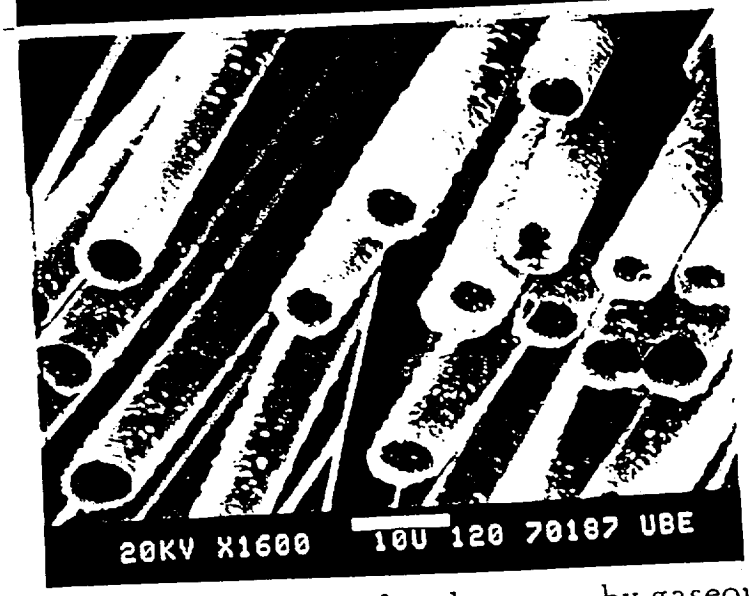

Figure 42 SiC fibers prepared by siliconizing of carbon core by gaseous SiO. (a) Graphitic(b) PAN based (c) PAN based

CO is very important for the surface morphology. The major advantage of the process is the fact that individual filaments in the carbon(or silicon carbide) tow are not glued together and that they keep their identity.The developed fibers are shown in Figure 41.

15 Summary and Conclusions

Small diameter (10-20μm) silicon carbide fiber was developed by using carbon tow as a core material in our batch process. The continuous system with a special seal arrangement can generate fiber continuously but the gluing is the main obstacle to scale-up. Different parameters were analyzed and briefly discussed. The thermal expansion mismatch and residual stresses were partially eliminated by incorporating secondary carbon deposition.

- Fibers obtained by us showed good physical properties. We are able to produce these fibers continuously with 30% gluing.
- Secondary spongy coating improved the fiber strength by reducing the stresses.
- The system we used to separate the individual filament separated approximately 60% of the filaments at the best.
- Further strides are required to quantify the advantages of these fibers over others. The heating system and the oxidation studies require additional attention.
- The thermodynamic studies for whole spectrum of conditions were discussed. An improvement over all the published result has been made.
- deposited film morphology with respect to different operating conditions were obtained and compared with theoretical result

16 REFERENCES

Airey,A.C., Cartwright,P.J., and Popper,P.,"Stresses Developed in Pyrolytic SiC Coatings During Deposition and Cooling", 147-157, in " Special Ceramics -6 (1974)", The British Ceramic Association, 1975.

Beutler, H., Oesterle, S.,and Yee,K.K., The Chemical Vapor Deposition,1975. 5.Intern. Conference,The Electro Chemical Society,Princeton,NJ. Ed. by Blocher,J.M., Hintermann,H.H., and Hall, L.H., 749,1975

Bhatt,R.T; "Effects of temperature, Matrix Density and Interfacial Shear Strength on the Mechanical Properties of SiC/RBSi_3N_4 Composites, HiTemp.Rev,57-1,1988

Blocher, J. M., Jr.,"Structure/Properties/Process Relations in Chemical Vapor Deposition(CVD)", J. Vac. Sci. Technol.,11,680 (1974).

Blocher, J. M., Browning, M. F.,and Barret, D. M.,"Chemical Vapor Deposition of Ceramic Materials", Mater. Sci. Res.,17, 299, 1984.

Brenner,W.,"Chemical Approach to the Synthesis of SiC" Proc. Conf. Boston,1959 "Silicon Carbide,A High Temperature Super Conductor" Eds.O'Conner,J.R.,and Smiltens; Paragon Press,New york, 110-114,1960

Brennfleck, K., Fitzer, E., Schoch, G. and Dietrich, M.; "CVD of SiC-interlayers and their interaction with carbon fibers and with multilayer NbN coatings.", Proc. 9th Int. Conf. on CVD, 649, 1984.

Bryant, W.A., Meier, G.H., "Factors affecting the adherence of chemically vapor deposited coatings," J. Vac. Sci. Technol., 11, No. 4, 719, 1974.

Buzhdam, Y.M., Kocheshkova,A.A., and Kuznetsov,F.A., "Analysis of Crystalization Condition of SiC from Gas Phase in the Si-C-Cl_2-H_2 System","Proc. Intl. Conf. on Chemical Vapor Deposition" Eds.Sedgwick,T.O., and Lydtin,H;The Electro Chemical Society,Princeton,NJ,412,1979

Cartwright, B. S. and Popper, P., "Deposition of Pyrolytic SiC from Methyltrichloro Silane" in "Science of Ceramics -5,473 (1970)", Research Paper No. 615, 1969, The British Ceramic Association,1970.

Chin, J., Gantzel, P. K. and Hudson, R. G.,"The Structure of Chemical Vapor Deposited Silicon Carbide", Thin Solid Films,40, 57, 1977.

Chin,J., and Ohkawa,T.;"In Situ Regeneration of Fusion Reactor First Walls",Nuclear Technology, 32,115-124,1977

Chin,J., and Gantzel,P.K.,"Structure of Chemical Vapor Deposited Silicon Carbide,GA-A-13845,General Atomic Co., San Diago,1976

Chiu, K.C. and Rosenberger, F.; "Mixed convection between horizontal plates I Entrance effects", Int. J. Heat Mass Transfer **30**, 1645- 1654,1987.

Christin, F., Naslain, R., Bernard, C., "A Thermodynamic and Experimental Approach of Silicon Carbide CVD. Application to the CVD- Infiltration of Porous Carbon Composites," Proc.7th Int. Conf. CVD., 499, 1979.

Coltrin, M.E., Kee, R.J. and Miller, J.A.; "A mathematical model of silicon chemical vapor deposition. Further experiments and the effect of thermal diffusion", J. Electrochem. Soc.**133**, 1206-1213 ,1986.

Di Carlo, J.A.; "Fibers for Structurally reliable metal and ceramic composites", J. Met.**37**, 44-49 ,1985.

Di Carlo, J.A.; "Ceramic matrix composites", Hitemp Rev., **9-1**, 1988.

Diefendorf, R. J. and Stover, E. R.,"Pyrolytic Graphites,How Structure Affects the Properties" Metal. Progr.,**81**, 103, 1962.

Doherty, J. E.,"Chemical Vapor Deposition of Structural Ceramic Materials", J.Met,**28**, 6, 1976.

Edie, D.D.,"Textile Structure and Their Use in Composite Materials", Int. Fiber. J.,**2(2)**, 6, 1987.

Edie, D. D.,and Dunham, M. G.,"Advanced Engineering Fibers", Chem. Eng. Edu., **21**, 186, 1987.

Federer, J. I.,"Parametric Study of Silicon Carbide Coatings Deposited in a Fluidized Bed", Thin Solid Films,**40**, 89, 1977.

Fitzer, E. and Kehr, D.,"Carbon, Carbide, and Silicides Coatings", Thin Solid Films, **39**, 55-67, 1976.

Fitzer, E.,Hegen, D.,and Pommer,H.;"Gas Phase Separation of SiC and Si_3N_4-A Contribution of Chemistry to the Development of Silicon Ceramics", Angew. Chemie, **91**, 316, 1979.

Gupte,S.M.: "Chemical Vapor Infiltration and Chemical Vapor Deposition of Silicon Carbide.", Ph.D. Thesis, SUNY-Buffalo, 1990

Gordon, S., McBride, B.J., "Computer program for calculation of complex chemical equilibrium compounds, rocket performance, incident and reflected shocks and Chapman-Jouget detonations," NASA SP - 273, 1971.

Guinn,K., and Middleman, S.,"continuous Filament Coating by Chemical Vapor deposition", J. Cryst. Growth, **96**, 589, 1989

Gulden, T. D., "Stacking Faults in Chemically Vapor Deposited Beta Silicon Carbide", J. Amer. Cer. Soc., **54**, 498, 1971

Gulden, T. D.,"Deposition and Microstructure of Vapor Deposited Silicon Carbide", J. Am. Ceram. Soc.,**51**, 424, 1968.

Harris, J. M., Gatos, H. C. and Witt, A. F.,"Growth Characteristics of Alpha SiC. I.Chemical Vapor Deposition", J. Electrochem. Soc., **118**, 335, 1971.

Hess, D.W., K.F. Jensen and T.J. Anderson; "Chemical Vapor Deposition: A chemical engineering perspective.", Rev. Chem. Eng., **3**, 97-186 (1985), Hitachi Japan Kokai Jokkyo **62**, 12671,1987.

Holliday, G. C. and Gooderham, W.J.,"Thermal Decomposition of Methane. I.The Homogeneous Reaction", J. Chem. Soc. (London),**1594**, 1931.

Holman, W. R. and Huegel, F. J.,"Chemical Vapor Deposition of Tungusten and Tungusten-Rhenium Alloys for Structural Applications" " Proceedings of the Conference on Chemical Vapor Deposition of Refractory Metals, Alloys, and Compounds",Gatisburg,TN Sept 12-14,1967,American Nuclear Society,Hinsdale, IL, **127** and 427,1967

Iwasa, M., Ide, M., Watanabe, S., and Tanji, H.,"Properties and Cycle-Life of Pyrolytic BN-Crucible", Proc.10^th Int. Conf. CVD, Eds. Cullen, G. W. and Blocher, J. M. Jr., 1106, 1987.

Ivanova, L. M., and Pletyushkin,A.A.,"Kinetics of the Formation of Beta-SiC from Gaseous Phase",Izvest.Akademii Nauk, SSSr. Neorgan Mater,.**3**,1817-1822,1967

Ivanova, L. M., and Pletyushkin, A. A.,"Thermal Decomposition of Methyl trichloro Silane Vapors".,Izvest.Akademii Nauk, SSSr. Neorgan Mater., 4,1089,1968

Janaf Thermochemical Tables, J. Phys. Chem. Ref. Data.,1990.

Janaf, "Thermochemical Tables," 2nd edn., D.R. Stull; H. Prophet et al., NSRS-NBS, 1970.

Johnson, S. M., Brittain, R. D., and Lamoreaux, R. H.,"Degradation of SiC Fibers", J. Electrochem. Soc., **134**, 470, 1987.

Kaae, J. L., Gulden, T. J.;"Structure and Mechanical Properties of Co-Deposited Pyrolytic C-SiC Alloys", Amer. Ceram. Soc., **54**, 605,1971

Kassel, L. S., "The Kinetics of Homogeneous Gas Reactions", Am. Chem. Soc. Monograph,J. Am. Chem. Soc.,**54**, 4121, 1932.

Knippenberg, W. F., Verspui, G., and Von Kemenade, A.W.C.,"Growth Mechanism of SiC in Vapor Deposition"," Silicon Carbide",Eds.Faust,J.W., and Ryan,C.E., 1973, Univ. of South Carolina Press, Columbia, SC, 92-107, 1974.

Knippenberg,W.F.,"Growth Phenomenon in Silicon Carbide", Philips.Res.Report,**18**,161-274,1963.

Knippenberg,W.F., and Verspui,G.; "Growth Mechanisms of SiC in Vapor Deposition. II",Silicon Carbide,Proc. Int. Conf., **3rd**,108,1973

Lavrov, N. V., Chernekov, I. I. and Emyashev, A. V.,Determination of Conditions for the Deposition of the Pyrolytic Material Based on the Thermodynamic Analysis of the Si-C-Cl_2-H_2 System", Dokl. Akad. Nauk, SSSR, **184**, 154, 1969.

Lewis, J., Ed. Henish, M.K. and Roy, R., Silicon Carbide, 1968 Paragon Press 1969, S321-332, Mat. Res. Bull.,**4**, 321, 1969.

Mah, T., Hecht, N. L., McCullum, D. E., Hoenigman, J. R., Kim, H. M., Katz, A. P., Lipsitt, H. A., Thermal Stability of SiC Fibers(Nicalon)", J. Mat. Sci.,**19**, 1191, 1984.

Mamet'ev, R. Yu., Pavlov, S.M., Sharpin, D.N., Yurkinskaya, L.V., "Static regularities of titanium diboride deposition from gaseous phase," Poroshk. Met., No.**3**, (135), 1974.

Merz, K. M.,"Crystals, Whiskers and Microcrystal Form of SiC", " Silicon Carbide,A High Temperature Super Conductor" Eds. O'Conner,J.R., and Smiiltens,J., Pargamon NY, Proc. Boston Conf(1959), 73, 1960.

Motojima, S., Yagi, H. Iwamori, N.,"Chemical Vapor Deposition of SiC and Some of its Properties", J. Mater. Sci. Lett.,5, 13, 1986.

Naslain, R.,Hannache,H.,Hearud, L., Rossingnol, J. Y., Christin, F., Bernard, C.,"Chemical Vapor Infiltration Technique",EURO CVD Four, Proc. Eur. Conf. on Chemical Vapor Deposition,4th, 293,1983

Naslain, R., Thebault, J., Hagenmuller, P. and Bernard, C.,"The Thermodynamic Approach to Boron Chemical Vapor Deposition Based on A Computer Minimization of Gibbs Free Energy", J. Less- Common Met.,**67**, 85, 1979.

Nickl, J. J. and Von Braunmuhl, C., "Gas Phasenabscheidung Im System Silicium-Kohlenstoff",J. Less-Common Metals,**25**, 303, 1971.

Nickl, J. J. and von Braunmuhl, C.,"Chemical Vapor Deposition in the Systems Silicon-Carbon and Silicon-Carbon-Nitrogen" J. Less-Common Metals,**37**, 317,1974.

Oxley, J. H., Secrest, A. C., Veigel, N. D. and Blocher, J. M., Jr., "Kinetics of Carbon Deposition in a Fluidized Bed", A. I. Ch. E.J.,7, 498, 1961.

Pampuch, R. and Stobierski, L., "Morphology of SiC Formed by Chemical Vapor Deposition",Ceramurgia Intern.,**3**, 43, 1977.

Pierson, H.O., Randich, E., "Titanium diboride coatings and their interaction with the substrates," Thin Solid Films,**54**, 119, 1978.

Pierson, H.O., Randich, E., Mattox, D.M., "The Chemical Vapor Deposition of TiB_2 on Graphite," J. Less-Common Met.,**67**, 381, 1979.

Popper,P., Mohyuddin,I., "Special Ceramics"1964 Ed. Popper,P., Academic Press,London,45, 1965

Poretr,G.,"Structure and Properties of Pyrolytic Silicon Carbide" Amer.Cera. Bull,**48**,859,1969.

Price, R. J.,"Structure and Properties of Pyrolytic Silicon Carbide" Amer. Ceram. Soc. Bull,**48**,859, 1969.

Pring, J. N. and Fielding, W.,"Preparation at High Temperatures, Refractory Metals from Their Chlorides" J. Chem. Soc.,**95**, 1497, 1909.

Powell, C.F., Campbell, I.E., Gonser, B.W., "Vapor-Plating,The Formation of Coatings by Vapor Deposition Techniques",71 and 120, John Wiley and Sons, Inc., N.Y., 1955.

Prewo, K.M.; "Fiber reinforced ceramics: New opportunities for ceramic materials.", Cer. Bull.,**68**, 395 (1989).

Reisch, M. S.,"High- Performance Fibers Find Expanding Military, Industrial Uses", C & EN, **65**, Feb. 2, 1987.

Revankar, V.V.S., Arya, P. V., and Hlavacek, V.,"Ceramic Fibers by Chemical Vapor Deposition", NASA Publication,1988.

Revankar, V.V.S.; Schultz, J.; Hlavacek, V.; "Synthesis of ceramic fibers by CVD, A model study;" Ceram. Eng. and Sci. Proc., 1988.

Revankar, V.V.S. and Hlavacek, V.; "Synthesis of SiC multifilaments by Chemical Vapor Deposition.", High temp. Mater. and Processes, in press (1991).

Richerson, S. M.,"Modern Ceramic Engineering", p 136, Marcel Dekker Publ.,N.Y, 1984.

Sandy, S.C.; "Physical vapor deposition on a multifilament tow.", Paper presented in AIChE conf. on Emerging Technology in Materials", Minneapolis, Minnesota, Aug. 18-20, 1987.

Scholtz, J.H.; "The coating of fibrous substrates by CVD: Modeling and simulation.", Ph.D. Thesis, SUNY-buffalo, 1991

Farrell,K., Houston,J.T., and Schaffhauser, A. C.,"The Growth of Grain Boundary Gas Bubbles in Chemically Vapor Deposited Tungusten" Ed., Proceedings of the Conference on Chemical Vapor Deposition of Refractory Metals, Alloys and Compounds, Gatlinburg, TN, Sept. 12-14, 1967, American Nuclear Society, Hinsdale, IL, 363,1967.

Schlichting, J.; "Chemical Vapor Deposition of Silicon Carbide", Powder Metall. Int.,**12**, 196-200, 1980.

Schlichting, J., Ceramic from Metal Alkoxides", Sci. Ceram,**10**,143, 1980a.

Sherman, A.," Chemical Vapor Deposition of Microelectronics Principles, Technology and Applications," Park Ridge,NJ., Noyes Publication, 1987.

Shinko, J. S. and Lennartz, J. W.,"CVD Silicon Nitride Crucible Produced Using SPC Techniques to Correlate and Optimize Processing Variables", Proc.10^th Int. Conf. CVD, Eds. Cullen, G. W. and Blocher, J. M. Jr., 1106, 1987.

Shorshorov, M. V., Alekhin, V. P., Savvateeva, S. N., Fedorov, V. B. and Chernyshova, I. A., "Plasticizing and Wettability Enhancing Coatings on Carbon, SiC, and B Fibers", Thin Solid Films.,**58**, 279,1978

Smoak, R. H., Korzekwa, T. M., Kunz, S. M., Howell, E.D.,"Silicon Carbide", 520-535 in "Encyclopedia of Chemical Technology," 2nd Edition, Vol. 4, Wiley (Interscience) Publisher, NY 1964.

Spear, K.E.; "Principles and Applications of Chemical Vapor Deposition", Pure Appl. Chem.,**54**, 1297-1311 (1982).

Spruiell, J. E.,"Chemical Vapor Deposition of SiC from $SiCl_4$-CH_4- H_2 Mixture",**ORNL-4326**, Oak Ridge National Lab., Tennessee, 1968.

Spruiell,J.E.,"Chemical Vapor Deposition of SiC from Silicon tetra chloride - Methane-Hydrogen Mixture.",Chemical Vapor Deposition;Intl. Conf. ,Eds. Blocher,J.M. Jr., and Withers,J.C.,The Electrochemical Soc., Princeton,NJ., 279, 1970

Susman, S., Springs, R. S. and Weber, H. S.,"Vapor Phase Growth of β-SiC Single Crystal", Proc of Conf. "Silicon Carbide - A High Temperature Semiconductor," Ed. by O'Connor, J. R. and Smittens, J.,Boston,(1959) Pergamon Press, Oxford, 94-109, 1960.

Storch, R. H.,"The Thermal Decomposition of Methane by a Carbon Filament", J.Am. Chem. Soc.,**54**, 4188, 1932.

Tukovic, A. and Marinkovic, S.,"Microhardness of Silicon-Containing Pyrolytic Carbon", J. Mat. Sci.,**5**, 541, 1970.

Van Kemenade, A.W.C. and Stemfoort, C. F., Formation of β-SiC from Pyrolysis of Methyltrichloro Silane in Hydrogen" J. Crystal Growth, **12**, 13,1972.

Vinson, J.R.; "Recent Advances in Technology for Composite Materials in the United States", Composites of Technology and Research, **59** ,1989

Wahl, G., and Schmadere, F.," Reviews in Chemical Vapor Deposition of Superconductor", J. Mater. Sci,**24**, 1141, 1989.

Warren, R.,Anderson, C. H., and Carlsson, M.,"High Temperature Capability of Carbon Fibers with Ni", J. Mat. Sci.,**13**, 178 ,1978

Wawner, F., Teng, A., Nutt, S., "Microstructural Characterization of SiC (SCS) Filaments," Metal Matrix Carbon and SiC Composites, NASA Conf. Pub. **2291**, 29, 1983.

Weiss, J. R. and Diefendorf, R. J.,"Relation of Structure to Properties in Chemical Vapor Deposited SiC", "Silicon Carbide - 1973," Ed. by Marshall, R. C., Faust, J. W., and Ryan, C. E., Univ. of South Carolina Press, Columbia, South Carolina,80-91, 1973.

Weiss, J. R., and Diefendorf, R. J., Silicon Carbide, 1973, University of South Carolina Press, Columbia, SC, 80-91, 1974.

Yajima,S., and Hirai,J.;"Siliconated Pyrolytic Graphait. I. Preparation and Properties, II. State of Si Present in Pyrolytic Graphite", J.Mat.Sci.,4,1969

Yajima,S., Hasegawa,Y.,Hayashi,J., and Imura,J.,"Synthesis of Continuous Silicon Carbide Fibers with High Tensile strength and Modulus" J.Mat.Sci.,**13**, 2569,1978

Yee, K. K, "Protective Coating for Metals by Chemical Vapor Deposition", Int. Met. Rev.,**23**, 19, 1978.

Zhao, G.Y., Revankar, V.V.S., Hlavacek, V., "Hydrogen-Chlorine Flame For Synthesis of Ultra Fine Powders," J. Less Common Metals, **163** , 269, 1990.